TECHNISCHE UNIVERSITÄT WIEN

Diplomarbeit

Salt hydrates as alternative thermochemical energy storage materials for industrial applications

ausgeführt am

Institute für Angewandte Synthesechemie

der Technischen Universität Wien

unter der Anleitung von

Associate Prof. Dipl.-Ing. Dr. techn. Peter Weinberger

und

Proj.-Ass. DI Jakob Smith

durch

Jakob Werner, BSc

01425051

[redacted]

[redacted]

Wien, im Oktober 2023

Abstract

Around 50 % of the global demand of primary energy is devoted to heat production, making heat the most abundant form of energy. A great part of the heat produced, is after the desired usage lost as low-grade waste heat. In order to increase energy efficiency, thermochemical energy storage is a promising technique to utilize and store the otherwise lost waste heat for later usage.

In this thesis the synthesis and characterization of promising salt hydrates as thermochemical materials is presented. A small library of calcium dicarboxylate salt hydrates was prepared to investigate and compare these compounds with each other to scan for promising candidates and get a deeper understanding of the chemical processes behind the de- and rehydration reactions.

Ca-terephthalate trihydrate has shown its potential as thermochemical material, showing a high storage potential, as well as good preliminary cycle stability results. A comparison with its derivatives resulted in the identification of the crystal structure of 2-fluoro calcium terephthalate trihydrate that could be investigated in collaboration with Priv.-Doz. Dr. Berthold Stöger.

Furthermore, the synthesis of ettringite, another promising material, had to be optimized.

The work can be considered successful, as a small library of 11 Ca-salts was prepared and characterized. Furthermore, the preparation method of ettringite could be optimized to a phase purity of 98.5 % confirmed with quantitative phase analysis for smaller scales.

Zusammenfassung

Ungefähr 50 % des globalen Primärenergiebedarfs entfallen auf die Produktion von Wärme. Ein Großteil der produzierten Wärme wird, nach dem geplanten Einsatzzweck, als Abwärme verloren. Um einen wichtigen Schritt in Richtung einer energieeffizienten Zukunft machen zu können, bietet sich thermochemische Energiespeicherung als vielversprechendes Konzept an, um die normalerweise verloren gehende Abwärme zugänglich und speicherbar zu machen.

Diese Arbeit befasst sich mit der Synthese und Charakterisierung von vielversprechenden Salzhydraten die als thermochemisches Material Einsatz finden sollen. Eine kleine Auswahl an Calcium Dicarboxalaten wurde hergestellt, und charakterisiert, um sie untereinander zu vergleichen und vielversprechende Kandidaten auswählen zu können. Darüber hinaus sollten die zugrundeliegenden chemischen Abläufe der De- und Rehydratationsreaktion untersucht werden.

Ca-Terephthalat Trihydrat tat sich dabei als vielversprechendes Material mit hohem Energiespeicherpotential, und vielversprechenden ersten Versuchen zur Zyklierbarkeit, hervor. Ein Vergleich mit einigen Derivaten ermöglichte außerdem, in Kollaboration mit Priv.-Doz. Dr. Berthold Stöger, die Aufklärung der Kristallstruktur der Verbindung 2-Fluoro Calcium Terephthalat Trihydrat.

Ein weiteres Ziel der Arbeit war die Optimierung der Synthese von Ettringit, einem anderen vielversprechenden thermochemischen Materials.

Insgesamt kann die Arbeit als erfolgreich durchgeführt angesehen werden. Eine Auswahl von insgesamt 11 Ca-Dicarboxylaten wurde hergestellt und charakterisiert. Die Syntheseoptimierung von Ettringit gelang in kleineren Ansätzen bis zu einer Phasenreinheit von 98.5 %, was mittels quantitativer Phasenanalyse ermittelt wurde.

Acknowledgements

The present work was accomplished at the Institute of Applied Synthetic Chemistry at TU Wien from October 2022 to September 2023. I want to thank Prof. Peter Weinberger for providing me a place in his group and the numerous chances of dissemination he offered me during my stay. Furthermore, I want to acknowledge DI Jakob Smith for his supervision and for never hesitating to put his own work on hold to help me.

I want to thank the whole Magneto- and Thermochemistry research group for the nice time and good collaboration, Priv.-Doz. Dr. Berthold Stöger for his contributions in measuring the crystal structure, and DI Werner Artner for his help with all X-ray devices.

Furthermore, I want to thank my whole family for their constant support and especially my parents for giving me the opportunity to choose this type of education. Special acknowledgements go to my father who introduced me to the topic of thermal energy storage. Last but not least, I want to thank my fantastic girlfriend Helene, who never got tired of listening to my thoughts, test presentations or any other chemical topics.

Without one of the mentioned persons, this work could not exist in the way it does, a deep thank you for your support!

Table of contents

Glossary **1**
List of symbols 1
Subscripts 1
List of abbreviations 2

1 Introduction **3**
1.1 Thermal energy storage – state of the art 3
1.1.1 Sensible heat storage 3
1.1.2 Latent heat storage 4
1.1.3 Thermochemical energy storage 4
1.2 Thermodynamics of thermal energy storage 6
1.3 Calcium dicarboxylate salt hydrates 8
1.4 Aim of the work 9

2 Results and discussion **10**
2.1 Synthesis of calcium dicarboxylate hydrates 10
2.1.1 Calcium oxalate monohydrate 10
2.1.2 Calcium malonate dihydrate 11
2.1.3 Calcium succinate monohydrate 11
2.1.4 Calcium glutarate monohydrate 11
2.1.5 Calcium terephthalate trihydrate 12
2.1.6 2-methyl calcium terephthalate n-hydrate 14
2.1.7 2-fluoro calcium terephthalate trihydrate 14
2.1.8 2-chloro calcium terephthalate n-hydrate 15
2.1.9 Tetrafluoro calcium terephthalate n-hydrate 15
2.1.10 Tetrachloro calcium terephthalate tetrahydrate 15
2.1.11 Cyclopropane-1,1-dicarboxylic acid calcium salt n-hydrate 16
2.2 Single crystal growth for X-ray analysis 16
2.2.1 2-fluoro calcium terephthalate trihydrate 16
2.3 Characterization of calcium dicarboxylate salt hydrates with STA 17
2.3.1 Enthalpy values calculation and comparison 20
2.4 In-situ PXRD measurements 22
2.4.1 Ca-malonate dihydrate 22
2.4.2 Ca-terephthalate trihydrate 24
2.4.3 2-fluoro Ca-terephthalate trihydrate 26
2.4.4 Tetrafluoro calcium terephthalate tetrahydrate 27
2.5 Ettringite 28
2.5.1 Negative synthetic approaches for ettringite 29

2.5.2 STA measurements 30
2.6 Ca-oxalate monohydrate synthesis comparison 30
2.7 Crystal structure identification of 2-fluoro calcium terephthalate trihydrate 33
2.8 Final conclusion and outlook 34

3 Experimental Part 35
3.1 General Methodology 35
3.1.1 Nuclear magnetic resonance spectroscopy (NMR) 35
3.1.2 X–ray powder diffraction 35
3.1.3 Single crystal XRD 35
3.1.4 Scanning electron microscope (SEM) 35
3.1.5 Simultaneous thermal analysis (TGA-DSC) 36
3.2 Synthesis of calcium oxalate monohydrate 36
3.3 Synthesis of calcium malonate dihydrate 36
3.4 Synthesis of calcium glutarate monohydrate 36
3.5 Synthesis of calcium terephthalate trihydrate 37
3.5.1 Negative synthetic approaches for 5a 37
3.6 Synthesis of 2-methyl calcium terephthalate n-hydrate 38
3.7 Synthesis of 2-fluoro calcium terephthalate trihydrate 38
3.7.1 Single crystal growth for X-ray diffraction 39
3.1 Synthesis of 2-chloro calcium terephthalate n-hydrate 40
3.2 Synthesis of Tetrafluoro calcium terephthalate tetrahydrate 40
3.1 Synthesis of Tetrachloro calcium terephthalate n-hydrate 41
3.2 Cyclopropane-1,1-dicarboxylic acid calcium salt n-hydrate 41
3.3 Synthesis of Ettringite 41
3.3.1 Negative synthetic approaches for ettringite 42
3.4 STA data 43

4 Contributions 44

Appendix 45
STA Curves 45
PXRD diffraction patterns 49
FTIR Spectra 59
References 66

Glossary

List of symbols

Symbol	Definition	Unit
Cp	Specific heat capacity	J K^{-1} mol^{-1}
CV	Specific heat capacity	J K^{-1} mol^{-1}
H	Enthalpy	J
m	Mass	kg
n	Moles of crystal water	mol
p	Pressure	Pa
Q	Quantity of heat	J
T	Temperature	K
U	Internal energy	J
V	Volume	m^3
W	Work	J
δ	Difference	1
δ (NMR)	Chemical shift	ppm
Δ	Difference	1
θ	Angle of diffraction	°
λ	X-ray wavelength	Å
v	Stoichiometric coefficient	1

Subscripts

Subscript	Description
deh	Dehydration
e	Evaporation
f	Formation
i	Substance i
I	State I
II	State II
net	net
p	Isobaric process
r	Reaction
t	Transition
V	Isochoric process
v	Vaporization
α	Characteristic X-ray emission line

List of abbreviations

Abbreviation	Description
DSC	Differential scanning calorimetry
Eq	Equation
h	Hour
HPLC	High pressure liquid chromatography
IEA	International Energy Agency
IR	Infrared
min	Minute
MOF	Metal organic framework
NMR	Nuclear magnetic resonance
PXRD	Powder X-ray diffraction
r.t.	Room temperature
SEM	Scanning electron microscopy
STA	Simultaneous thermal analysis
TCES	Thermochemical energy storage
TCM	Thermochemical material
TG	Thermogravimetry
TGA	Thermogravimetric analysis
vol	Volume
VSD	Volumetric storage density
XRD	X-ray diffraction

1 Introduction

Record breaking heat waves, extreme weather events and ecological calamities are reported more and more frequently. The world's climate is changing. Furthermore, events like the COVID-19 pandemic and the war in Ukraine have shown that Europe has to continue its work towards energy independence.

In 2021 the global demand of primary energy was as high as 595.15 EJ, of which 82 % were covered by fossil fuels [1]. According to the International Energy Agency (IEA) around 50 % of the world's final energy consumption are correlated to the production of heat making it the most abundant form of energy to be used [2, 3]. In industry heat is the most common form of energy, including power plants, to produce electricity or driving processes. After all processes and as a consequence of the work produced, most heat is degraded and lost as low-grade waste heat, as it is released into the environment [4]. While in 2019 globally about 50 % of total heat produced were used in industrial processes, another 46 % were consumed by the domestic sector [5]. Not only is heat production the primary usage of fossil fuels, but also a considerable part remains unutilized, due to the losses of waste heat. This points out that the discussion about reducing primary energy consumption oftentimes lacks a part of equal importance – increasing energy efficiency. Further speaking increasing the efficiency of all energy conversion processes and (re)utilizing waste heat are key approaches towards a more sustainable energy management [6-8].

1.1 Thermal energy storage – state of the art

Three main approaches were established in terms of thermal energy storage. To give a brief, general overview they are discussed in this chapter. The thermodynamic basics can be found in chapter 1.2.

1.1.1 Sensible heat storage

In sensible heat storage systems thermal energy is stored as kinetic energy in liquid or solid storage medias. The thermodynamic quantity behind this storage concept is the specific heat capacity of the storage medium. Through heat exposure the atoms and molecules of the storage material are excited, resulting in an increase in internal kinetic energy, which causes an increase of the temperature of the storage medium [9].

To perform well, a sensible heat storage material is required to have a high specific heat capacity and long-term stability towards thermal exposure. Furthermore, it needs to be compatible with its containment and low cost. Sensible heat storage is widely investigated and mostly categorized according to the state of the storage materials: liquid media storage (water, oil, molten salts etc.) and solid media storage (rocks, metals etc.) [7, 10].

The biggest issues for sensible heat storage are the requirement to thermally insulate the storage tank and the difficulty in long-term storage due to a constant loss of heat despite of thermal insulation [11].

1.1.2 Latent heat storage

Latent heat storage systems rely on phase change materials (PCMs) as storage materials. It is a very attractive technique since it shows significantly higher storage densities than purely sensible storage systems. If a material undergoes a change of phase, the corresponding energy is expressed via the transition enthalpy ΔH_t [12]. There are three possible phase transformations for PCMs: solid-solid, liquid-gas, and solid-liquid. However, only the solid-liquid transformations show practical relevance.

A variety of different applications can be found for latent heat storage such as waste heat recovery, cooling applications, solar thermal energy storage, building applications and medical applications [13].

1.1.3 Thermochemical energy storage

The third technique follows the idea to utilize reversible chemical reactions to store thermal energy. Reaction 1.1 shows the description of a TCES system in a most general way.

$$A + B \rightleftharpoons AB + \Delta H_r \qquad 1.1$$

According to [14] such an equation states an existing equilibrium between two or more educts and their corresponding products plus the associated enthalpy of reaction. As long as the educts A and B are kept separated, the system remains in a charged state. Due to spatial separation, energy losses during the storing period are prevented.

Thermochemical energy storage can be divided into sorption systems and chemical reactions. Sorption systems are related to adsorption or absorption effects [15, 16]. The focus of this work lies on materials feasible for thermochemical reactions between a solid and a gaseous component. Substances like H_2O, CO_2, or O_2 are highly abundant and easy to use as gaseous components. H_2, SO_2, and NH_3 are further possible candidates [17]. The biggest advantage of thermochemical heat storage over the previously mentioned techniques is the significantly higher energy storage density [18]. Figure 1 highlights the proportions of energy density between the three storage methods, with dividing TCES into sorption and reaction systems.

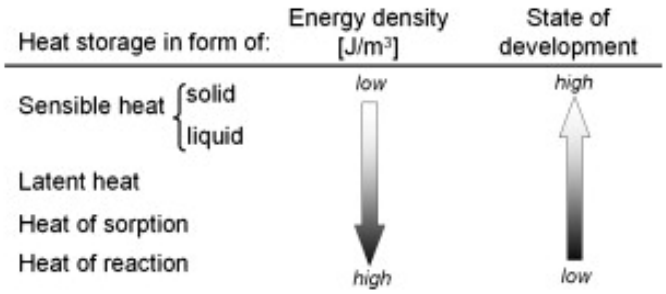

Figure 1: Energy density comparison of the three storage principles [19]

Salt hydrates are a feasible material class for TCES and extensively studied in literature [20-24]. They are compounds incorporating crystal water within the molecular crystal lattice fundamentally different from their anhydrous compounds in most cases as they possess unique chemical and physical properties [23]. In literature salt hydrates are sometimes classified as adsorption materials [25] or, more frequently as thermochemical reaction materials [16, 26].

$$A + n\,H_2O \rightleftharpoons A{\cdot}nH_2O + \Delta H_r \qquad (1.2)$$

Figure 2 illustrates the principle of a TCES system based on salt hydrates beginning with the fully hydrated TCM (discharged state). Through heat exposure the salt is dehydrated quantitatively and as long as the two components remain separated, the thermal energy from the previous charging step is stored. To discharge, the anhydrous salt reacts with water releasing the equivalent amount of heat.

The main requirements for salt hydrates as TCMs are [27, 28]:

- high energy density
- high cycle stability
- non-toxic
- low cost
- non-corrosive
- fast reaction time

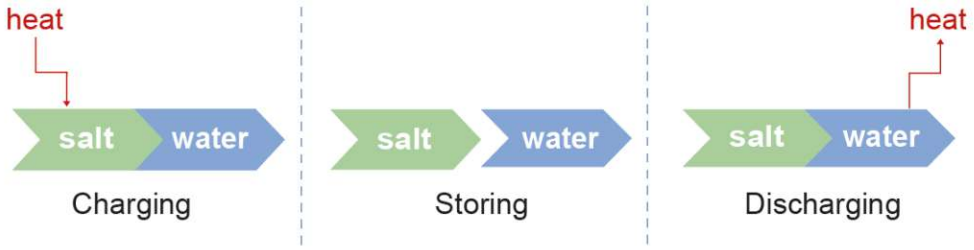

Figure 2: Storage principle for a TCES-system using salt hydrates as TCMs

Within the past years numerous salt hydrates were characterized with respect to their potential as TCM. Prominent and extensively studied examples are: $MgSO_4$ [29-32], $MgCl_2$ [30, 33, 34], $CaCl_2$ [35-37], Na_2S [38], K_2CO_3 [33, 39], $SrCl_2$ [40, 41], $SrBr_2$ [42, 43].
However, it has been reported that in practical applications, salt hydrates fail to meet the expectations and are underperforming [44]. For some salts theoretically 2 GJ/m^3 volumetric storage densities (VSD) could be expected, however, even achieving densities over 1 GJ/m^3 was difficult [37, 45]. To unlock the strengths of salt hydrates as TCM promised by theoretical calculations it is necessary to investigate the correlation between thermophysical and thermochemical properties with the chemical structure of the compounds.

1.2 Thermodynamics of thermal energy storage

The aim of this chapter is to give a brief overview of the thermodynamic fundamentals necessary to discuss thermal energy storage, however, an extended discussion of all thermodynamic coherences would exceed the frame of this work.
According to the first law of thermodynamics the internal energy of a system is the sum of the work and heat exchanged with the surroundings of the system (eq. 1.3).

$$\Delta U = W + Q \qquad 1.3$$

In TES the form of energy that is from utmost importance is heat. In thermodynamics heat is defined *"as the quantity of energy that flows across the boundary between the systems and surroundings because of a temperature difference between the systems and the surroundings"* [12]. Heat and work are path functions, meaning that they cannot be "possessed" by a system. Heat and work only exist in a process, meaning that a transfer of heat and/or work from a system to its surroundings (or vice versa) results in a change of the system's internal energy. The system has changed its states from a state I with an internal energy U_I to state II with an internal energy U_{II}.

To determine the energy released or taken up by a system undergoing a process – such as a chemical reaction it is required to determine ΔU. From the first law of thermodynamics for a

process with constant volume eq. 1.4 shows that ΔU can be determined by measuring the exchanged heat between the system and its surroundings.

$$\Delta U = Q_V$$

1.4

If the investigated process is a chemical reaction, the assumption of a constant volume is pointless. It is more realistic to carry out a reaction at constant pressure. On this behalf the energy function enthalpy H was defined (eq.1.5). The enthalpy is the sum of the internal energy U and the product of system pressure p and volume V.

$$H = U + pV$$

1.5

$$\Delta H = Q_p$$

1.6

In a closed system at constant pressure the enthalpy change is given by the heat exchanged with the systems surroundings Q_p (eq.1.6).

The amount of energy (as heat) required to raise the temperature of a system by 1 °C is called heat capacity. It can also be described as the thermal response of a system to heat flow [12]. A certain amount of heat δQ can only be supplied to the system if either the volume, or the pressure of the system remains constant. The specific heat capacity at constant pressure is expressed as C_p, and at constant volume by C_V. The corresponding specific heat capacities are defined as the heat capacity related to mass.

$$c_p = \frac{Cp}{m}$$

1.7

$$c_V = \frac{C_V}{m}$$

1.8

Enthalpy itself is a function of temperature changing according to equation 1.9.

$$h_{T_1} = h_{T_2} + \int_{T_1}^{T_2} c_p dT$$

1.9

For a TCES system the most important quantity in respect to thermal energy storage is the enthalpy of reaction ΔH_r. Following Hess' law of enthalpy summation [12, 46], the enthalpy of

reaction can be calculated by the sum of the enthalpies of formation times the stoichiometric coefficients ν_i of all reactants. ΔH_r^0 is the enthalpy of reaction at standard state, which means a pressure of 1 bar and a temperature of 298.15 K [12].

$$\Delta H_r^0 = \sum_i \nu_i \Delta H_{f,i}^0$$

1.10

Rewritten for a chemical reaction:

$$\Delta H_r^0 = \sum_i \nu_i \Delta H_{\mathrm{f},products}^0 - \sum_i \nu_i \Delta H_{\mathrm{f},reactants}^0$$

1.11

Precision for the thermophysical characterization of salt hydrates

For the process of de- and rehydrating a salt hydrate the involved enthalpy of the reaction is accessible by DSC measurements. The peak area of the corresponding peak in the DSC signal gives the value of the total energy necessary to dehydrate the salt. The enthalpy accessed this way is a combination of two energies.

$$\Delta H_{deh} = \Delta H_r + \Delta H_v$$

1.12

To vaporize the crystal water a certain amount of energy is required, which is covered by ΔH_v. The remaining part comes from the chemical bonds as reaction enthalpy ΔH_r.

1.3 Calcium dicarboxylate salt hydrates

A systematic search algorithm screening chemical databases to identify possible candidate reactions proposed the calcium oxalate monohydrate/calcium oxalate system as potential reaction for medium temperature heat storage applications [47]. First investigations showed a number of promising strengths of the $CaC_2O_4{\cdot}H_2O/CaC_2O_4$ system, such as complete reversibility of de- and rehydration reaction, high cycle stability with over 100 cycles investigated, and fast rehydration times [48]. Investigations for a feasible reactor design using the calcium oxalate system were conducted [49, 50]. Calcium salts of higher dicarboxylic acids form salt hydrates as well. Calcium malonate forms a dihydrate, with a published thermal characterization [51] and a study based on the infrared spectroscopic influences of the coordinated water [52]. It is recorded that Ca-succinate forms a trihydrate in single-crystals [53, 54], however, as powder it is only available as monohydrate. Thermal analysis data for Ca-succinate monohydrate, as well as for Ca-glutarate monohydrate are not available in literature. Ca-terephthalate trihydrate is of essential meaning as precursor for metal organic

frameworks (MOFs) [55-57] as well as in macromolecular chemistry [58, 59]. Its crystals are monoclinic in the $P2_1/c$ space group [60].

1.4 Aim of the work

The main goal of this work is to characterize potential materials that can be applied in thermochemical energy storage systems. Previous work in the group studied calcium oxalate monohydrate showing its huge potential as a TCM [48]. The question arose whether other calcium dicarboxylate hydrates share the strengths of the Ca-oxalate or can even outperform it. To accomplish this goal a small library of calcium dicarboxylate salt hydrates was characterized, the salts that were not commercially available were synthesized. To get a better understanding of the chemical behavior of hydrate water, derivatives of calcium terephthalate trihydrate were synthesized and characterized to investigate the effect of minor functionalizations on the thermophysical properties. The ultimate goal would be the tuneability of thermophysical properties by manipulating the chemical structure of the material. Furthermore, the synthesis of another potential TCM, ettringite, was to be optimized.

2 Results and discussion

2.1 Synthesis of calcium dicarboxylate hydrates

2.1.1 Calcium oxalate monohydrate

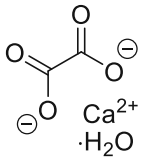

1

Calcium oxalate monohydrate was commercially available and used without further purification.

As a comparison to the frequently applied mechanochemical synthesis procedure the formation of calcium oxalate monohydrate with mechanochemical means was investigated.

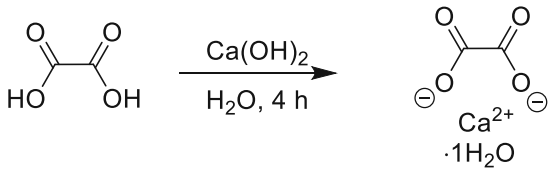

1

1 was obtained by milling oxalic acid with calcium hydroxide as calcium source in a ball mill. After milling for 4 h the product was obtained as a white powder. Product formation was confirmed by IR-spectroscopy and PXRD.

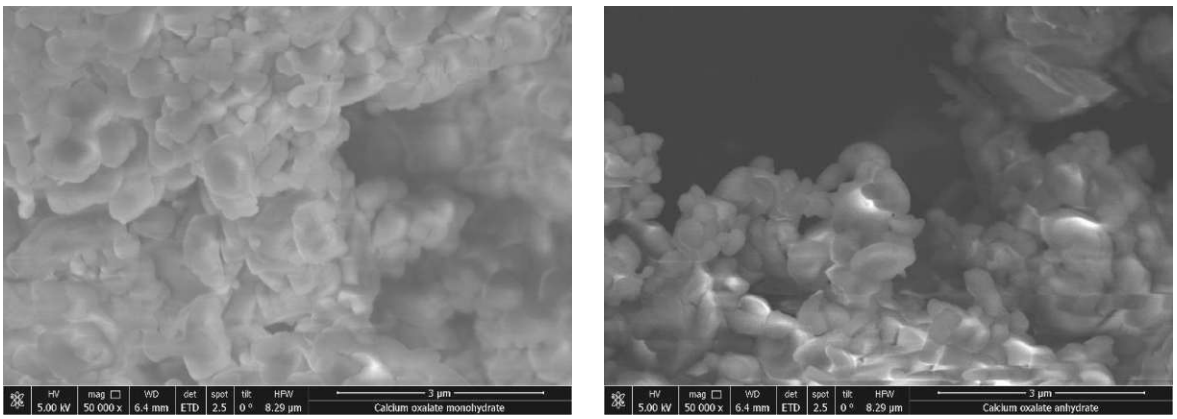

Figure 3: SEM-pictures of Ca-oxalate monohydrate (left) and Ca-oxalate anhydrate (right) at 50k magnification

2.1.2 Calcium malonate dihydrate

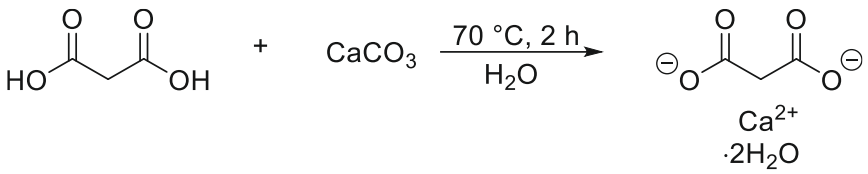

2

The product (**2**) was obtained by reaction of malonic acid with calcium carbonate in distilled water. After CO_2 formation was completed, a white precipitate was formed, that could be isolated as white powder. Product formation was confirmed by IR-spectroscopy.

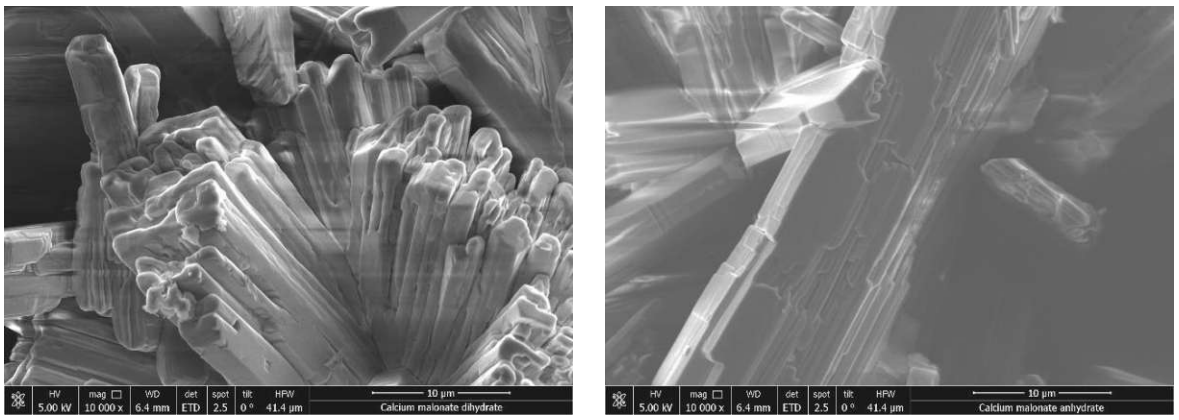

Figure 4: SEM-pictures of Ca-malonate dihydrate (left) and Ca-malonate anhydrate (right) at 10k magnification

2.1.3 Calcium succinate monohydrate

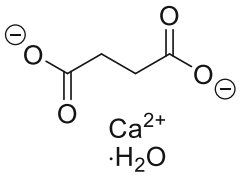

3

Calcium succinate was purchased from Santa Cruz Biotechnology and used as supplied.

2.1.4 Calcium glutarate monohydrate

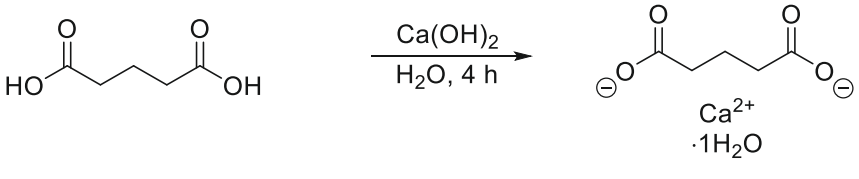

4

The product (4**)** was obtained by mechanochemical synthesis. Glutaric acid was milled with calcium hydroxide as calcium source in a ball mill. After milling for 4 h the product was obtained as white powder. Product formation was confirmed by IR-spectroscopy.

2.1.5 Calcium terephthalate trihydrate

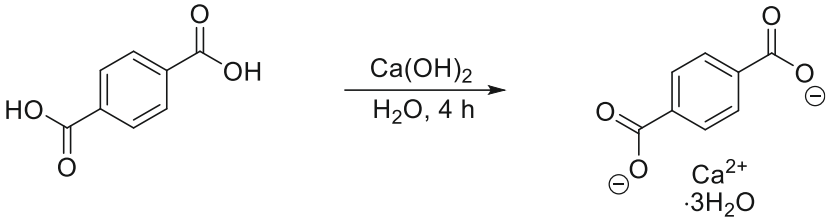

5a

The product (**5a)** was obtained by mechanochemical synthesis following literature procedure [61]. Terephthalic acid was milled with calcium hydroxide as calcium source in a ball mill. After milling for 4 h the product was obtained as a white powder. Product formation was confirmed by IR-spectroscopy and PXRD.

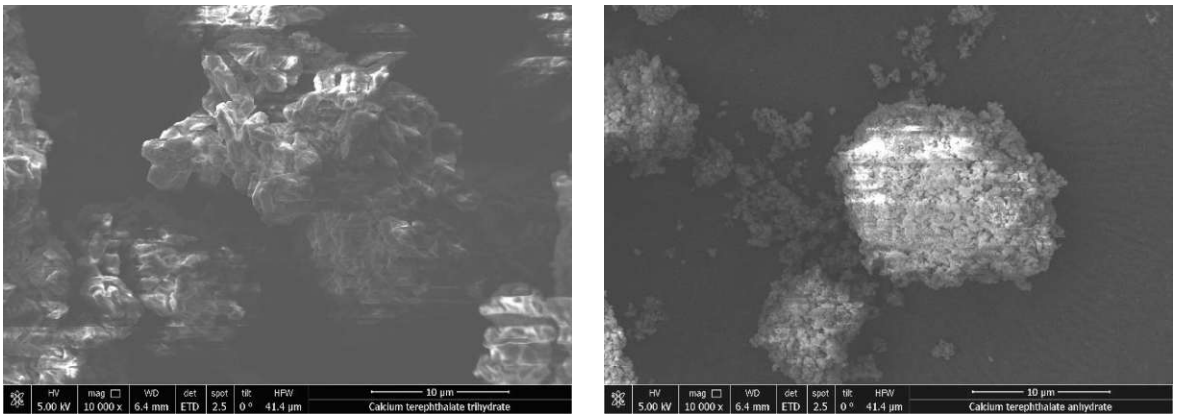

Figure 5: SEM-pictures of Ca-terephthalate trihydrate (left) and Ca-terephthalate anhydrate (right) at 10k magnification

2.1.5.1 Negative synthetic approaches for 5a

This part gives a brief overview over preparation methods for **5a** that, in our hands, did not lead to the desired product.

Alternative approach 1

Following the procedure suggested by [59].

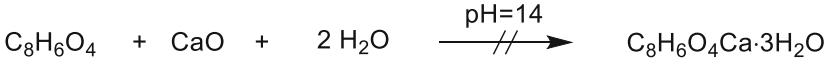

5a

Terephthalic acid was dissolved in an alkaline solution of water and NH_3 under heating and stirring CaO was added giving a white precipitate. After the work up IR-spectroscopy revealed that product formation was not successful.

Alternative approach 2

In approach 1 it was observed that CaO as calcium source seems to be problematic, since it is not soluble in water. So as a modification CaO was replaced by $CaCl_2$ as calcium source leaving the general methodology unchanged.

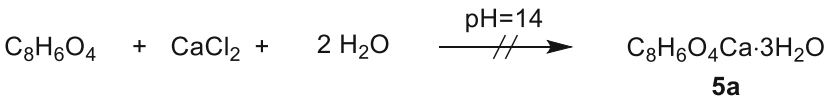

IR-spectroscopy did not indicate a successful product formation.

Alternative approach 3

Exact same procedure as approach 2 with reaction time elongated to 24 h, no product formation observable.

Alternative approach 4

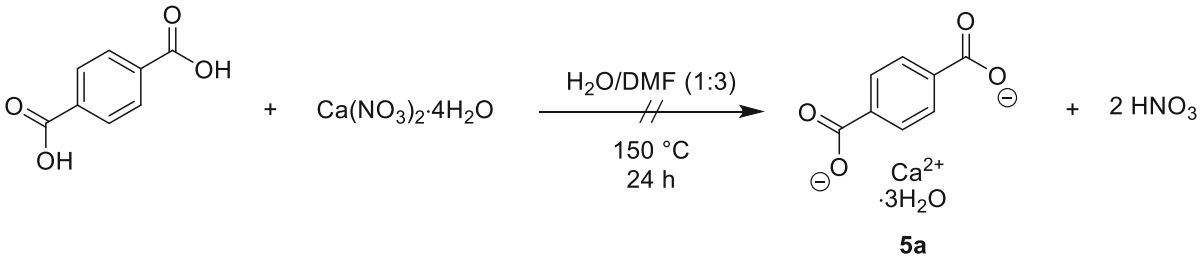

Based on the paper by Yang et. al. [62] a solvothermal pathway was considered by letting terephthalic acid react with calcium nitrate tetrahydrate as calcium source in water and DMF as solvent mixture. Reaction was carried out in an autoclave reactor at 150 °C and autogenous pressure. IR-spectroscopy and PXRD indicated product formation, however, thermal analysis showed a shift in onset temperature from 104 °C to 124 °C and a drastically reduced enthalpy of dehydration.

Mazaj et. al. [57] reported the formation of a compound with coordinated DMF molecules in the crystal structure. This compound with the assigned formula of Ca(BDC)(DMF)(H_2O) crystallizes in triclinic and orthorhombic conformations both of which are formed via crystal-to-crystal transformations of Ca-terephthalate trihydrate.

Since at this point the mechanochemical synthesis of **5a** had already been well established, further investigations regarding the true composition of products were dismissed. It is expectable that a compound mixture of Ca-terephthalate and Ca(BDC)(DMF)(H_2O) in a sample will influence the thermophysical properties observed in TGA-DSC, explaining the

divergence of onset temperature of dehydration and dehydration enthalpy from the product of the mechanochemical pathway.

2.1.6 2-methyl calcium terephthalate n-hydrate

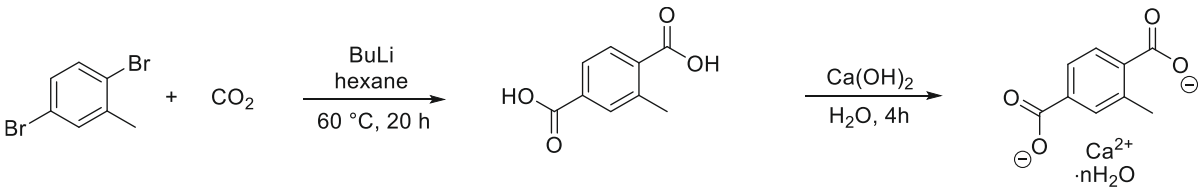

5b

5b was prepared in two steps. At first 2,5-dibromtoluene and BuLi were heated in hexane for 20 h. Pouring the solution on dry ice in diethyl ether and acidification with HCl gave 2-methyl terephthalic acid as a brown powder. The formation of the intermediate was confirmed by ^{1}H NMR spectroscopy. **5b** was prepared by milling the previously prepared 2-methyl terephthalic acid with calcium hydroxide as calcium source in a ball mill. After milling for 4 h the product was obtained as a white powder. Product formation was monitored via IR-spectroscopy.

2.1.7 2-fluoro calcium terephthalate trihydrate

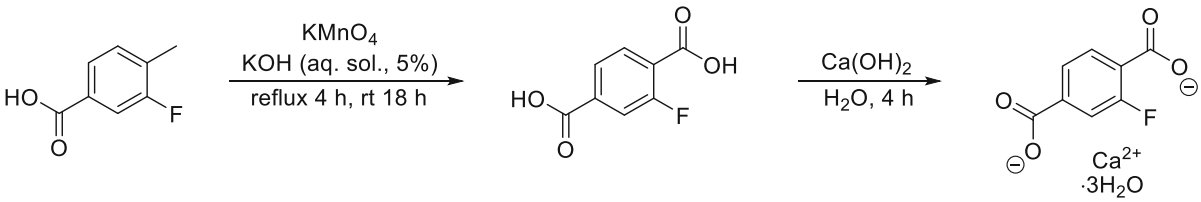

5c

5c was prepared in two steps. At first 3-fluoro-4-methylbenzoic acid was refluxed in 5 % aqueous KOH solution with $KMnO_4$ for 4 h and then stirred at rt for another 18 h. Acidification with HCl gave 2-fluoro terephthalic acid as a white powder. The formation of the intermediate was confirmed by ^{1}H NMR spectroscopy. **5c** was prepared by milling the previously prepared 2-fluoro terephthalic acid with calcium hydroxide as calcium source in a ball mill. After milling for 4 h the product was obtained as a white powder. Product formation was monitored via IR-spectroscopy.

2.1.8 2-chloro calcium terephthalate n-hydrate

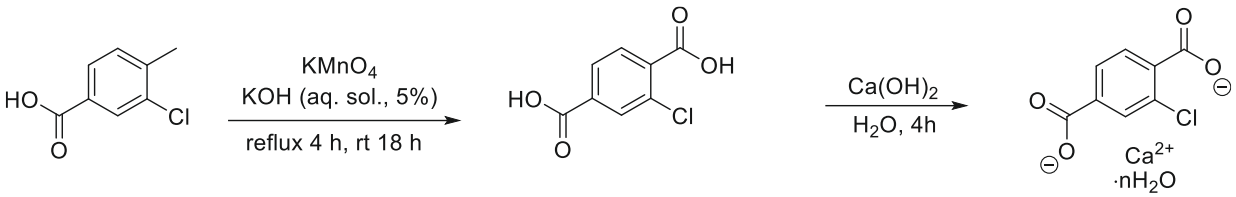

5d

5d was prepared in two steps. At first 3-chloro-4-methylbenzoic acid was refluxed in 5 % aqueous KOH solution with $KMnO_4$ for 4 h and then stirred at room temperature for another 18 h. Acidification with HCl gave 2-chloro terephthalic acid as a white powder. The formation of the intermediate was confirmed by ^1H NMR spectroscopy. **5d** was prepared by milling the previously prepared 2-chloro terephthalic acid with calcium hydroxide as calcium source in a ball mill. After milling for 4 h the product was obtained as a white powder. Product formation was monitored via IR-spectroscopy.

2.1.9 Tetrafluoro calcium terephthalate n-hydrate

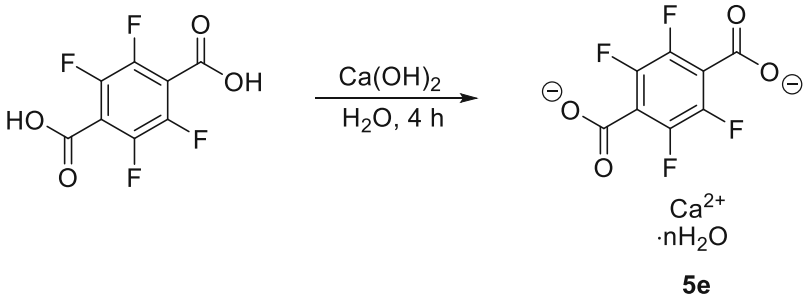

5e

5e was prepared by milling tetrafluoro terephthalic acid with calcium hydroxide as calcium source in a ball mill. After milling for 4 h the product was obtained as a white powder. Product formation was monitored via IR-spectroscopy.

2.1.10 Tetrachloro calcium terephthalate tetrahydrate

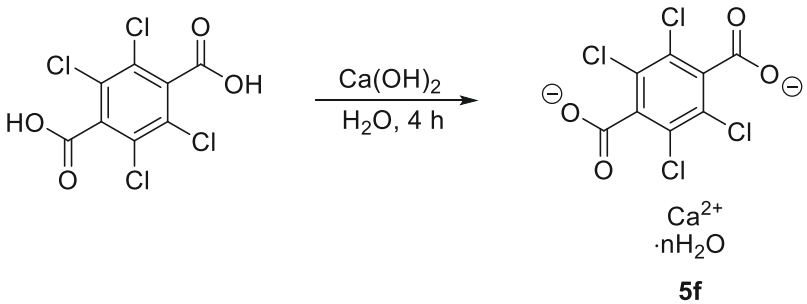

5f

5f was prepared by milling tetrachloro terephthalic acid with calcium hydroxide as calcium source in a ball mill. After milling for 4 h the product was obtained as a white powder. Product formation was monitored via IR-spectroscopy.

2.1.11 Cyclopropane-1,1-dicarboxylic acid calcium salt n-hydrate

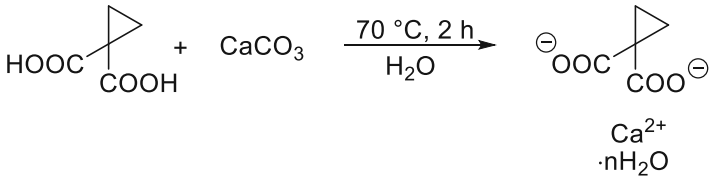

6

The product (**6**) was obtained by reaction of 1,1-cyclopropane-dicarboxylic acid with calcium carbonate in distilled water. After CO_2 formation was completed, a white precipitate was formed, that could be isolated as white powder. Product formation was monitored by IR-spectroscopy.

2.2 Single crystal growth for X-ray analysis

2.2.1 2-fluoro calcium terephthalate trihydrate

Two different approaches were tried to grow single crystals in a quality suitable for structural identification via single crystal XRD. Since 2-fluoro calcium terephthalate trihydrate is insoluble in water, a crystallization approach by dissolving the component and evaporating the solvent is not available. Since it is important to get a single crystal of the trihydrate, it is not possible to search for other possible solvents to carry out this technique. However, the disodium salt of 2-fluoro terephthalate can easily be dissolved in water.

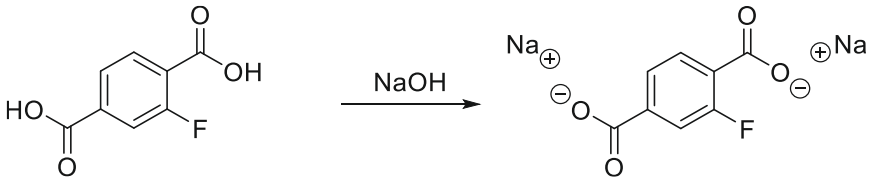

The 2-fluoro terephthalic acid disodium salt was obtained by dissolving 2-fluoro terephthalic acid to a solution of NaOH in water. Stirring and pouring the reaction mixture on cold acetone gave a white precipitate. After filtration, several washing steps and drying the product could be obtained as a white/slightly yellow powder.

2.2.1.1 Approach 1: Reaction and evaporation

The first approach was to form suitable single crystals by reaction of 2-fluoro terephthalic acid disodium salt with $CaCl_2$ as calcium source following the procedure proposed by [63].

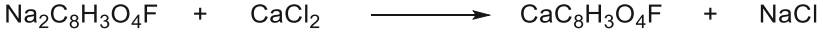

Aqueous solutions of $CaCl_2$ and 2-fluoro terephthalic acid disodium salt were mixed carefully, resulting in a slight turbidity. After two weeks of crystallization at room temperature, red single crystals were obtained.

*Figure 6: Single crystals of **5c** formed with approach 1*

2.2.1.2 Approach 2: Reaction and diffusion

For a slower crystallization approach a glass containment in the form of an “H” (H-tube reactor) was used for crystallization. The reactor consists of two chambers in which the two solutions can be filled. Slower crystal growth is provided by the required diffusion of the reactants through a glass frit. One chamber was filled with an aqueous solution of 2-fluoro terephthalic acid disodium salt the other one with an aqueous solution of $CaCl_2$ After seven weeks red single crystals were obtained.

Both methods led to single crystals in a quality sufficient for X-ray analysis. After a comparison under a light microscope the crystals from **approach 1** were chosen for single crystal analysis.

2.3 Characterization of calcium dicarboxylate salt hydrates with STA

To get information about the thermophysical properties STA measurements (TGA-DSC) were performed, which is also the most common technique used in literature to evaluate the performance of TCM. The investigated salts are considered as potential candidates for medium temperature heat storage (100-400 °C), ideally working in the 100 to 200 °C range. From the DSC curves an onset point of dehydration was extrapolated, representing a first impression of a possible operating temperature of the TCM. Table 1 shows the onset temperatures of dehydration in °C and the dehydration enthalpies (ΔH_{deh}) in J/g obtained from the DSC curves for all calcium dicarboxylate hydrates.

Table 1: STA data of calcium dicarboxylate hydrates

Substance	Number	Onset temperature of dehydration in °C	ΔH_{deh} in J/g
Ca-oxalate monohydrate	1	156	489
Ca-malonate dihydrate	2	127	637
Ca-succinate monohydrate	3	166	314
Ca-glutarate monohydrate	4	145	418
Ca-terephthalate trihydrate	5a	104	695
2-methyl Ca-terephthalate n-hydrate	5b	93	220
2-fluoro Ca-terephthalate trihydrate	5c	126	483
2-chloro Ca-terephthalate n-hydrate	5d	*	*
Tetrafluoro Ca-terephthalate n-hydrate	5e	99	657
Tetrachloro Ca-terephthalate n-hydrate	5f	*	*
Cyclopropane-1,1-dicarboxylic acid calcium salt n-hydrate	6	*	*

* *No valid data obtained by STA measurements*

This first characterization regarding the thermophysical properties of the calcium salts gives numerous interesting insights. At first it can be noted that all measured onset temperatures of dehydration lie in the temperature interval 100-200 °C, indicating that, theoretically, all of the investigated salts are applicable for medium temperature heat storage. Secondly, neither for onset temperature, nor for enthalpy of dehydration a linear trend in respect to the chain length between the two carboxylate groups is observable.

Three salts (**2**, **5a** and **5e**) show higher enthalpies of dehydration than Ca-oxalate. While it is not documented in literature how many moles of hydrate water tetrafluoro calcium terephthalate (**5e**) holds, the other two form higher hydrates than the oxalate. Calcium malonate forms a dihydrate, calcium terephthalate a trihydrate. Figure 7 shows the TG (red) and the DSC (blue) curves of **2**. The curves indicate a loss in slight steps with first mass loss of 7.5 % and a second one of 10.4 % following subsequently adding up to 17.9 % mass loss, indicating a loss of 1.72 moles of hydrate water. In theory a full dehydration of pure calcium malonate dihydrate should result in a mass loss of 20.2 %. Published thermal analysis have

shown that full dehydration of **2** is possible effortlessly [51, 64, 65]. The total energy corresponding to both dehydration steps is 637 J/g.

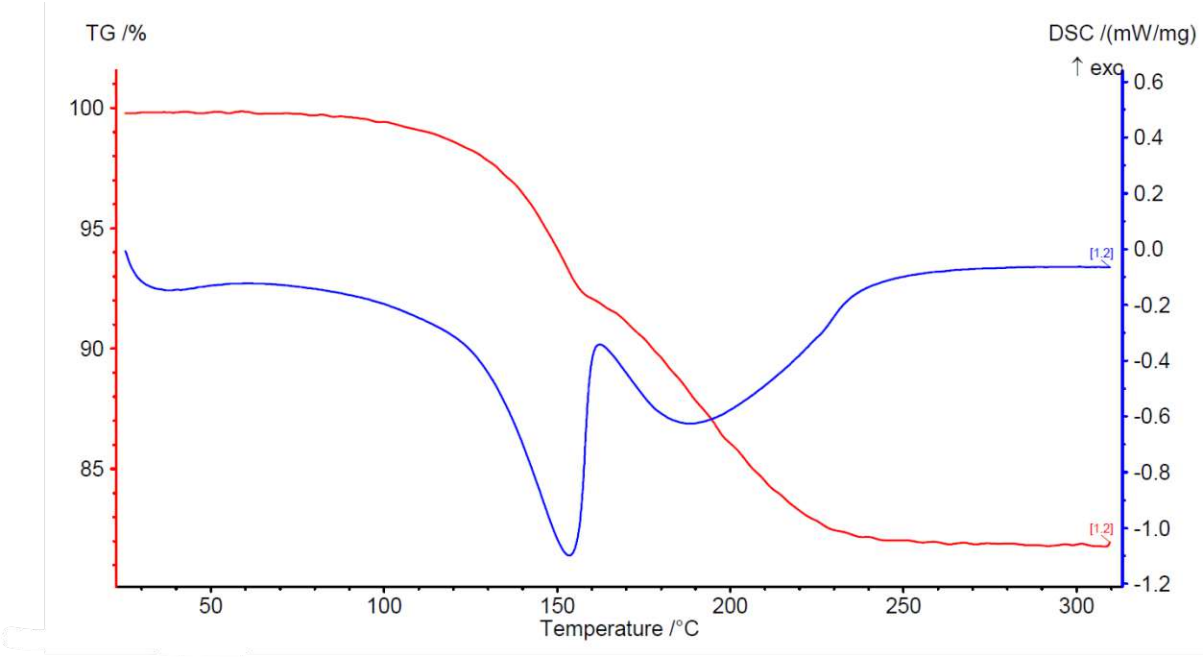

*Figure 7: DSC-TGA curve of **2***

Figure 8 shows the TGA-DSC curves of Ca-terephthalate trihydrate. The red TG-curve shows the stepless loss of three hydrate water molecules with a mass change of -20.1 % being in good correlation with a theoretically possible mass loss of 20.9 %. The blue curve represents the DSC signal, with a prominent endothermic peak coming from the dehydration process. Integration of the peak area gave 659 J/g for ΔH_{deh}.

In Table 1 for three TCMs no results could be given (**5d**, **5f**, **6**). The chlorinated derivatives (**5d**, **5f**) have shown an almost linear mass loss in the TG signal. It was not possible to extrapolate meaningful enthalpy values from the DSC signals. The measurements can be found in the appendix (Figure 29, Figure 30, and Figure 32). Cyclopropane-1,1-dicarboxylic acid calcium salt n-hydrate gave TG and DSC curves that were not to be analyzed. Potentially, different measurement conditions could result in obtaining meaningful data. A representative comparison of the calcium dicarboxylate salt hydrates demands identical analysis conditions, which is why no other data of the three components are included in this work.

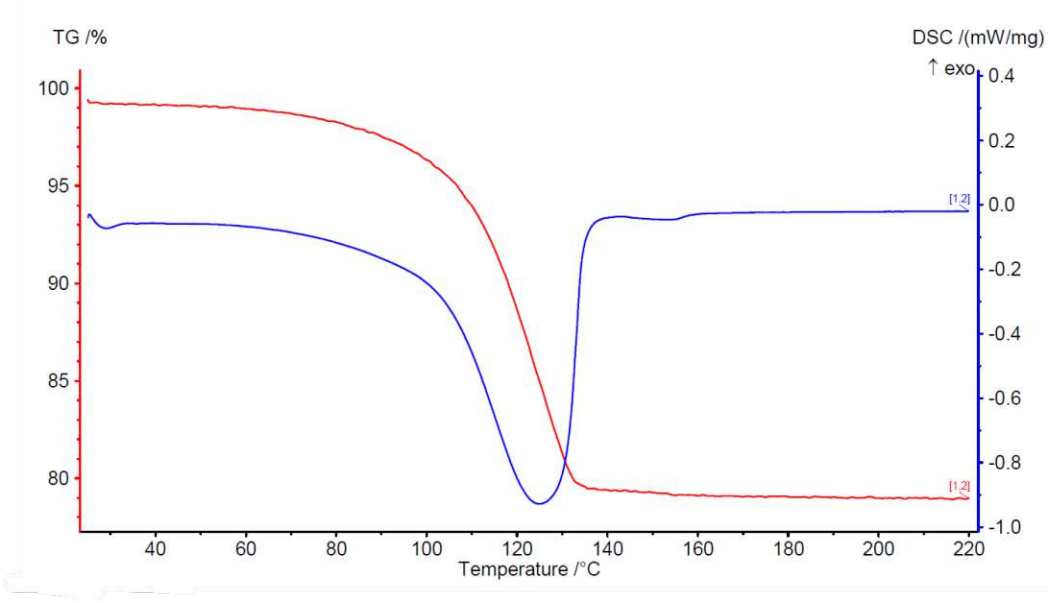

*Figure 8: DSC-TGA curve of **5a***

The results of the characterization of the calcium dicarboxylate hydrates via STA match the thermodynamical expectations. It can be concluded from eq. 1.12 that the enthalpy of dehydration must increase with the moles of crystal water molecules per mole of salt, due to the contribution of latent heat of vaporization.

2.3.1 Enthalpy values calculation and comparison

The measured dehydration enthalpies can give a direct impression of the storage potential for each salt. To enable a better comparison of the investigated calcium salt hydrates, the enthalpies measured via DSC were transformed into the corresponding molar enthalpies of dehydration Δh_{deh} in kJ/mol of hydrated TCM. In order to identify the storage potential of a salt hydrate it is advisable to consider the contributions of the required phase transition of crystal water. In equation 2.1 the molar enthalpy of dehydration Δh_{deh} is diminished by the energy required for the evaporation process Δh_e multiplied by the number of hydrate water molecules n. The energy required for the evaporation process Δh_e is built up by two parts. Δh_v represents the latent part corresponding to the vaporization enthalpy of water at the temperature T_2. If the evaporator temperature T_2 is higher than the water storage temperature T_1, sensible heat contributions need to be considered.

$$\Delta h_{net} = \Delta h_{deh} - n \cdot \Delta h_e$$

2.1

$$\Delta h_e = \Delta h_v + \int_{T_1}^{T_2} c_p \, dT$$

2.2

The Δh_{net} values show the TCMs contribution to the dehydration enthalpy. According to [66] the specific enthalpy of vaporization for water is 2441.7 kJ/kg at 25 °C (43.99 kJ/mol) and 2256.4 kJ/kg at 100 °C (40.65 kJ/mol). It is obvious that the storage temperature of water has a direct influence on the total enthalpy value related to the whole reaction. Table 2 shows the specific enthalpies of dehydration calculated with the ideal theoretical values for moles of crystal water, assuming full dehydration. Furthermore, net storage enthalpies, calculated for $T_1 = T_2 = 25$ °C (Δh_{net_25}) are included. Δh_{net_25} represents a rehydration at room temperature. It is only possible to calculate the theoretical values for compounds with an unambiguous crystal structure since the moles of crystal water per mole of hydrated salt needs to be considered. **5c** could be included since a structural analysis via single crystal XRD led to the insight of **5c** forming a trihydrate. Details about the crystal structure can be found in chapter 2.7. The enthalpies were calculated according to eq. 2.1, however, referring to [6, 44] the contributions of sensible heat were neglected.

Table 2: Theoretical enthalpies of the calcium dicarboxylates

TCM	Moles of crystal water	Δh_{deh}	Δh_{deh}/n H_2O	Δh_{net_25}
		kJ/mol	kJ/mol H_2O	kJ/mol
1	1	71.44	71.44	27.45
2	2	113.47	56.74	25.49
3	1	54.69	54.69	10.70
4	1	78.72	78.72	34.73
5a	3	179.38	59.79	47.41
5c	3	133.38	44.64	1.94

Table 3: Enthalpies of the calcium dicarboxylates calculated with TGA-DSC data

TCM	Moles of crystal water	Moles of water lost in TGA	Δh_{deh}	Δh_{deh} /n H_2O	Δh_{net_25}
			kJ/mol	kJ/mol H_2O	kJ/mol
1	1	0.99	71.33	72.20	27.87
2	2	1.72	110.26	64.10	34.59
3	1	0.98	54.60	55.46	11.29
4	1	1.35	81.36	60.29	21.99
5a	3	2.85	177.52	62.26	52.09
5c	3	2.29	127.73	34.65	27.00
5e	4	3.65	224.66	61.55	64.10

2.4 In-situ PXRD measurements

The rehydration process is a crucial step in a TCES system and often the limiting factor. Ideally rehydration is, like dehydration, studied with a combined TGA-DSC device equipped with a water vapor generator. Unfortunately, within the timeframe of this work it was not possible to get access to a STA suitable for rehydration measurements.

De- and rehydration measurements were performed using an Anton Paar XRK 900 reaction chamber. The reactions were monitored by collecting powder X-ray diffractograms. For the dehydration measurements, isothermal conditions were applied with $T_{deh} = T_{onset} + 10$ °C. T_{onset} corresponds to the onset temperature of dehydration observed in the STA experiments.

2.4.1 Ca-malonate dihydrate

Calcium malonate dihydrate was measured for two cycles. A first cycle of de- and rehydration could be investigated successfully. Figure 9 shows the diffraction patterns of **2** after dehydration. In the second dehydration, numerous reflections of the hydrate pattern remain present, indicating that a quantitative dehydration in the second cycle was not achieved. Figure 10 shows the corresponding rehydration measurements, compared to Ca-malonate dihydrate after preparation.

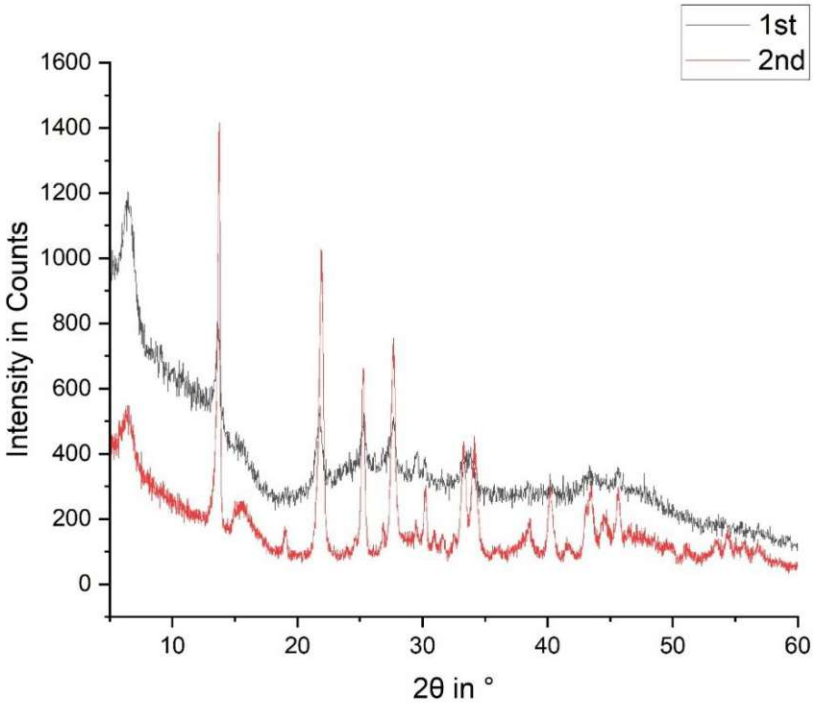

*Figure 9: Diffraction patterns after dehydration of **2** performed for two cycles*

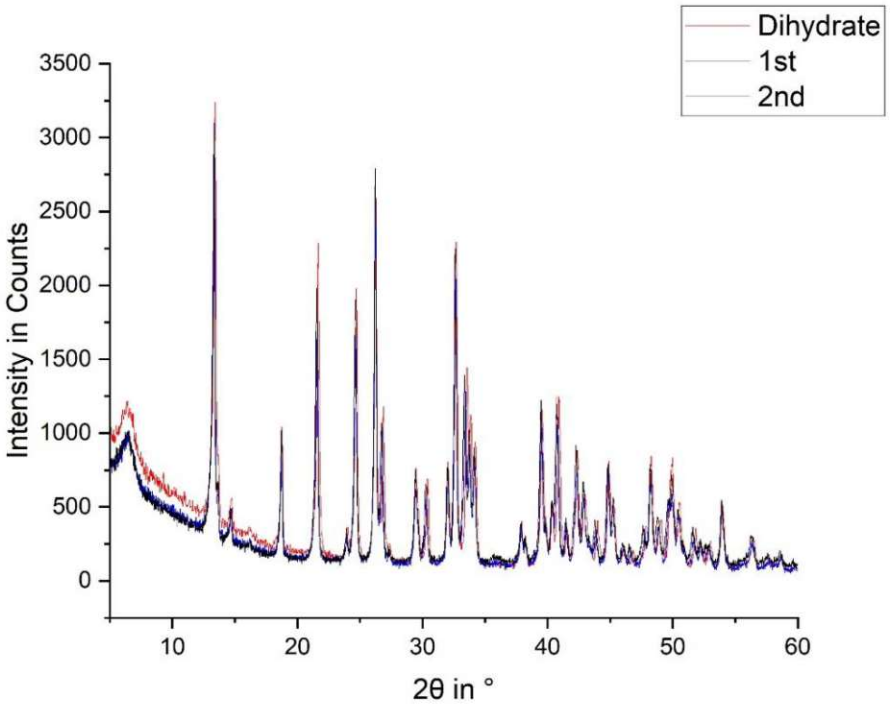

*Figure 10: Diffraction patterns of prepared **2** (red) and after rehydration performed for two cycles*

2.4.2 Ca-terephthalate trihydrate

De- and rehydration of Ca-terephthalate trihydrate were successful. The corresponding diffractograms can be found in the appendix. Furthermore, three full cycles were investigated, starting from the trihydrate. Figure 12 shows three diffraction patterns collected from dehydration measurements Figure 13 shows the corresponding rehydration measurements. The shift in the background occurs due to sample loss within every measurement cycle. This loss is inevitable due to the reaction chamber construction. After each hydration measurement the chamber has to be flushed with gas again, blowing out some sample. After the 3rd rehydration the remaining sample amount was too low to continue. The crystal structure of calcium terephthalate anhydrate is not documented in literature, also a powder diffraction pattern is not available. To confirm that the anhydrous diffraction pattern is obtained from a fully dehydrated sample, the IR spectra of the fully hydrated and the anhydrous state were measured (Figure 11). The red curve shows a prominent, broad absorption band at 3600-2900 cm^{-1} from OH stretching vibrations of the bound water molecules. The broadening is an effect of H-bonds. In the spectrum of anhydrous **5a** no bands occur in this region, confirming a full dehydration of the sample.

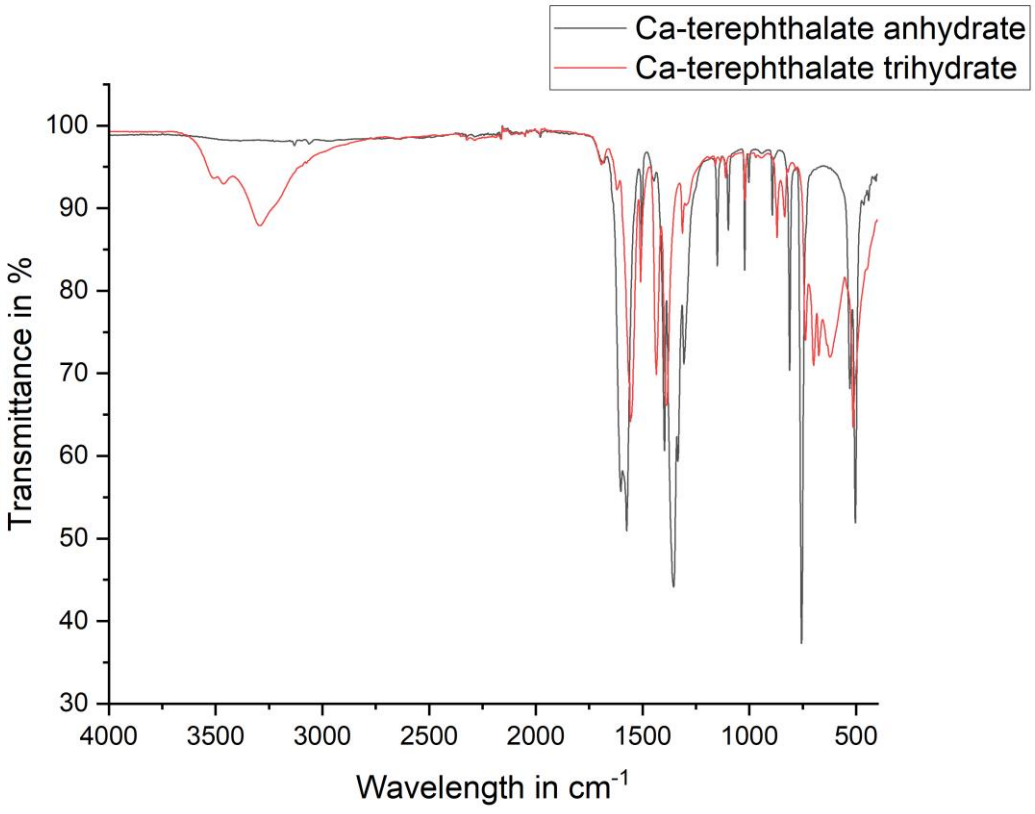

*Figure 11: FTIR spectra of **5a** trihydrate (red) and anhydrate (black)*

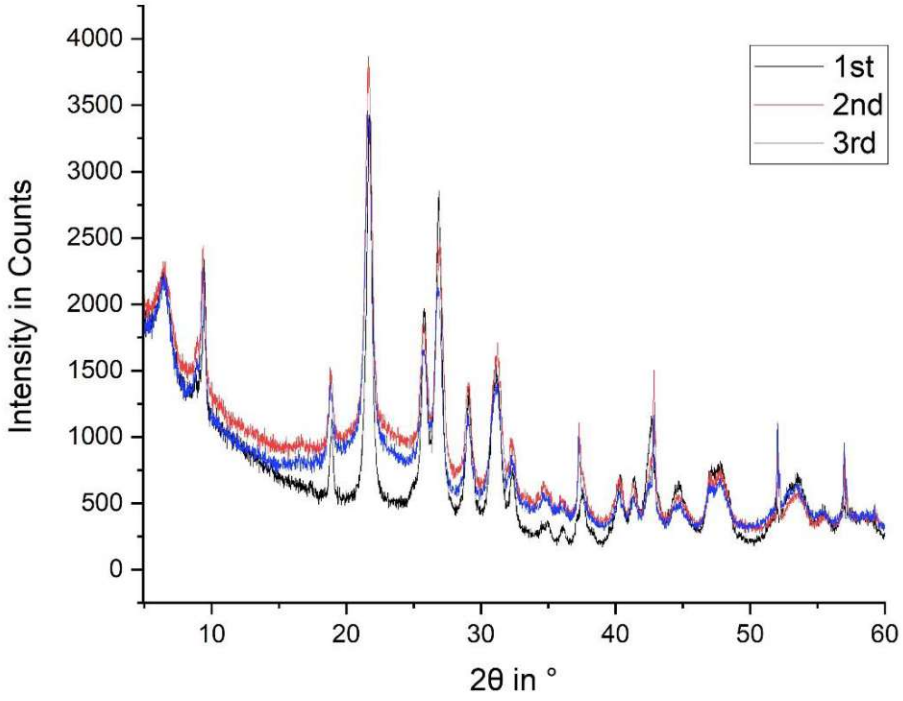

*Figure 12: Diffraction paterns of **5a** after three cycles of dehydration*

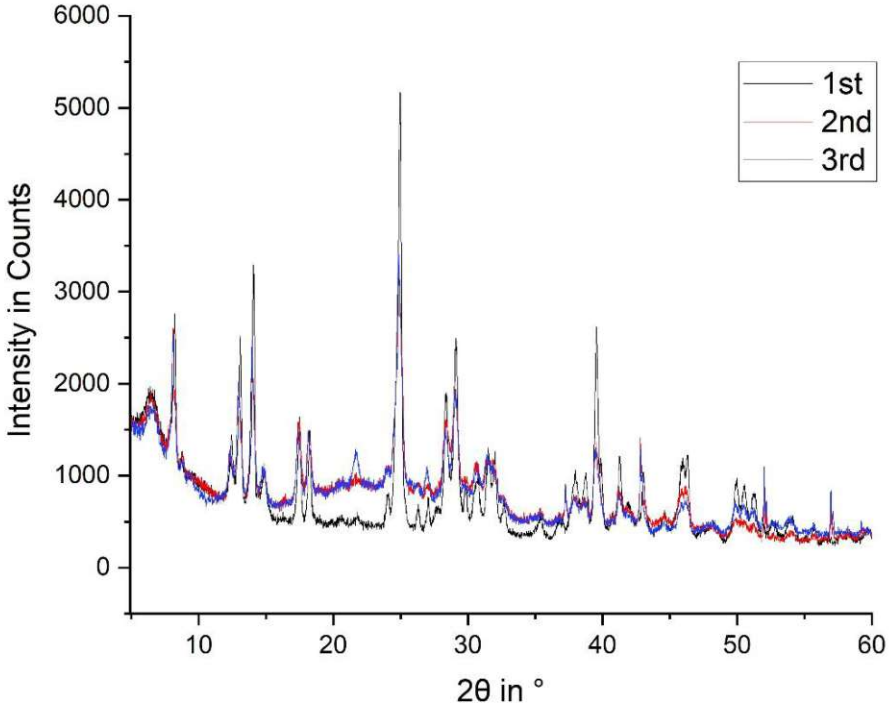

*Figure 13: Diffraction paterns of **5a** after three cycles of rehydration*

2.4.3 2-fluoro Ca-terephthalate trihydrate

The diffraction patterns of the salt after preparation and the rehydrated salt are displayed in Figure 14. Figure 15 shows the diffraction pattern of the anhydrate. A comparison of the diffraction patterns from the initial hydrate and the rehydrated compound indicates that full rehydration was achieved.

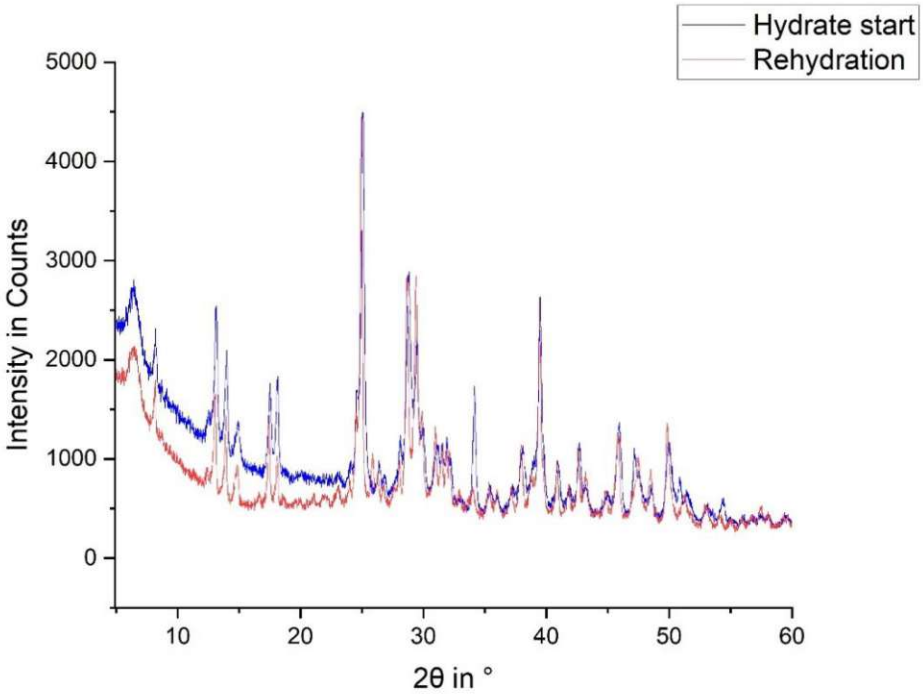

Figure 14: Hydrate and rehydrated diffraction patterns of **5c**

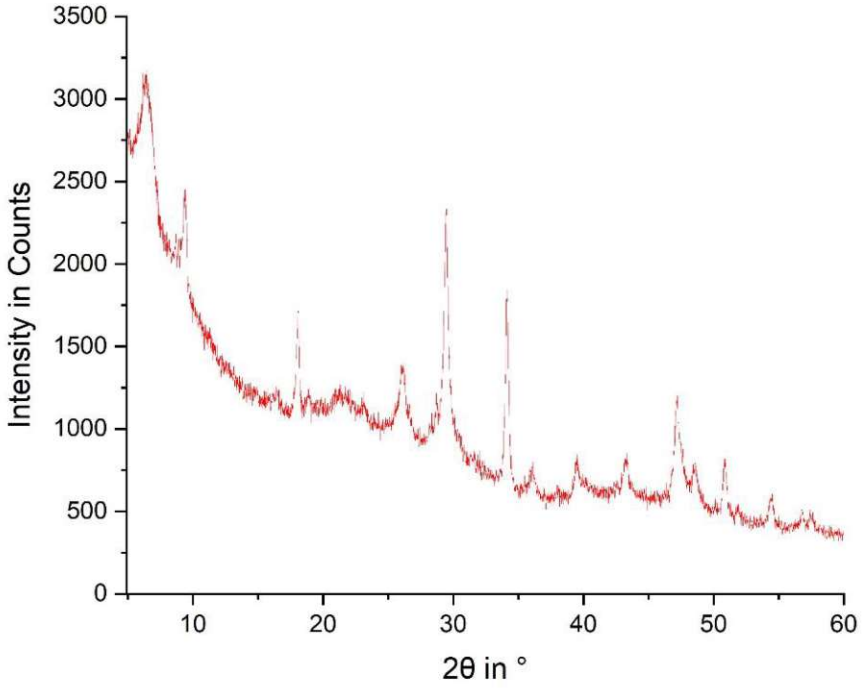

*Figure 15: Diffraction pattern of anhydrous **5c***

2.4.4 Tetrafluoro calcium terephthalate tetrahydrate

Figure 16 shows the diffractograms of the initial salt in its hydrated form and the rehydrated salt. Figure 17 shows the diffraction pattern of the anhydrate. A comparison of the diffraction patterns from the initial hydrate and the rehydrated salt indicates that a full rehydration was achieved.

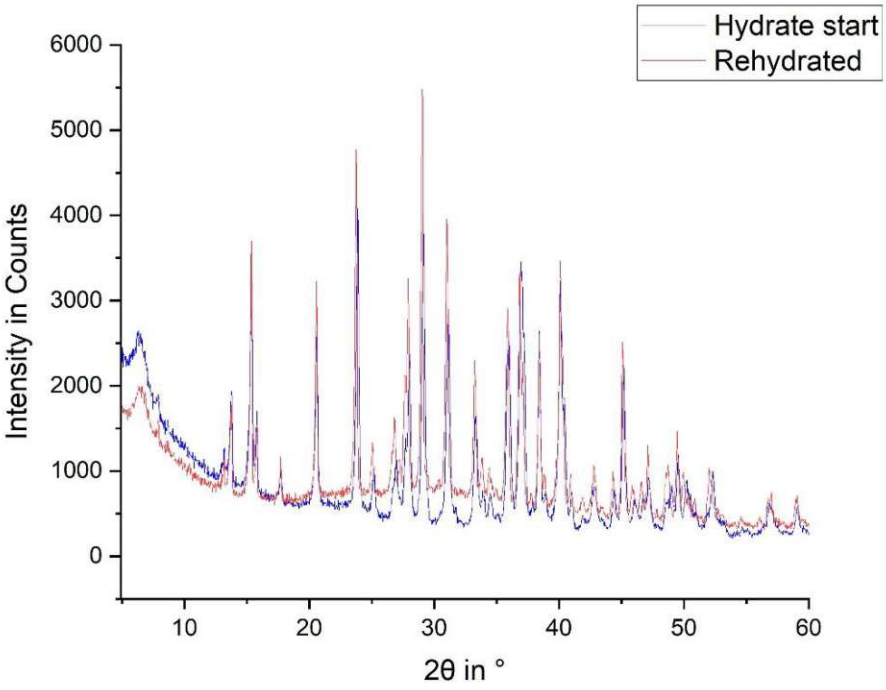

Figure 16: Hydrate and rehydrated salt diffraction patterns of **5e**

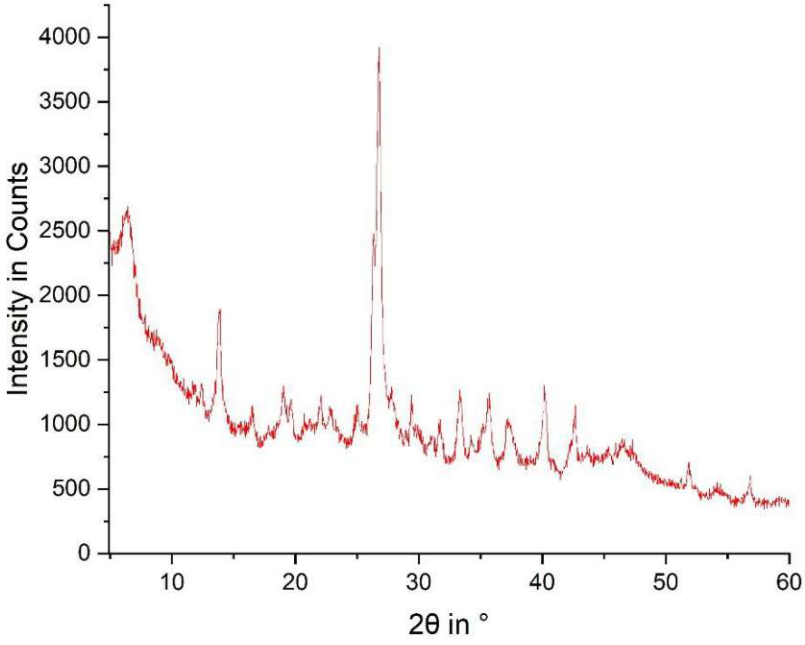

*Figure 17: Diffraction pattern of anhydrous **5e***

2.5 Ettringite

Ettringite was prepared following the proposed conversion scheme based on solutions referenced in literature [67]. The main conversion process is expressed by the following reaction:

$$Al_2(SO_4)_3 \cdot 18\ H_2O + 6\ Ca(OH)_2 + 8\ H_2O \longrightarrow Ca_6Al_2(SO_4)_3(OH)_{12} \cdot 26\ H_2O$$

A saturated $Ca(OH)_2$ suspension was prepared and after cooling in a fridge a solution of aluminum sulfate octadecahydrate was added. After stirring at room temperature, a slow evaporation of the solvent at 4 °C allowed a slow and pure ettringite crystallization. After final washing steps with water and ethanol the product was isolated as a white powder. Product formation as well as phase purity were confirmed with PXRD. With this method it is possible to prepare ettringite with a purity of 98.5 % ettringite and 1.5 % calcium sulfate impurities. Figure 18 shows a measured powder X-ray diffraction pattern, Figure 51 shows the result of a quantitative phase analysis via the Rietveld refinement method.

This synthesis is the outcome of several optimization steps. Typically, such a standard procedure requires a glovebox to create the most reproducible environment for ettringite growth. Since glovebox access is not possible for aqueous reactions at our university facilities, a preparation procedure outside a glovebox had to be established.
Calcinating the required CaO freshly prior to the synthesis provides a big impact in achieving higher phase purity of the product. Adding aluminum sulfate octadecahydrate to a heated $Ca(OH)_2$ suspension either as solid or as aqueous solution, or generally heating the reaction mixture as proposed in [68] has turned out to result in higher impurities.

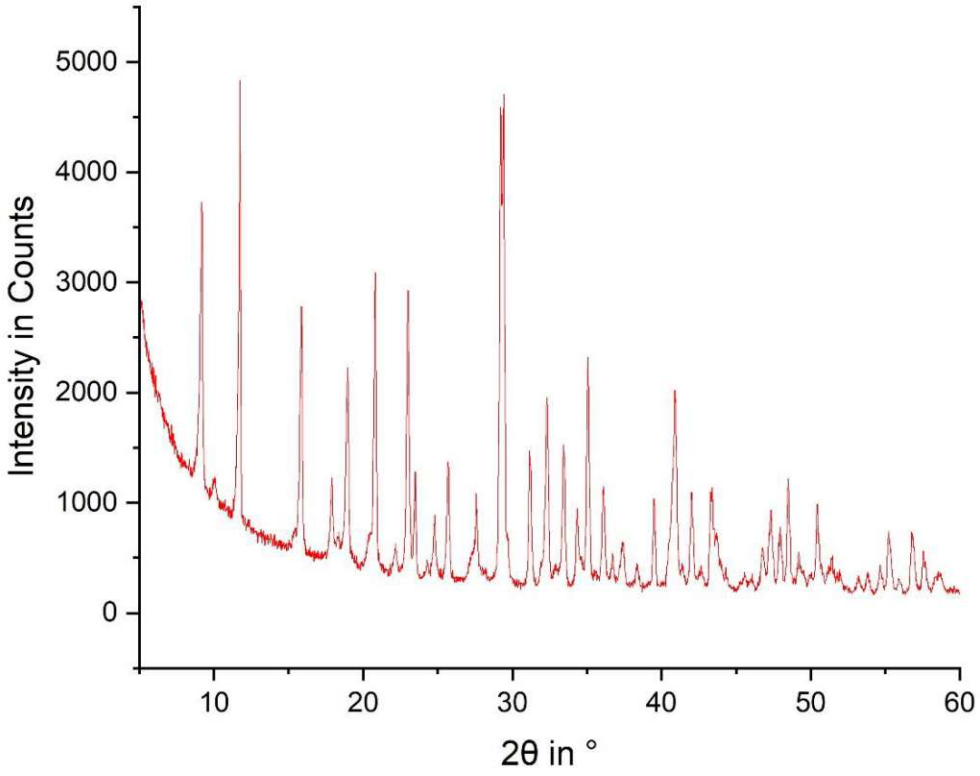

Figure 18: PXRD of ettringite

2.5.1 Negative synthetic approaches for ettringite

This part gives a brief overview over preparation methods for ettringite that, in our hands, did not lead to the desired product or to a product of insufficient purity.

1st approach

A $Ca(OH)_2$ suspension obtained by CaO hydration was heated in a beaker until boiling. Addition of $Al_2(SO_4)_3 \cdot 18\ H_2O$ (180 g, 270 mmol) under stirring, heating for 2 h and solvent evaporation in a refrigerator gave a white, brittle solid that was ground, washed once with cold water and dried at 40 °C in vacuo. PXRD indicated that no phases from ettringite were present in the samples measured.

2nd approach

A $Ca(OH)_2$ suspension obtained by CaO hydration was heated in a beaker until boiling. Addition of $Al_2(SO_4)_3 \cdot 18\ H_2O$ (180 g, 270 mmol) under stirring, heating for 2 h and storing the mixture at 400 mbar in Ar-atmosphere. Freshly refluxed H_2O was used for all steps. PXRD indicated that no phases from ettringite were present in the samples measured.

2.5.2 STA measurements

The DSC and TG curves for ettringite are shown in Figure 19. The TG signal shows a mass loss of 27.5 % with an onset temperature of 92.4 °C. The corresponding enthalpy of dehydration is 553.3 J/g. The observed mass loss indicates a loss of 19.16 moles of water. Based on TGA Perkins et al. [68] observed a dehydration in four steps. The first and major loss of about 23 moles of hydrate water (33 % mass loss) occurs between 40 and 180 °C, 3 moles lost between 200-280 °C, three between 280 and 500 °C and a mass loss of around 2.5 moles of water between 600 to 900 °C. Assuming a full dehydration this would add up to 31.5 moles of hydrate water. Synthesized ettringite can hold up to 32 moles of hydrate water [67], a full dehydration can even require temperatures up to 1000 °C [69].

The synthesized ettringite was characterized from 25 to 220 °C showing good correlation with literature data, however, only a loss of 19.16 moles of water could be observed in the investigated temperature interval. Perkins et al. [68] state that the water lost in the 40 to 180 °C temperature interval, is mostly the loosely bound water. It is possible that a small amount of water was lost undetected (in the drying process or prior to the start of the measurement). Also, the present calcium sulphate impurity can affect the dehydration.

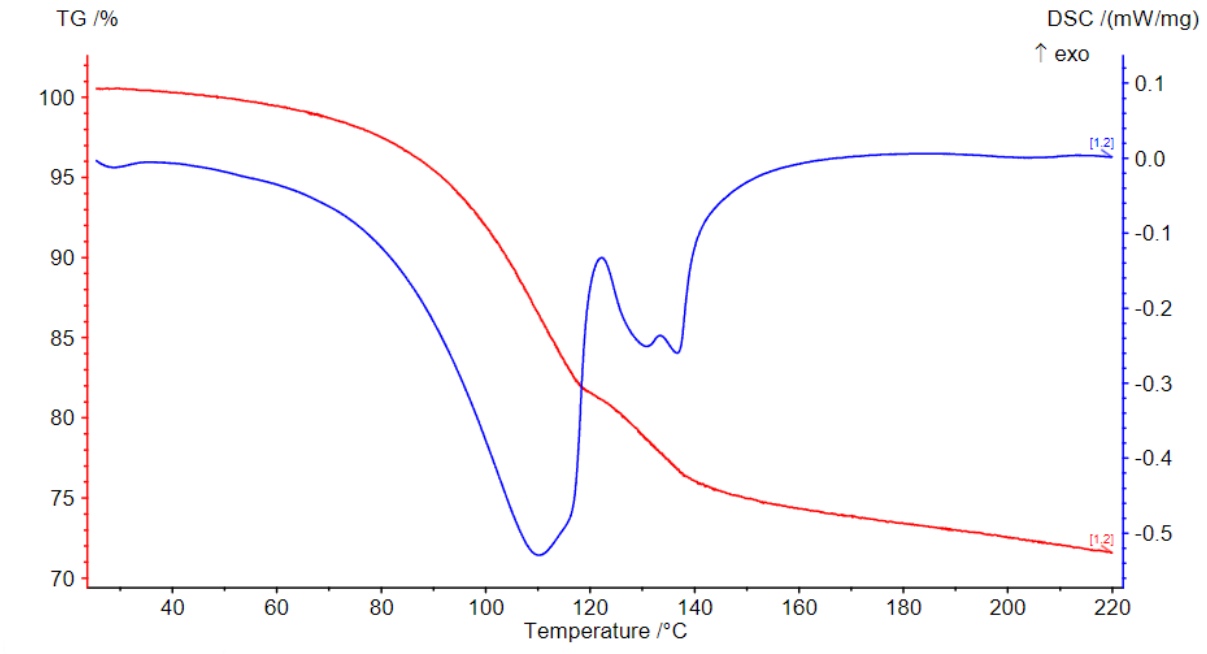

Figure 19: Measured STA curve of ettringite

2.6 Ca-oxalate monohydrate synthesis comparison

It was specifically requested by a project partner to investigate the synthesis of Ca-oxalate monohydrate via the mechanochemical pathway, that was also applied for Ca-glutarate monohydrate and all Ca-terephthalate hydrates. The synthetic details can be found in chapters 2.1.1 and 3.2. Relevant data collected via STA is displayed in Table 4. For purchased **1** TG-

analysis shows a mass loss of 12.2 % being in good correlation with the theoretically possible value of 12.3 %. For the product of the mechanochemical preparation method, a mass loss of 12.6 % was observed. The two DSC curves (Figure 21) both show an endothermic peak with the peak maximum slightly shifted. For purchased **1** the maximum is at 197 °C, for the synthesized compound at 180 °C. The two peak areas, and the corresponding enthalpies of dehydration correlate well. The two onset temperatures of dehydration are the same.

Table 4: STA data of purchased and synthesized Ca-oxalate monohydrate

	Ca-oxalate monohydrate, purchased	**Ca-oxalate monohydrate, synthesized**
Mass loss	12.2 %	12.6 %
ΔH_{deh}	464 J/g	489 J/g
Peak max. (DSC)	180 °C	197 °C
Onset temperature of dehydration	156 °C	156 °C

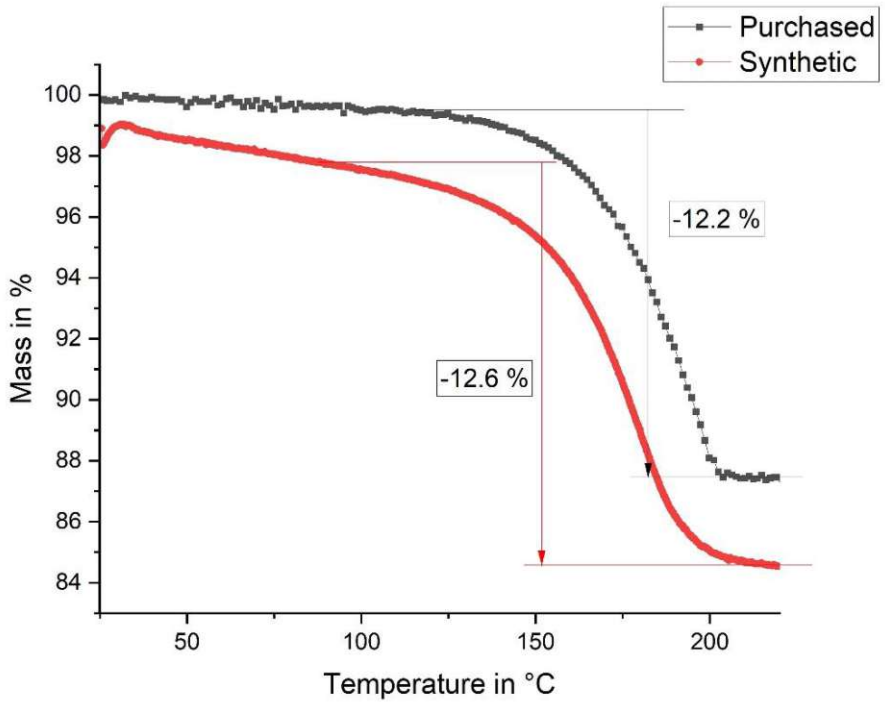

Figure 20: TGA curves of purchased Ca-oxalate monohydrate (black) and prepared (red)

Figure 22 shows the IR-spectra of purchased and prepared Ca-oxalate monohydrate. Although that for the synthesized compound some bands show lower intensity than for the purchased one, it is clearly visible that the spectra are coming from chemically identical compounds.

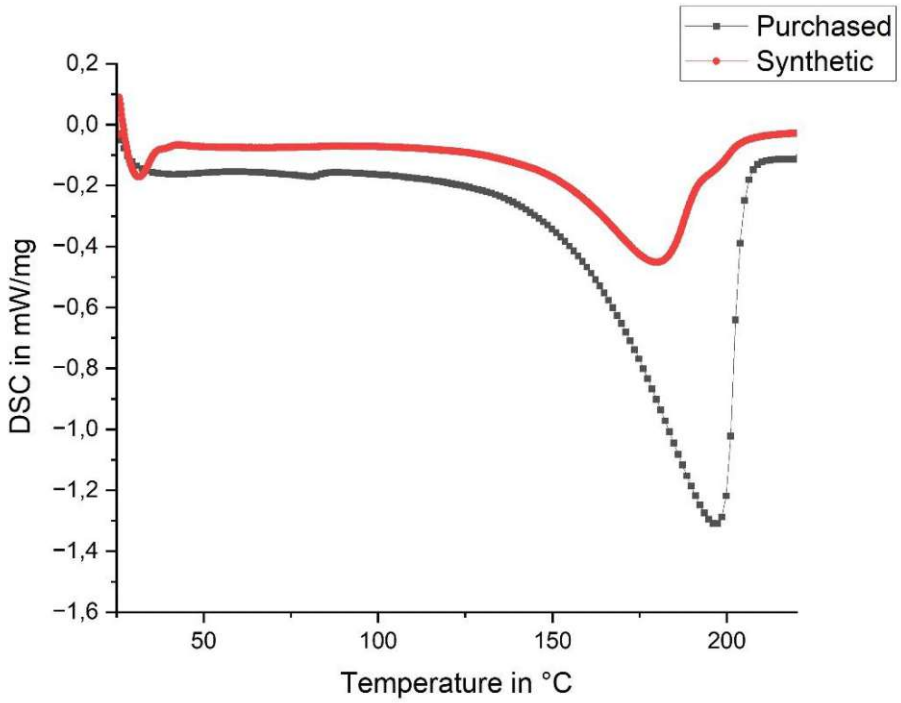

Figure 21: DSC curves of purchased Ca-oxalate monohydrate (black) and prepared (red)

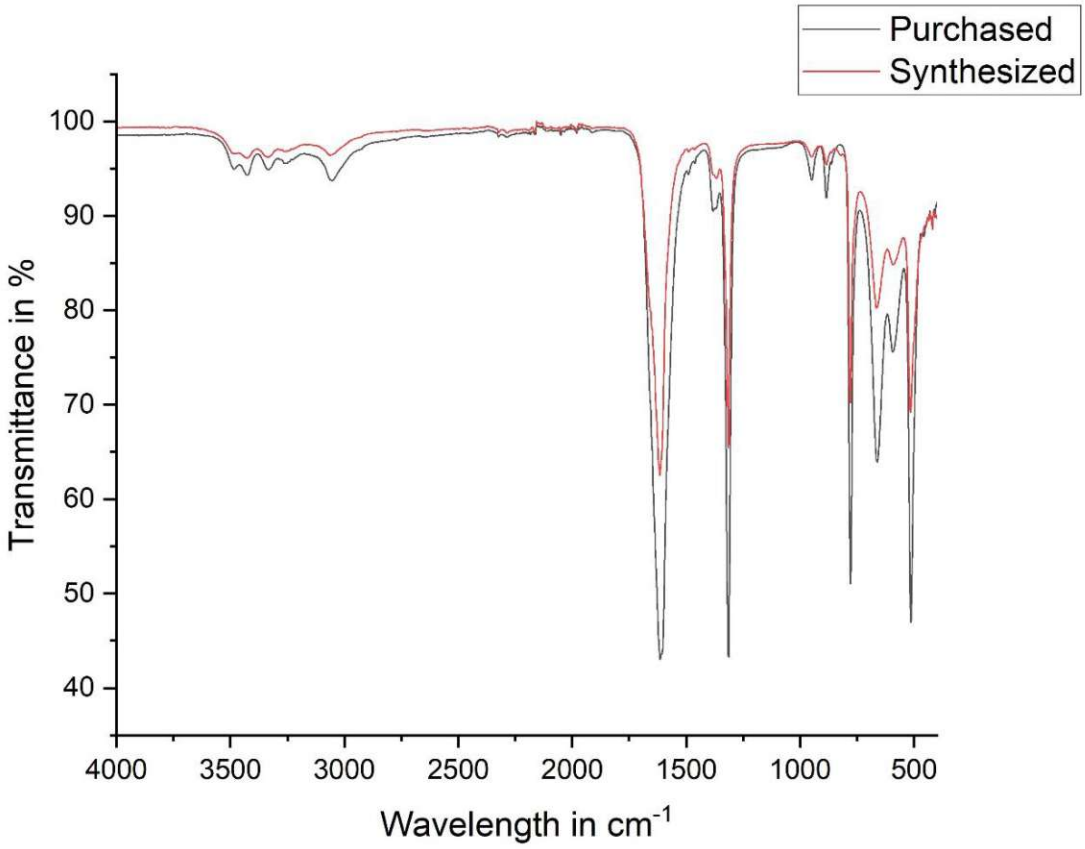

Figure 22: FTIR spectra of purchased (black) and prepared (red) ***1***

2.7 Crystal structure identification of 2-fluoro calcium terephthalate trihydrate

2-fluoro calcium terephthalate trihydrate crystallizes in the Pmna system (Z = 4, Z' = ½). The structure is built of infinite chains of Ca-atoms located on the the $m_{[100]}$ reflection plane, connected by monofluorinated terephthalate ions. Coordinated water molecules extend the [100] direction. Two adjacent Ca-atoms in the infinite chains are connected by a bridging water molecule on a $2_{[010]}$ rotation axis. Two more water molecules located on $m_{[100]}$ are coordinated to one Ca-atom. The measured single crystal formed a trihydrate. The infinite chains are connected by H-bonds between the water molecules and the oxygen of the non-coordinating carboxylate group.

The structure is highly related to Ca-terephthalate trihydrate [60], which is built of the same kind of infinite chains. Furthermore, a similar H-bond formation is observable.

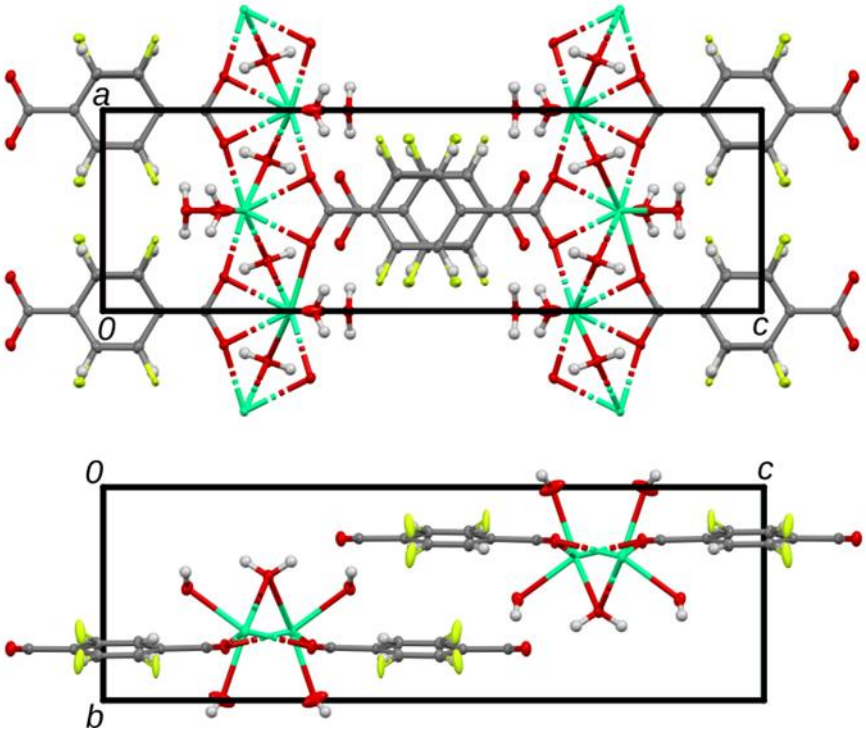

Figure 23: Crystal structure of 2-fluoro Ca-terephthalate trihydrate viewed along (top) [010] and (bottom) [100]. Ca (green), F (yellow), O (red) and C (grey) atoms are represented by ellipsoids drawn at the 50% probability levels, H atoms by spheres of arbitrary radius.

The monofluorinated-para-phenylene moiety is disoriented around the $m_{[100]}$ reflection plane of the Pmna space group (Figure 23). In addition, the F-atom is disoriented itself, with possible locations at three out of the four crystallographic C-atom positions.

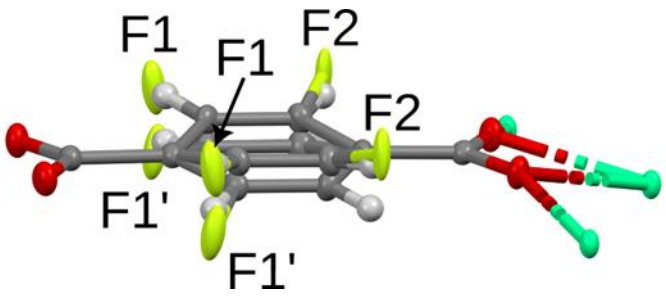

Figure 24: The mono-F-terephthalate molecule and coordinating Ca atoms. Colors as in Figure 23

2.8 Final conclusion and outlook

As described in the introduction the major goal of this work was to investigate calcium dicarboxylic acid salt hydrates regarding their potential as thermochemical materials. On this behalf, a library of eleven salts was characterized. Ten of the salts were synthesized successfully with facile synthetic procedures, easy to reproduce. Due to previous investigations in our group calcium oxalate monohydrate was used as reference material. A first characterization via thermal analysis indicated several interesting candidates (especially **2**, **5a**, **5e**) amongst the calcium salt hydrates. To extend the characterization of the candidates, powder diffractograms of the hydrated and dehydrated compounds were collected and SEM pictures of both states were recorded. To study the de- and rehydration reactions in-situ measurements of some promising candidates (**2**, **5a**, **5c**, **5e**) were conducted, also investigating cyclability for a small number of cycles. All of these investigations led to the conclusion, that the class of calcium dicarboxylic acid salt hydrates is definitely worth screening for thermochemical materials.

To determine a correlation between chemical composition of the TCM and the tuneability of its thermophysical and thermochemical properties, the scope of this work must be expanded. As a first attempt into understanding the dehydration and hydration procedure on a more fundamental level derivatives of calcium terephthalate trihydrate were synthesized and analyzed. The crystal structure of 2-fluoro calcium terephthalate could be determined via sc-XRD.

Another goal was to optimize the preparation of ettringite. It was possible to prepare ettringite with 98.5 % phase purity confirmed by quantitative phase analysis. What is still to be optimized is the reaction time and upscaling of the reaction. At the moment the most successful procedure requires a complete evaporation of all used water, which increases with an increasing scale of the reaction. It was observed that smaller scales resulted in higher phase purities of ettringite.

Future investigations would concentrate on studying the rehydration reaction, ideally by getting access to a STA-system suitable for rehydration experiments. Furthermore, the cycle stability of the most promising salts needs to be investigated.

3 Experimental Part

3.1 General Methodology

3.1.1 Nuclear magnetic resonance spectroscopy (NMR)

All spectra were recorded in dry, deuterated solvents and evaluated with MestReNova version 14.2.0-26256.

^{1}H and ^{13}C spectra were recorded on a Bruker Avance UltraShield 400 MHz and on a Bruker DXP 200 MHz FS FT – NMR spectrometer. The NMR chemical shifts are reported in ppm; ^{1}H and ^{13}C shifts are established based on the residual solvent method.

3.1.2 X–ray powder diffraction

The powder X–ray diffraction measurements were carried out on a PANalytical X'Pert diffractometer in Bragg-Brentano geometry using Cu $K_{\alpha1,2}$ radiation and a X'Celerator linear detector with a mirror. Sample spinning with back loading zero background sample holders were used, 2θ = 5 – 60 °, T = 297 K at the X–ray Center at Vienna University of Technology in collaboration with Werner Artner. The diffractograms were evaluated by the means of PANalytical program suite HighScore Plus v5.1. A background correction and a $K_{\alpha2}$ strip were applied. If necessary, the samples were manually ground in a mortar before being measured. For the in-situ experiments an Anton Paar XRK 900 chamber was used. The sample was mounted on a hollow ceramic mount, enabling a complete perfusion of the sample with gas. The reaction chamber can be operated between 25 and 900 °C. For dehydration measurements N_2 was used with a gas flow of 0.4 L min^{-1}. The rehydration measurements were performed with water vapor, which was generated by pumping distilled water through a capillary with a HPLC pump. Before entering the reaction chamber the capillary was heated to 300 °C creating water vapor. A flow rate of 2 ml min^{-1} was used. The sample temperature was controlled by a NiCr-NiAl thermocouple.

3.1.3 Single crystal XRD

The X-ray diffraction measurements of the single crystals were carried out at the X-ray Center at Vienna University of Technology by Dr. Berthold Stöger. The measurements were performed on a STOE STADIVARI diffractometer system equipped with a Dectris Eiger CdTe hybrid photon counting detector using Cu-K_α radiation (λ = 1.54186 Å). As measurement conditions T = 100 K and a dry nitrogen environment were chosen.

3.1.4 Scanning electron microscope (SEM)

SEM images were taken on a FEI Quanta 200 F. The measurements were performed with an acceleration voltage of 5 kV and a working distance of 6-7 mm. The samples were placed on

a sample holder and coated with an 8 nm AuPd layer to ensure the required conductivity. The sputtering was performed using a Baltec Med020 Coating system.

3.1.5 Simultaneous thermal analysis (TGA-DSC)

For TGA-DSC analysis a Netzsch STA 449 F1 Jupiter® system was used. The measurements were conducted under N_2 atmosphere, with a heating rate of 2 K/min in a temperature range between 25 °C and 300 °C. For many substances a temperature range of 25 to 220 °C was sufficient. 10 – 12 mg sample masses were measured in Al_2O_3 crucibles.

3.2 Synthesis of calcium oxalate monohydrate

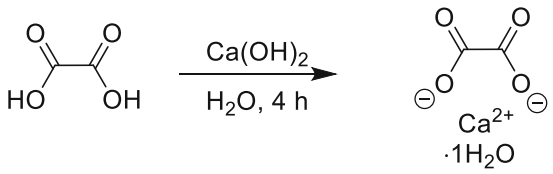

1

Oxalic acid (0.55 g, 6.11 mmol) and calcium hydroxide (0.45 g, 6.11 mmol) were put in a ball mill, 130 µl deionized water were added and milled for 4 h. The product was obtained as white powder (802 mg, 5.49 mmol, 89,63 %).

3.3 Synthesis of calcium malonate dihydrate

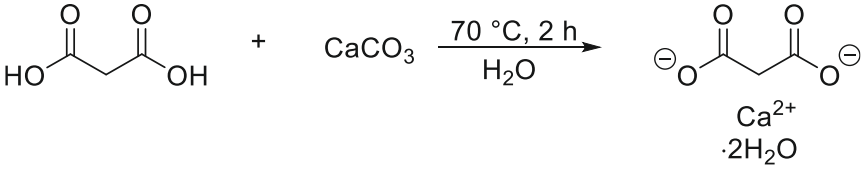

2

To a solution of malonic acid (5.2 g, 50 mmol) in 250 ml deionized water, calcium carbonate (5 g, 50 mmol) was slowly added. The reaction was stirred until no further CO_2 formation could be observed, giving a white suspension which was then heated to 70 °C for 2 h. The suspension was allowed to cool to room temperature and left over night. The white precipitate was collected by filtration, washed with deionized water twice, and dried at 40 °C in vacuo. The product was obtained as a white solid (7 g, 49.25 mmol; 98.5 %) [51].

3.4 Synthesis of calcium glutarate monohydrate

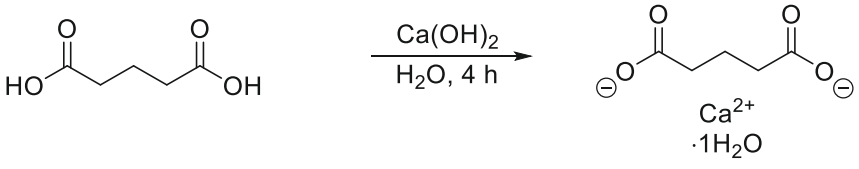

4

Glutaric acid (0.64 g, 4.8 mmol) and calcium hydroxide (0.36 g, 4.8 mmol) were put in a ball mill, 130 µl deionized water were added and milled for 4 h. The product was obtained as light brown powder (0.75 g, 4.41 mmol, 91.8 %).

3.5 Synthesis of calcium terephthalate trihydrate

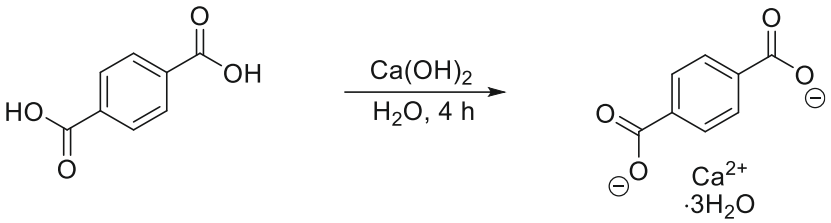

5a

Terephthalic acid (0.69 g, 4.15 mmol) and calcium hydroxide (0.31 g, 4.15 mmol) were put in a ball mill, 130 µl deionized water were added and milled for 4 h. The product was obtained as white powder (0.84 g, 4.11 mmol, 99.1 %).

3.5.1 Negative synthetic approaches for 5a

Alternative approach 1

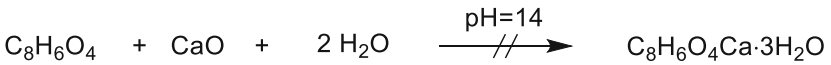

5a

Terephthalic acid (1.5 g, 9.03 mmol) was dissolved in an alkaline solution of water and NH_3 and stirred at 80 °C for 1 h. CaO (0.52 g, 9.03 mmol) was added resulting in a white turbidity, stirring and heating were continued for 30 min. After filtering the precipitate, three washing steps with water the white residue was dried over night at 85 °C.

Alternative approach 2

Terephthalic acid (1 g, 6.02 mmol) was dissolved in an alkaline solution of water and NH_3 and stirred at 80 °C for 1 h. $CaCl_2$ (0.67 g, 6.02 mmol) was added and stirred for 30 min. After filtering the precipitate, three washing steps with water the white residue was dried over night at 85 °C.

Alternative approach 3

Exact same procedure as approach 2 with reaction time elongated to 24 h, no product formation observable.

Alternative approach 4

A mixture of terephthalic acid (1.33 g, 8.01 mmol) and calcium nitrate tetrahydrate (1.89 g, 8.01 mmol) was stirred in a mixture of deionized water (20 ml) and DMF (60 ml) for 30 min at

room temperature. The solvothermal synthesis reaction was carried out in an autoclave reactor with a silicon reaction vessel (100 ml) at 150 °C for 24 h at autogenous pressure. The obtained white precipitate was washed with methanol (95 vol%) twice, filtered by centrifugation (5 min, 5000 rpm). The white solid was dried in vacuo at 50 °C, giving 1.49 g (91.1 %).

3.6 Synthesis of 2-methyl calcium terephthalate n-hydrate

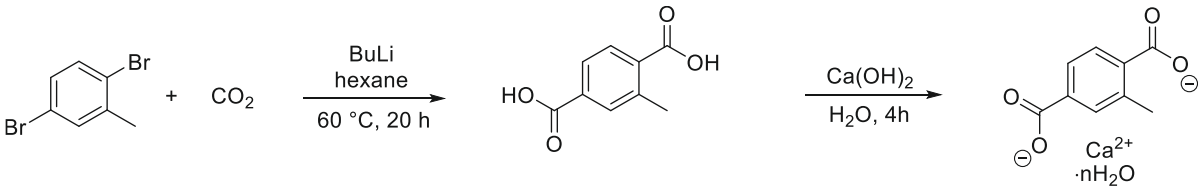

5b

Preparation of 2-methyl terephthalic acid

To a solution of 2,5-dibromtoluene (4.23 ml, 30 mmol) in hexane (60 ml) 1.6 M n-butyllithium in hexane (70 ml, 841 mmol) was added. The mixture was heated to 60 °C for 20 h, cooled to rt and poured to a mixture of dry ice in 600 ml diethyl ether. After the mixture warmed up to room temperature, 3 N HCl was added until pH 1 was reached. The mixture was extracted with Et_2O, washed with water, dried over $MgSO_4$. Removing the solvent under reduced pressure yielded the product as a brown powder (3.9 g, 21.6 mmol). To remove hexane completely, the product was dried at 70 °C under vacuo.

Preparation of 2-methyl calcium terephthalate

2-methyl terephthalic acid (0.53 g, 6.49 mmol) and calcium hydroxide (0.21 g, 6.49 mmol) were filled into a ball mill, 130 µl deionized water were added and milled for 4 h. The product was obtained as white powder (0.44 g, 1.98 mmol, 69.8 %).

3.7 Synthesis of 2-fluoro calcium terephthalate trihydrate

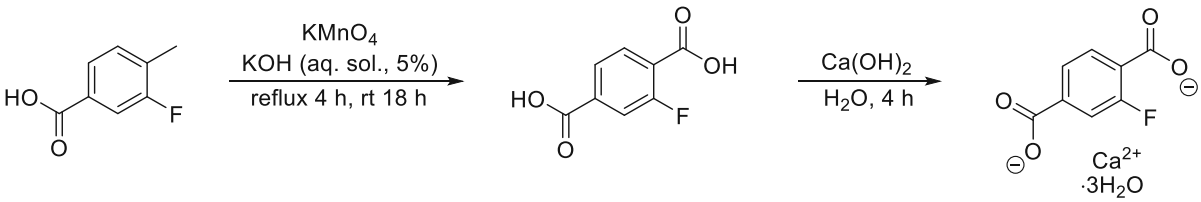

5c

Preparation of 2-fluoro terephthalic acid

3-fluoro-4-methylbenzoic acid (2 g, 12.3 mmol) and $KMnO_4$ (6.7 g, 42.4 mmol) were dissolved in an aqueous KOH solution (70 ml, 5 %). The solution was refluxed for 4 h, cooled to room temperature and stirred for 18 h. Afterwards the solution was filtered, and diluted with 50 ml

distilled water. The filtrate was acidified by the addition of concentrated HCl until pH 1 was reached. The formation of a white precipitate could be observed, which was collected by filtration, washed with water three times, and dried in vacuo (50 °C). 2-fluoro terephthalic acid was obtained as a white powder (1.79 g, 9.72 mmol).

^{1}H NMR (400 MHz, DMSO) δ 7.97 (t, 1H), 7.83 (dd, 1H), 7.73 (dd, 1H).

Preparation of 2-fluoro calcium terephthalate

2-fluoro terephthalic acid (0.53 g, 6.49 mmol) and calcium hydroxide (0.21 g, 6.49 mmol) were filled into a ball mill, 130 µl deionized water were added and milled for 4 h. The product was obtained as white powder (0.44 g, 1.98 mmol, 69.8 %).

3.7.1 Single crystal growth for X-ray diffraction

Two different approaches were tried to grow single crystals in a quality suitable for structural identification via single crystal XRD both starting from the corresponding 2-fluoro terephthalate disodium salt.

Preparation of 2-fluoro terephthalate disodium salt

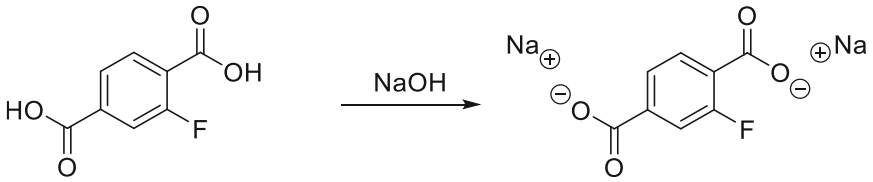

2-fluoro terephthalic acid (0.5 g, 2.72 mmol) was added to a solution of NaOH (0.22 g, 5.43 mmol) in 50 ml distilled water. After a complete dissolution was observed the mixture was stirred for 1 h and poured into cold acetone. The white precipitate was filtered, washed with Et_2O twice and dried in vacuo at 80 °C for 2 h. The product was isolated as a white/ slightly yellow solid (0.58 g, 2.54 mmol).

3.7.1.1 Approach 1: Reaction and Evaporation

$$Na_2C_8H_3O_4F + CaCl_2 \longrightarrow CaC_8H_3O_4F + NaCl$$

An aqueous solution of $CaCl_2$ (6.3 mg, 0.05 mmol) was carefully added to a solution of 2-fluoro terephthalic acid disodium salt (10.5 mg; 0.05 mmol) resulting in a slight turbidity. After two weeks of crystallization at room temperature, red single crystals were obtained.

3.7.1.2 Approach 2: Diffusion

A H-tube glass reactor was filled on one side with an aqueous solution of 2-fluoro terephthalic acid disodium salt (100 mg, 0.438 mmol) the other one with an aqueous solution of $CaCl_2$ (48.7 mg, 0.438 mmol). After seven weeks red single crystals were obtained.

3.1 Synthesis of 2-chloro calcium terephthalate n-hydrate

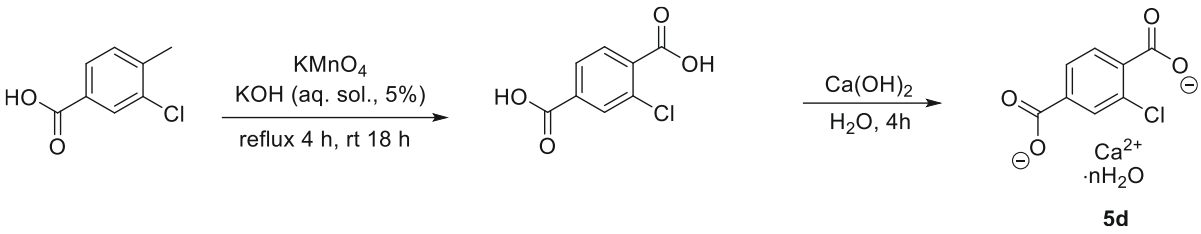

5d

Preparation of 2-chloro terephthalic acid

3-chloro-4-methylbenzoic acid (4 g, 23.2 mmol) and $KMnO_4$ (12.23 g, 77.38 mmol) were dissolved in an aqueous KOH solution (130 ml, 5 %). The solution was refluxed for 4 h, cooled to room temperature and stirred for 18 h. Afterwards the solution was filtered, and diluted with 100 ml distilled water. The filtrate was acidified by the addition of concentrated HCl until pH 1 was reached. The formation of a white precipitate could be observed, which was collected by filtration, washed with water three times, and dried in vacuo (50 °C). 2-chloro terephthalic acid was obtained as a white powder (3.75 g, 18.7 mmol, 80.59 %).

Preparation of 2-chloro calcium terephthalate n-hydrate

2-chloro terephthalic acid (0.8 g, 3.99 mmol) and calcium hydroxide (0.21 g, 3.99 mmol) were filled into a ball mill, 130 µl deionized water were added and milled for 4 h. The product was obtained as white powder (0.9 g, 3.75 mmol, 93.99 %).

3.2 Synthesis of Tetrafluoro calcium terephthalate tetrahydrate

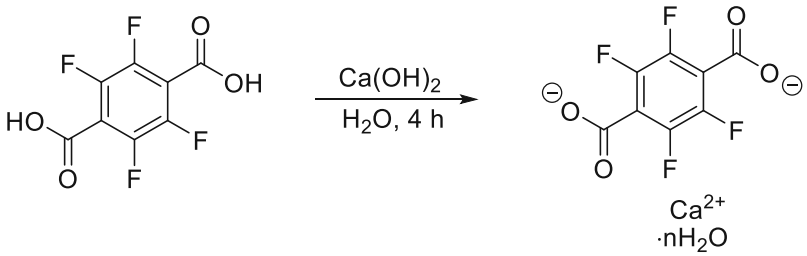

5e

Tetrafluoro terephthalic acid (0.76 g, 3.1 mmol) and calcium hydroxide (0.24 g, 3.1 mmol) were filled into a ball mill, 130 µl deionized water were added and milled for 4 h. The product was obtained as white/light grey powder (0.76 g, 2.75 mmol, 86.27 %).

3.1 Synthesis of Tetrachloro calcium terephthalate n-hydrate

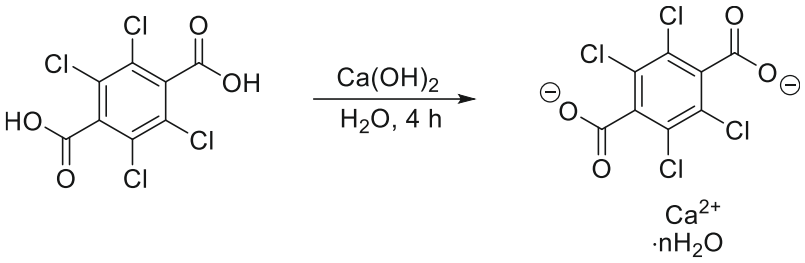

5f

Tetrachloro terephthalic acid (0.8 g, 2.5 mmol) and calcium hydroxide (0.2 g, 2.5 mmol) were filled into a ball mill, 130 µl deionized water were added and milled for 4 h. The product was obtained as white powder (0.81 g, 2.37 mmol, 90.06 %).

3.2 Cyclopropane-1,1-dicarboxylic acid calcium salt n-hydrate

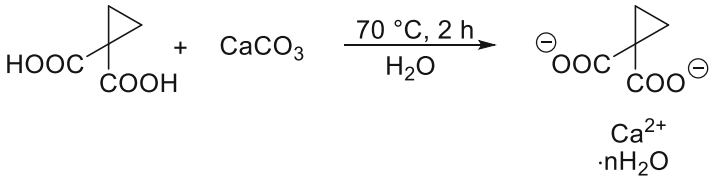

6

To a solution of cyclopropane-1,1-dicarboxylic acid (1.29 g, 9.91 mmol) in 50 ml deionized water, calcium carbonate (1 g, 9.91 mmol) was added in small amounts. The reaction was stirred until no further CO_2 formation could be observed, giving a white suspension which was then heated to 70°C for 2 h. The suspension was allowed to cool to room temperature and left over night. The white precipitate was collected by filtration, washed with deionized water twice, and dried at 40 °C in vacuo. The product was obtained as a white solid (437 mg, 2.6 mmol, 27.02 %).

3.3 Synthesis of Ettringite

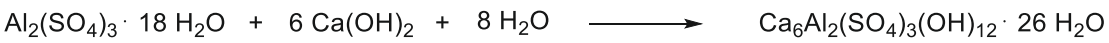

A saturated $Ca(OH)_2$ suspension was prepared by hydrating freshly calcinated calcium oxide (5 g, 89.22 mmol) with distilled, decarbonized water. The suspension was cooled in a fridge before adding a solution of aluminum sulfate octadecahydrate (10 g, 14.87 mmol). The suspension was stirred for 3 h at room temperature and afterwards stored in a fridge to slowly

evaporate the water. After a complete evaporation of the solvent the white solid was ground, washed with distilled water and EtOH, filtered, and dried in vacuo.14 g of white solid were isolated (76 %).

3.3.1 Negative synthetic approaches for ettringite

1st approach

CaO (60.59 g, 1050 mmol) was hydrated with distilled water in a beaker to create a $Ca(OH)_2$ suspension. After the suspension was heated until boiling, $Al_2(SO_4)_3 \cdot 18\ H_2O$ (180 g, 270 mmol) was added under stirring. The mixture was covered with a watch glass and heated for 2 h. Afterwards the reaction mixture was refrigerated at 4 °C to slowly evaporate the solvent. This gave a white, brittle solid that was ground, washed once with cold water and dried at 40 °C in vacuo.

2nd approach

Distilled water was heated to reflux for 30 min. CaO (28.52 g, 498 mmol) was hydrated with distilled water in a beaker to create a $Ca(OH)_2$ suspension. After the suspension was heated until boiling, $Al_2(SO_4)_3 \cdot 18\ H_2O$ (84.72 g, 172.1 mmol) was added under stirring. The mixture was covered with a watch glass and heated for 2 h. Afterwards the reaction mixture was stored in a desiccator at 400 mbar in argon atmosphere.

3.4 STA data

The measured TG-DSC curves that are not shown in the result chapter, can be found in the appendix.

	DSC-onset (°C)	DSC-peak$_{max}$ (°C)	Heat flow (J g^{-1})	Mass-loss (%)
Ca-oxalate monohydrate	158	197	466	12.2
Ca-malonate dihydrate	127	154	637	17.9
Ca-succinate monohydrate	166	191	313	10.2
Ca-glutarate monohydrate	148	189	398	12.1
Ca-terephthalate trihydrate	103	125	695	20.1
2-methyl Ca-terephthalate n-hydrate	88	113	262	15.8
2-fluoro Ca-terephthalate trihydrate	126	157	483	15.6
2-chloro Ca-terephthalate n-hydrate	88	113	262	15.8
Tetrafluoro Ca-terephthalate tetrahydrate	99	126	657	19.0

4 Contributions

Three poster presentations were held at three different events in the year of 2023.

1. “Synthesis and characterization of novel calcium salt dicarboxylate hydrates as thermochemical energy storage materials” at the 36th Workshop on "Novel Materials and Superconductors 2023, Schladming. (https://repositum.tuwien.at/handle/20.500.12708/153160)
2. “From waste to resource: investigating calcium dicarboxylate hydrates as thermochemical energy storage materials for waste heat storage” at the Exner Lectures 2023, Vienna, which was awarded with the poster award “fundamental milestone”.
3. “Solving energy challenges through chemical bonds: calcium dicarboxylate hydrates as thermochemical energy storage materials” at the 6th EuChemS Inorganic Chemistry Conference, Vienna (Book of abstracts: ISBN 978-3-9504809-5-5).

A part of this work is being prepared as a journal article in the special issue “Research in Thermal Energy Storage Materials” in the Crystals journal (ISSN 2073-4352).

Appendix

STA Curves

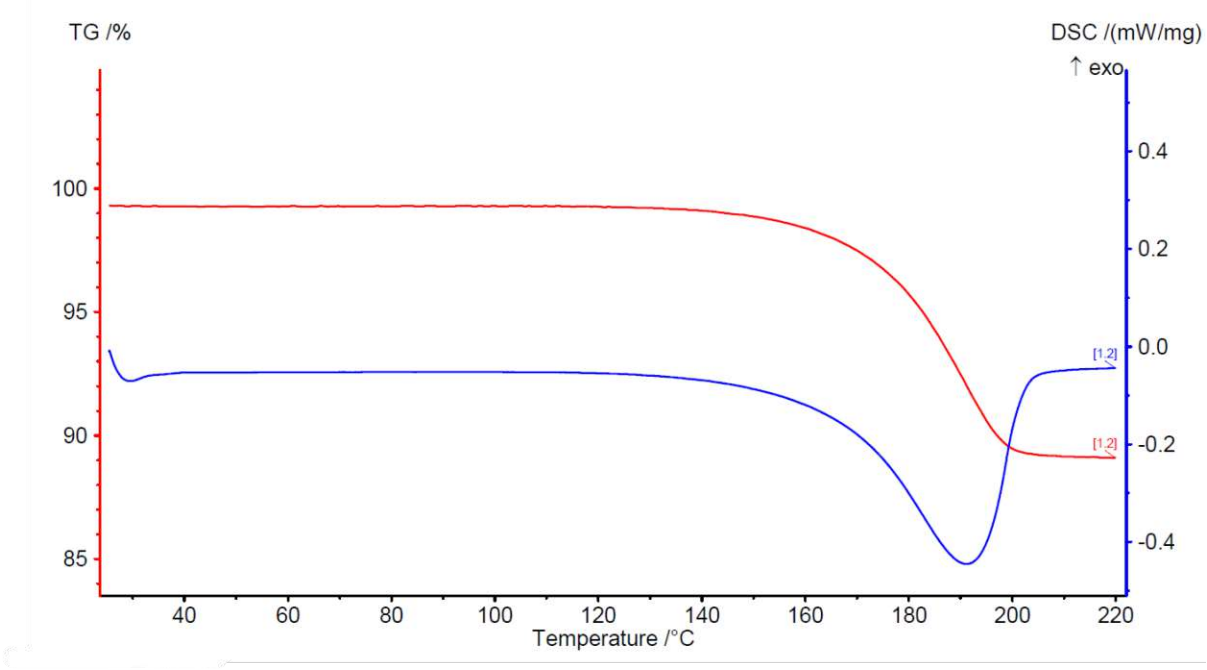

*Figure 25: STA of Ca-succinate monohydrate (**3**)*

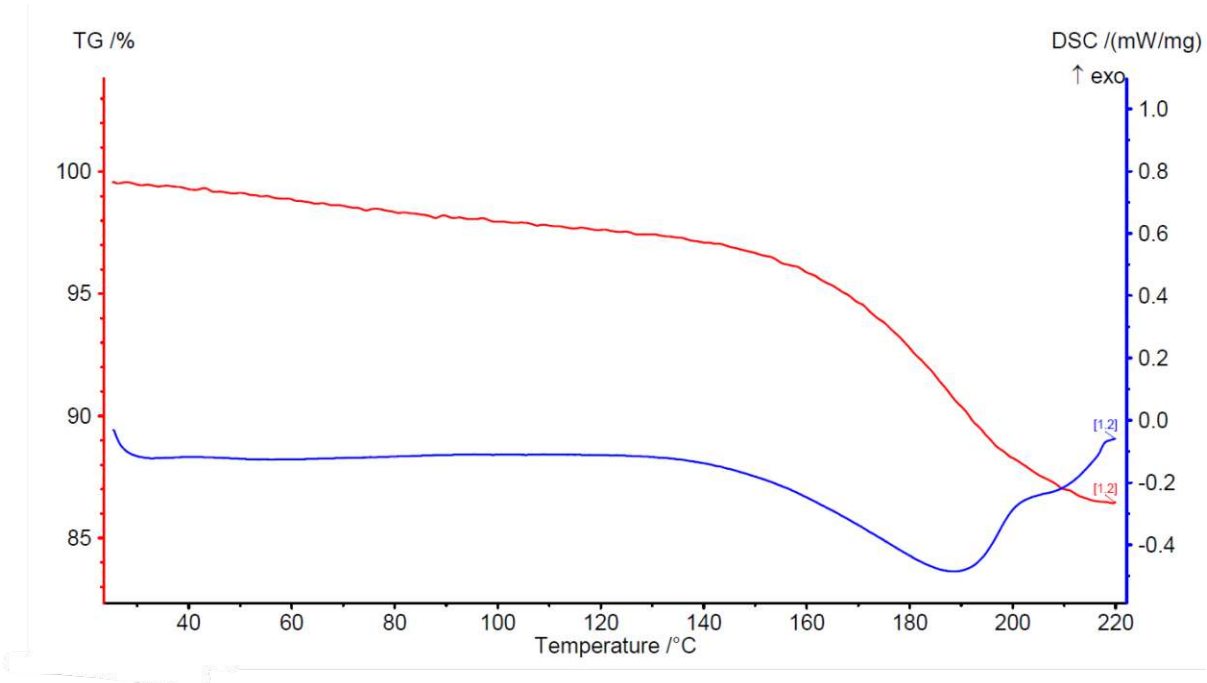

*Figure 26: STA of Ca-glutarate monohydrate (**4**)*

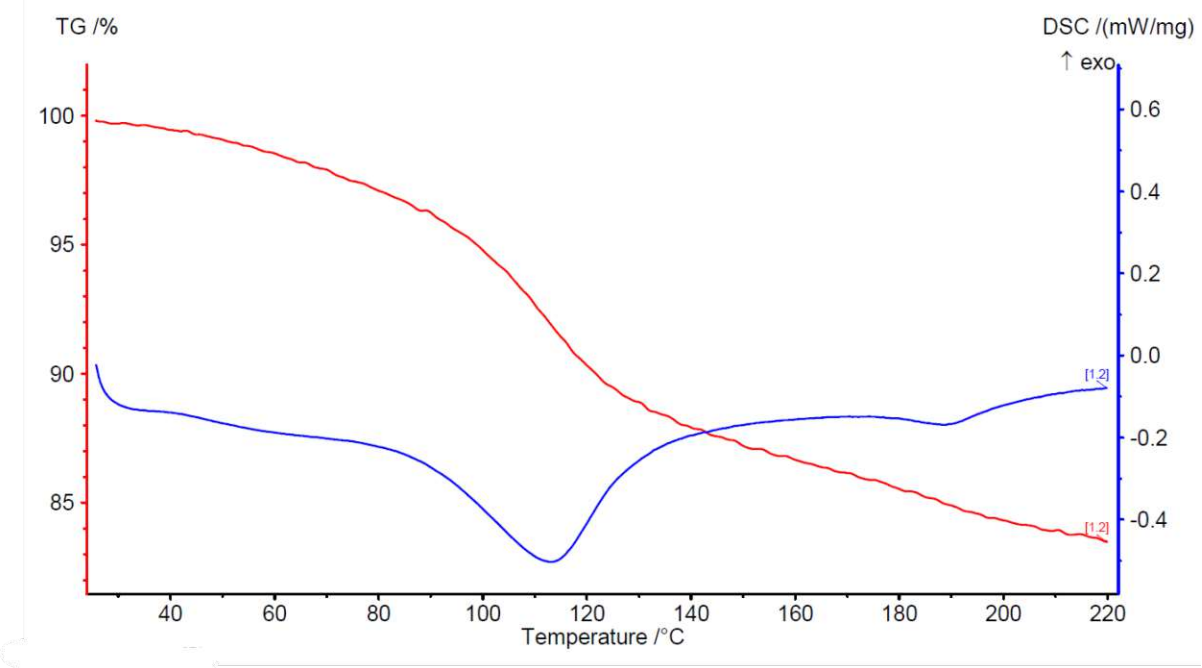

*Figure 27: STA of 2-methyl calcium terephthalate n-hydrate (**5b**)*

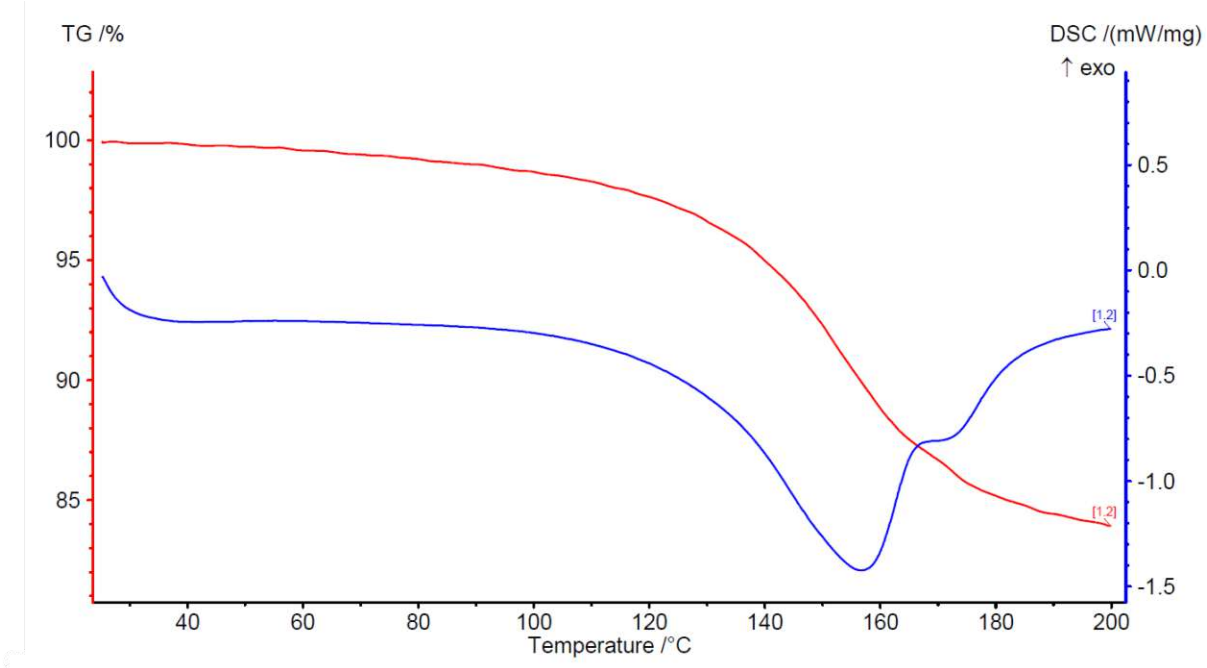

*Figure 28: STA of 2-fluoro calcium terephthalate trihydrate (**5c**)*

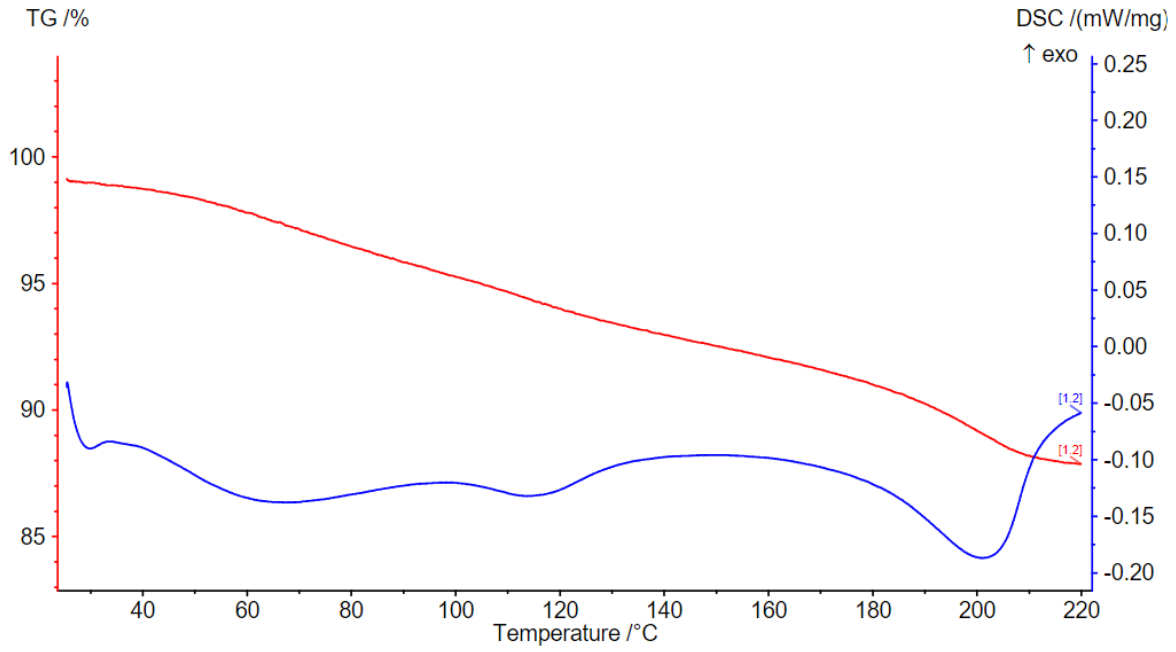

*Figure 29: STA of 2-chloro calcium terephthalate n-hydrate (**5d**, 1st measurement)*

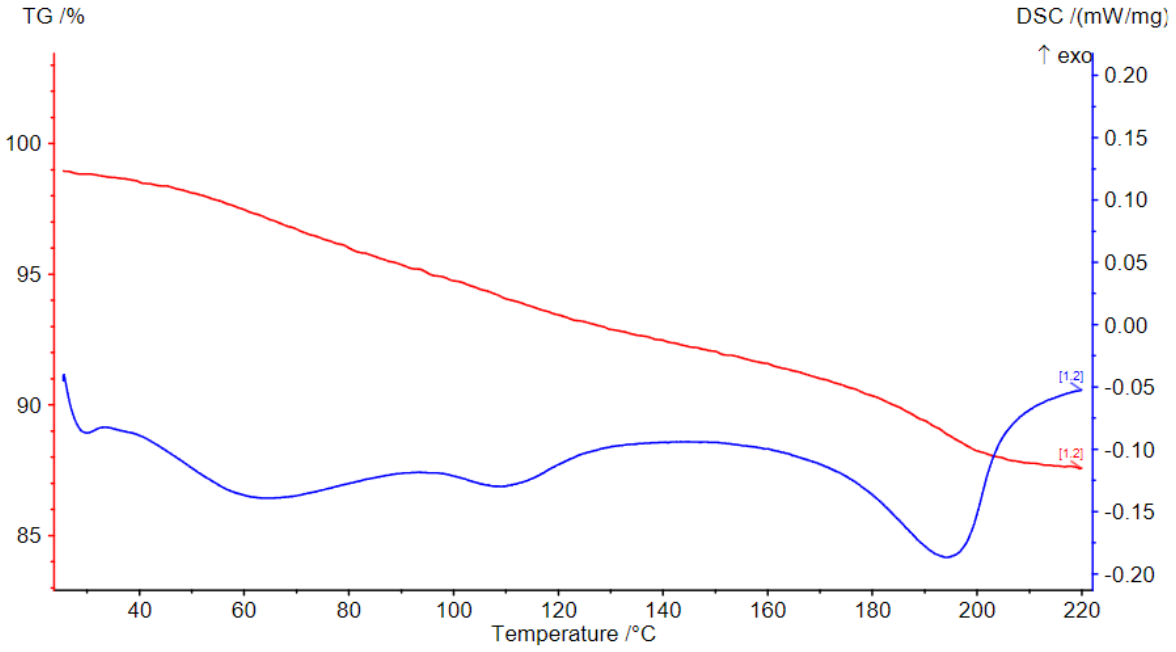

*Figure 30: STA of 2-chloro calcium terephthalate n-hydrate (**5d**, 2nd measurement)*

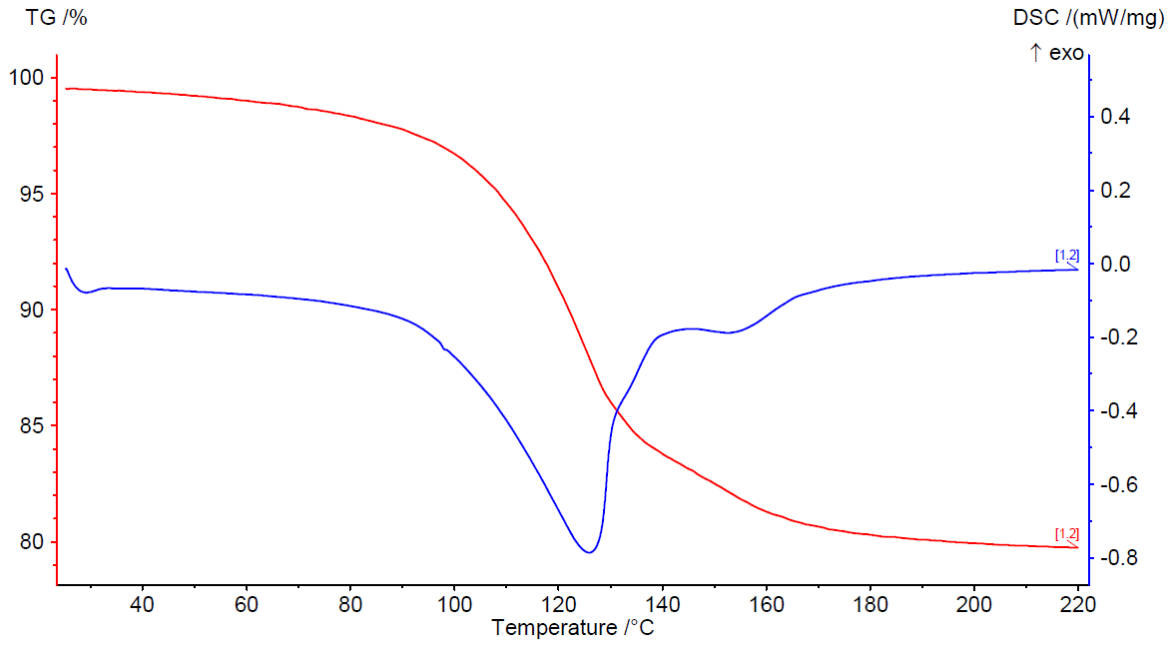

*Figure 31: STA of Tetrafluoro calcium terephthalate tetrahydrate (**5f**)*

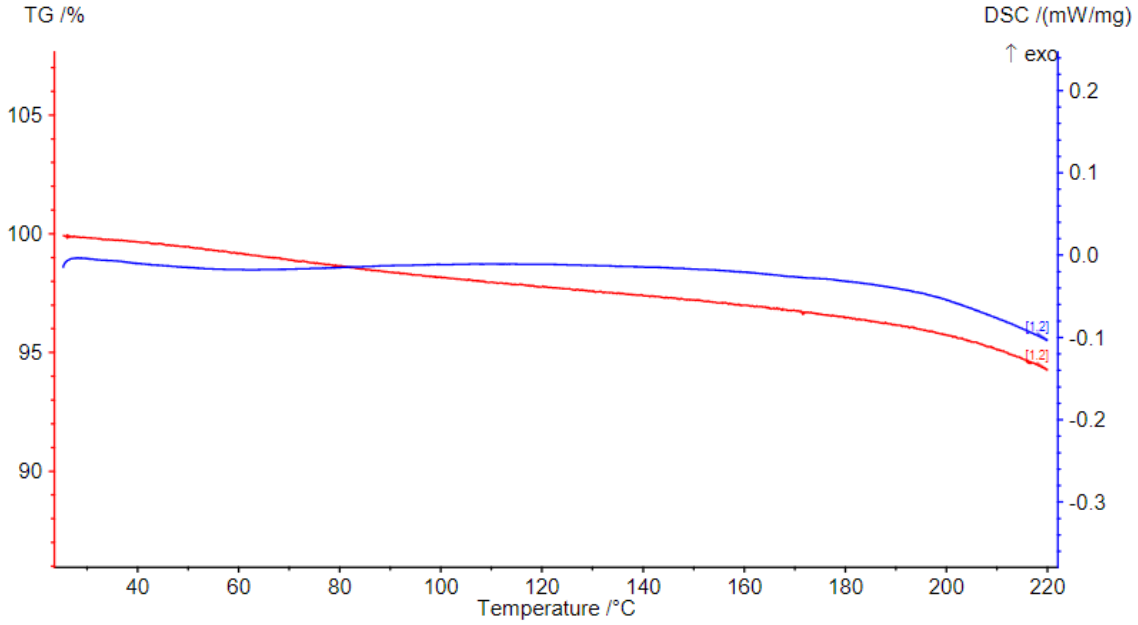

*Figure 32: STA of Tetrachloro calcium terephthalate n-hydrate (**5f**)*

PXRD diffraction patterns

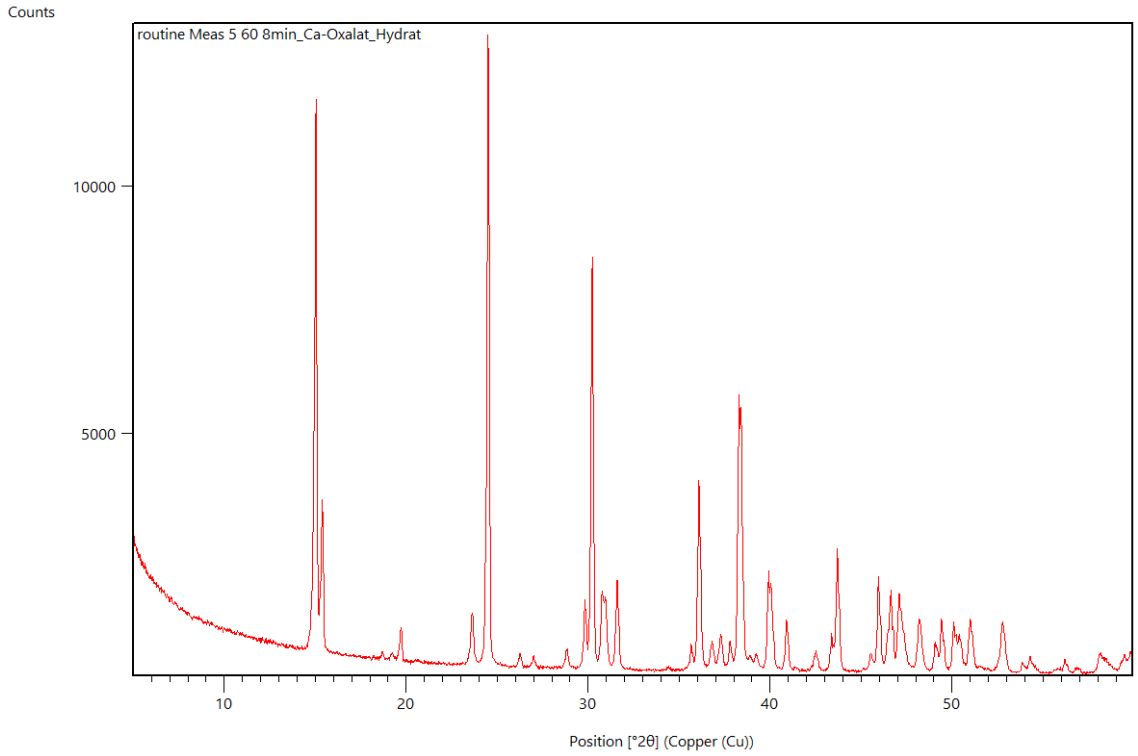

Figure 33: PXRD of Ca-oxalate monohydrate

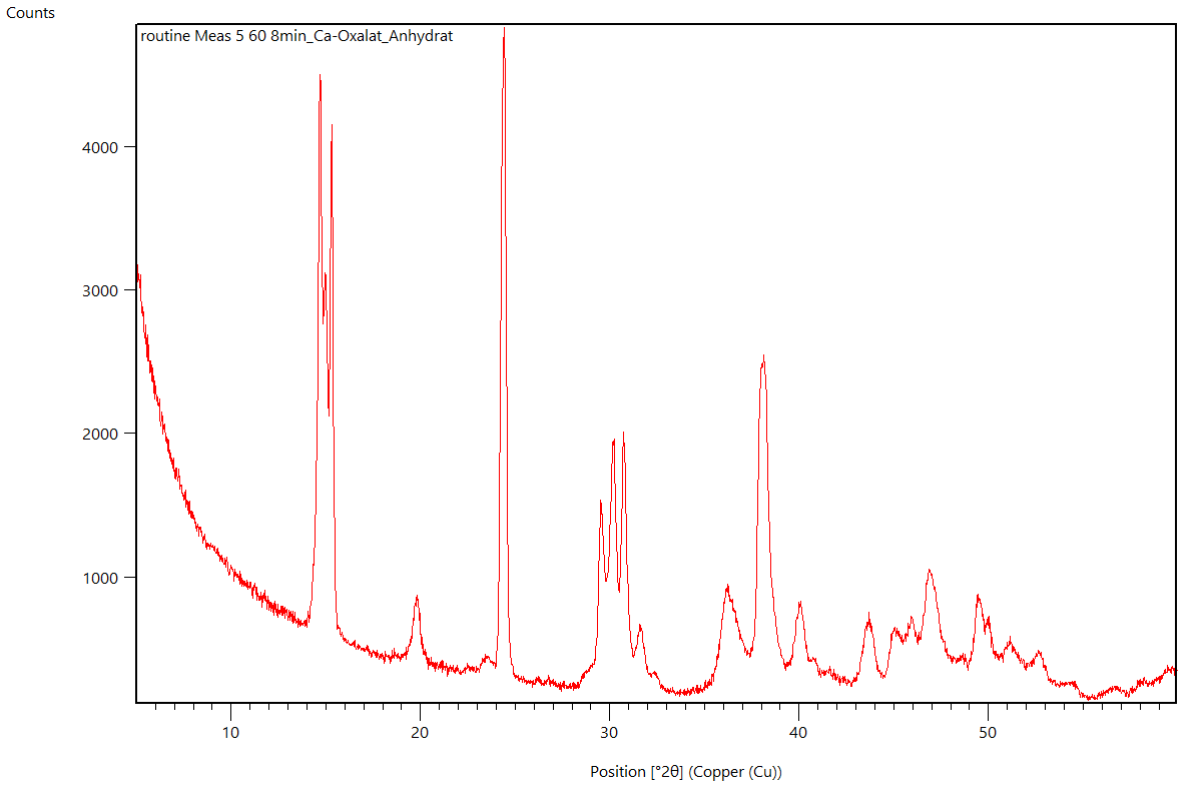

Figure 34: PXRD of Ca-oxalate anhydrate

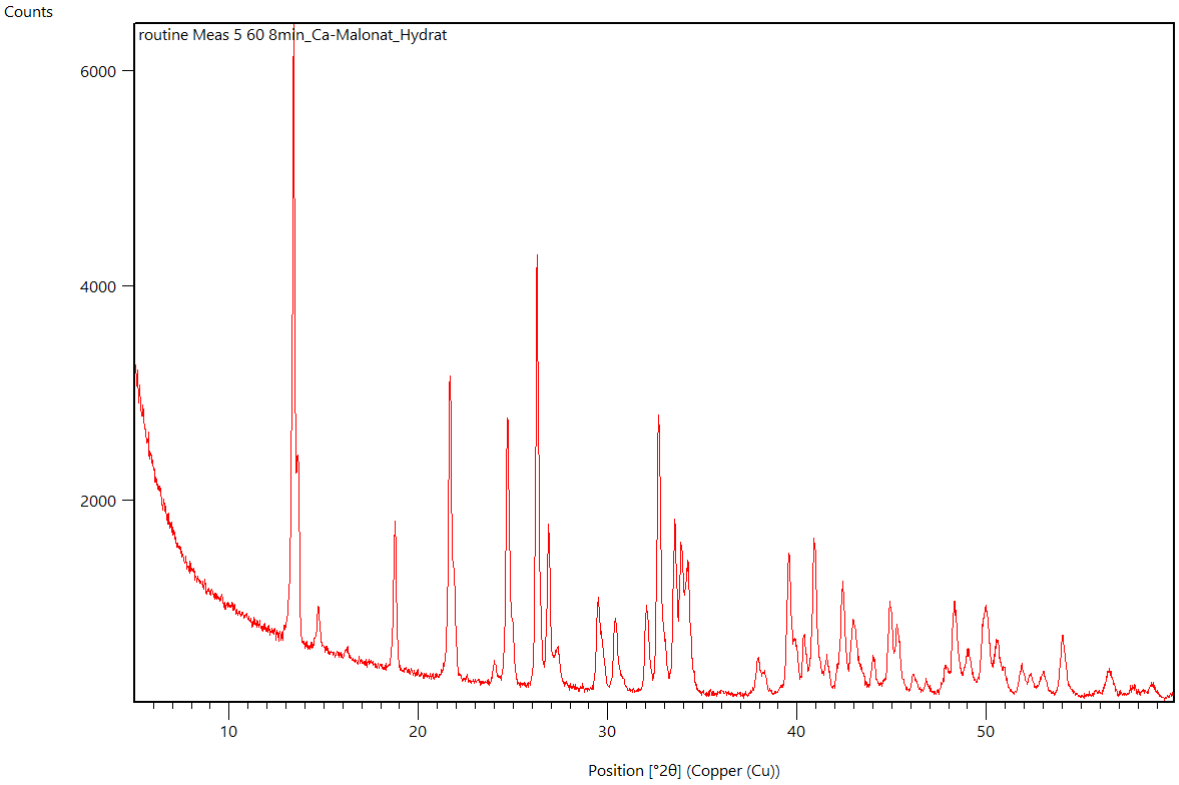

Figure 35: PXRD Ca-malonate dihydrate

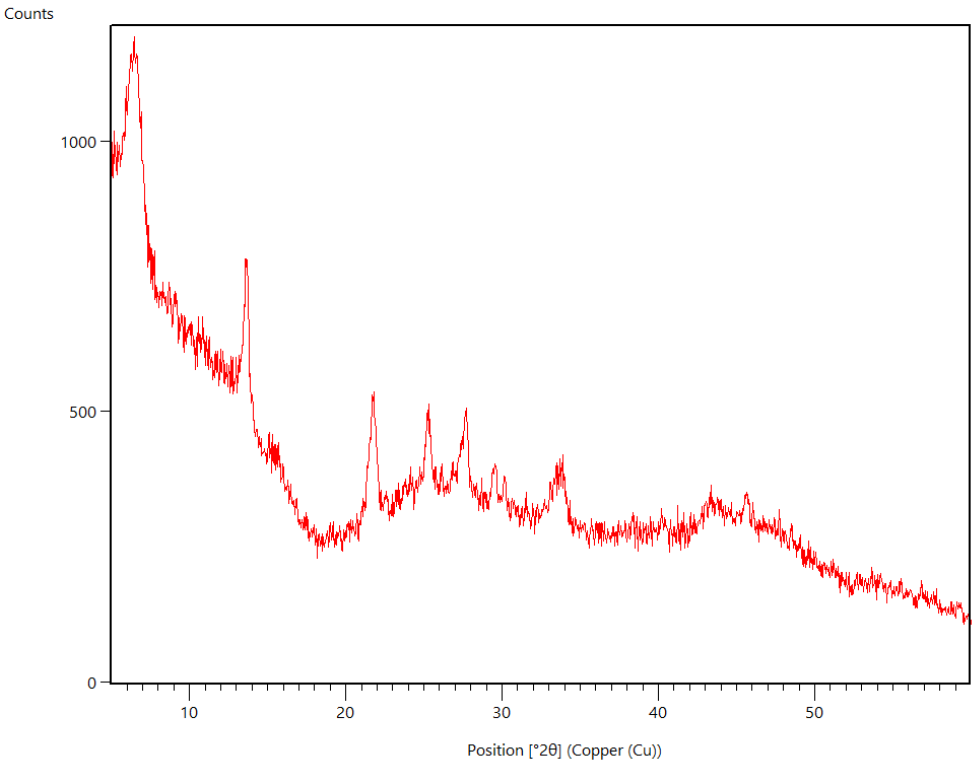

Figure 36: PXRD of Ca-malonate anhydrate

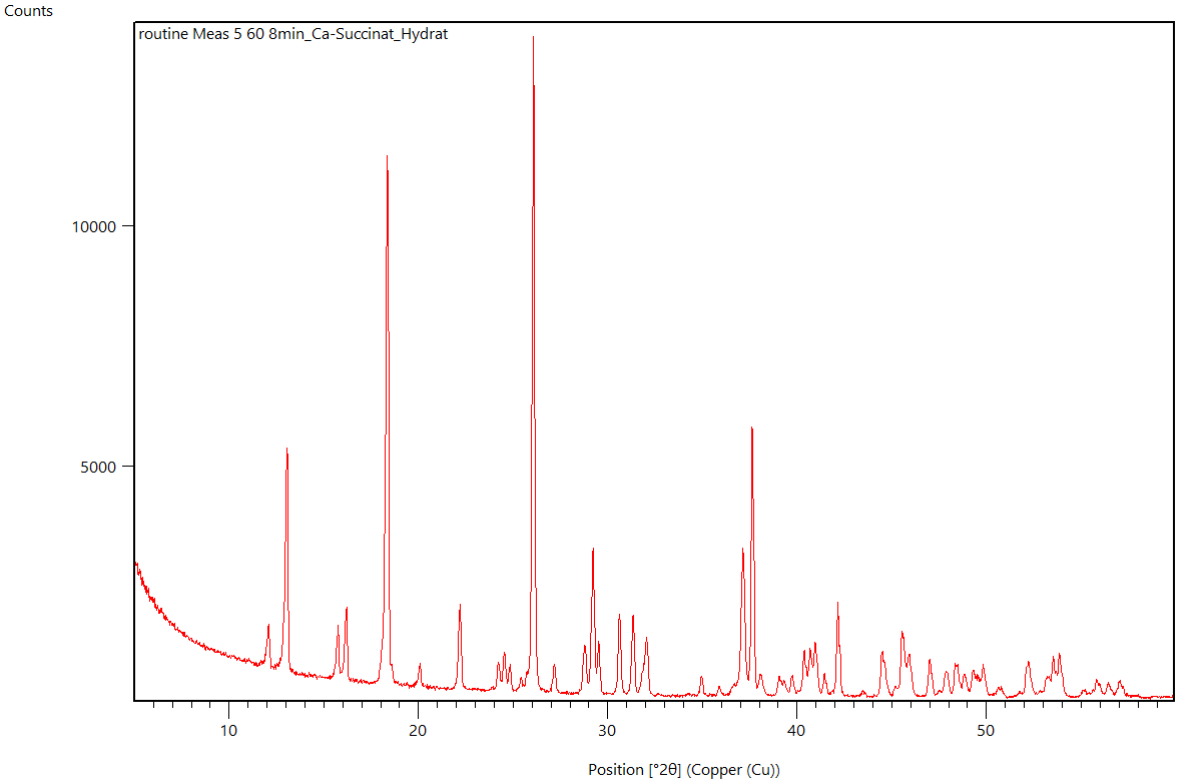

Figure 37: PXRD of Ca-succinate monohydrate

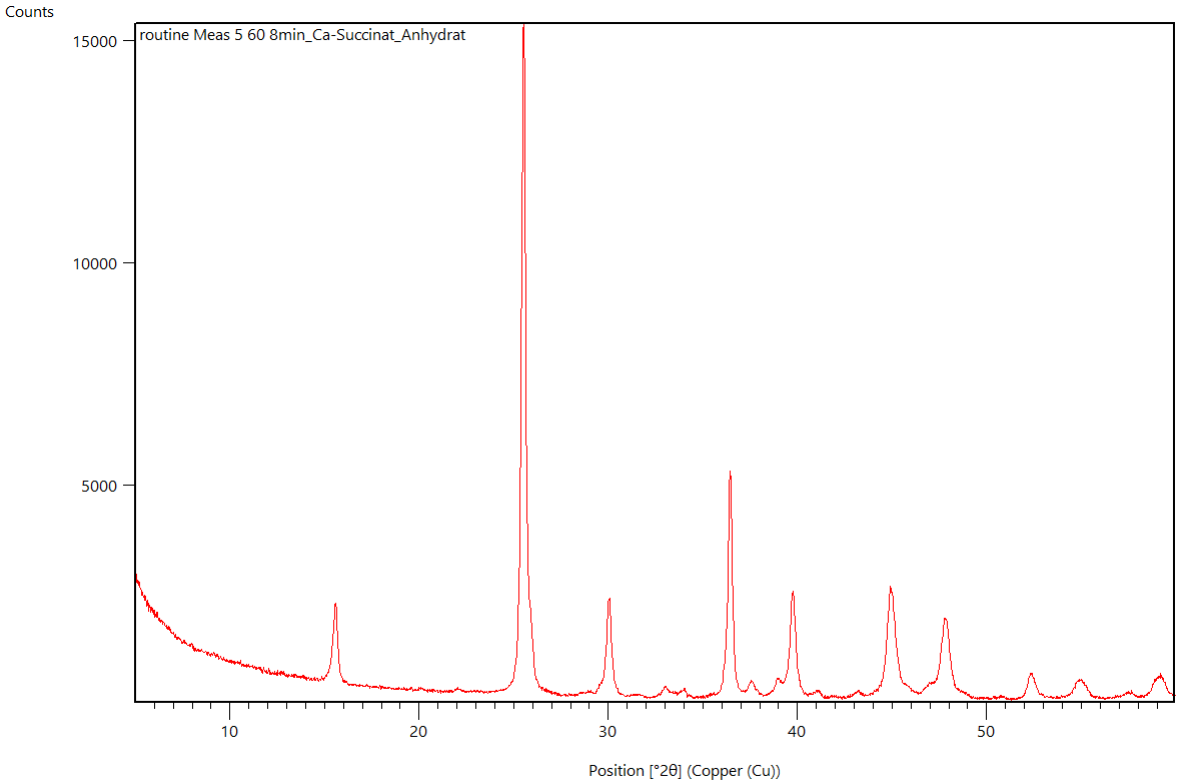

Figure 38: PXRD of Ca-succinate anhydrate

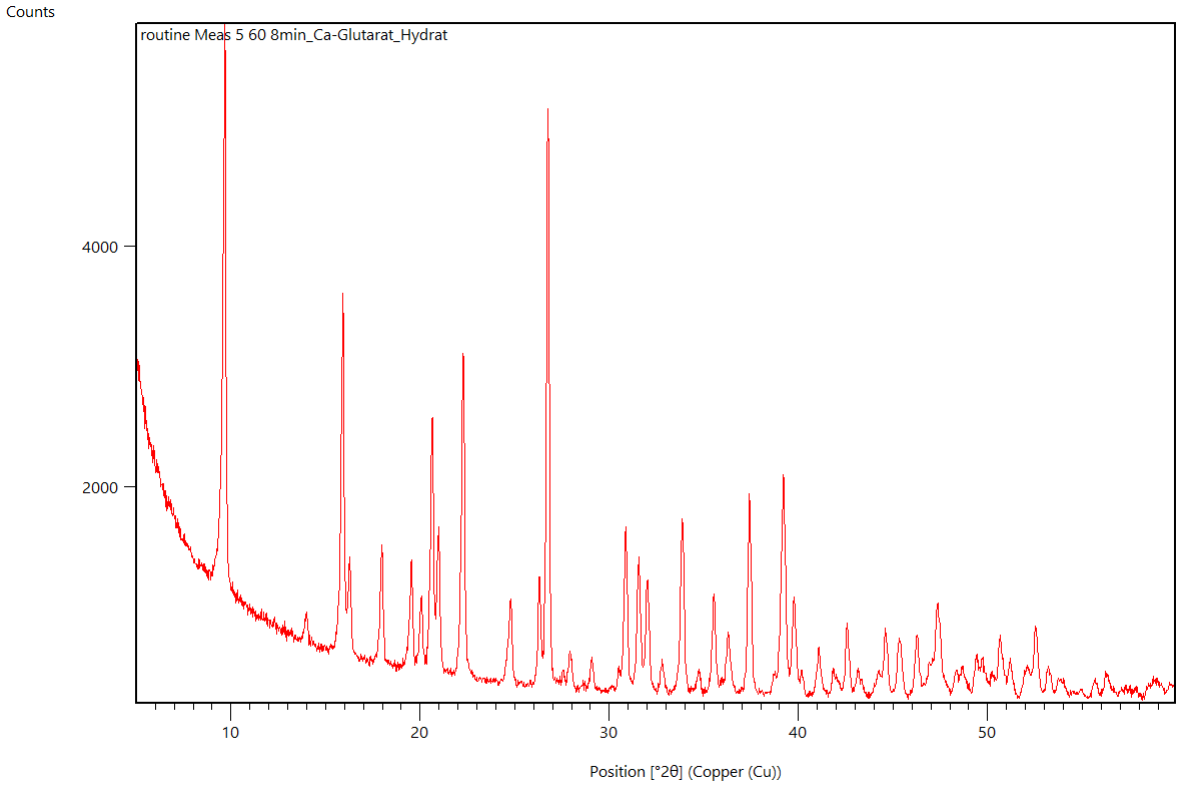

Figure 39: PXRD of Ca-glutarate monohydrate

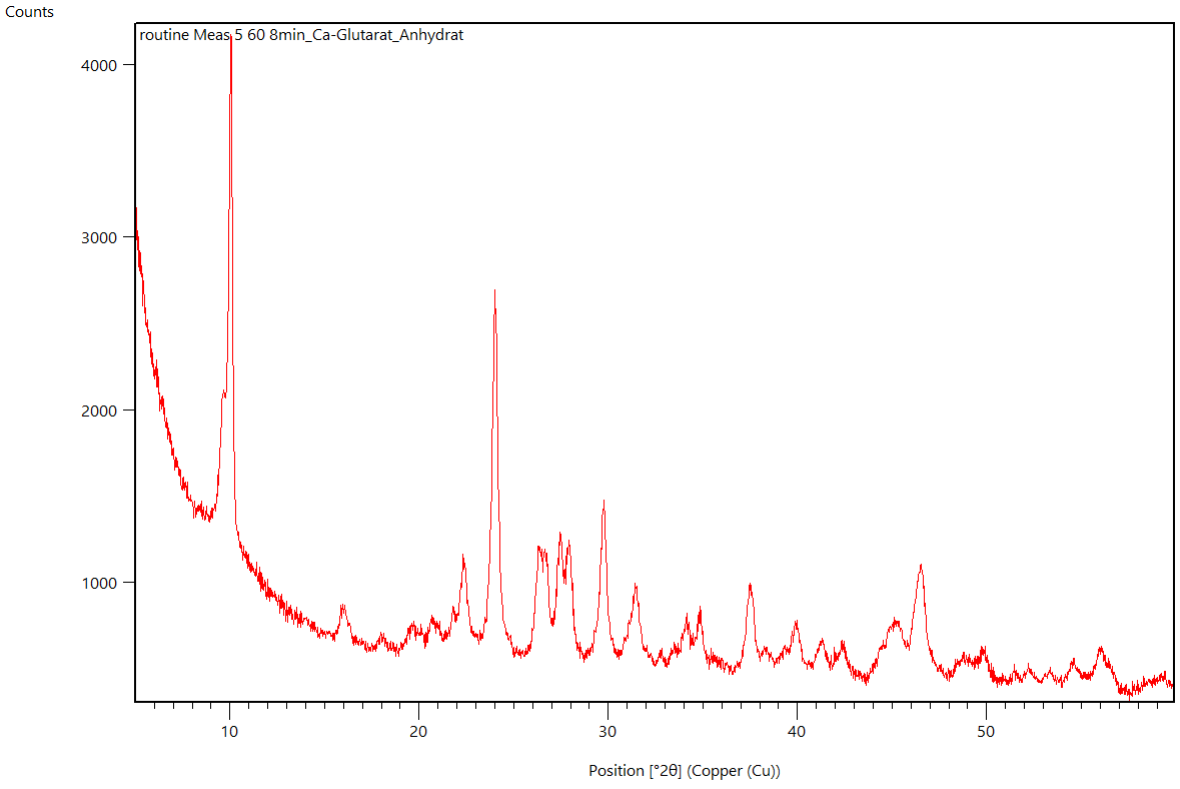

Figure 40: PXRD of Ca-glutarate anhydrate

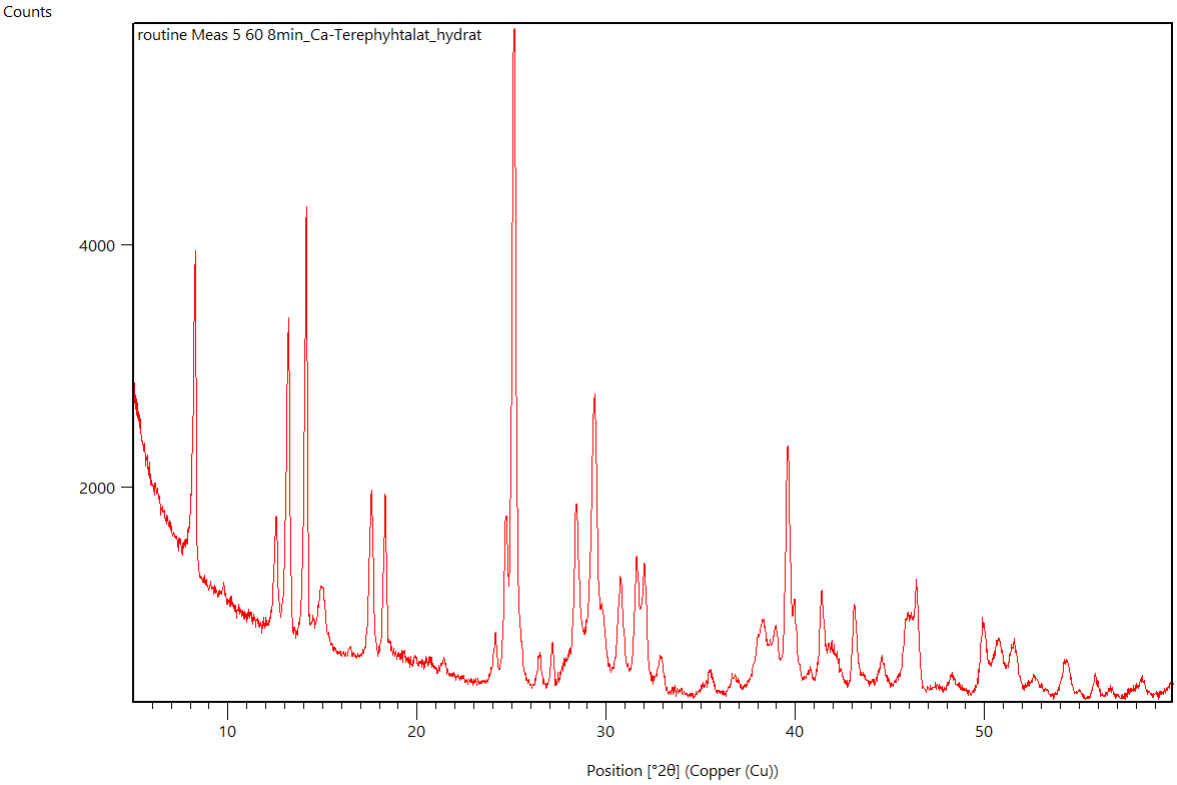

Figure 41: PXRD of Ca-terephthalate trihydrate

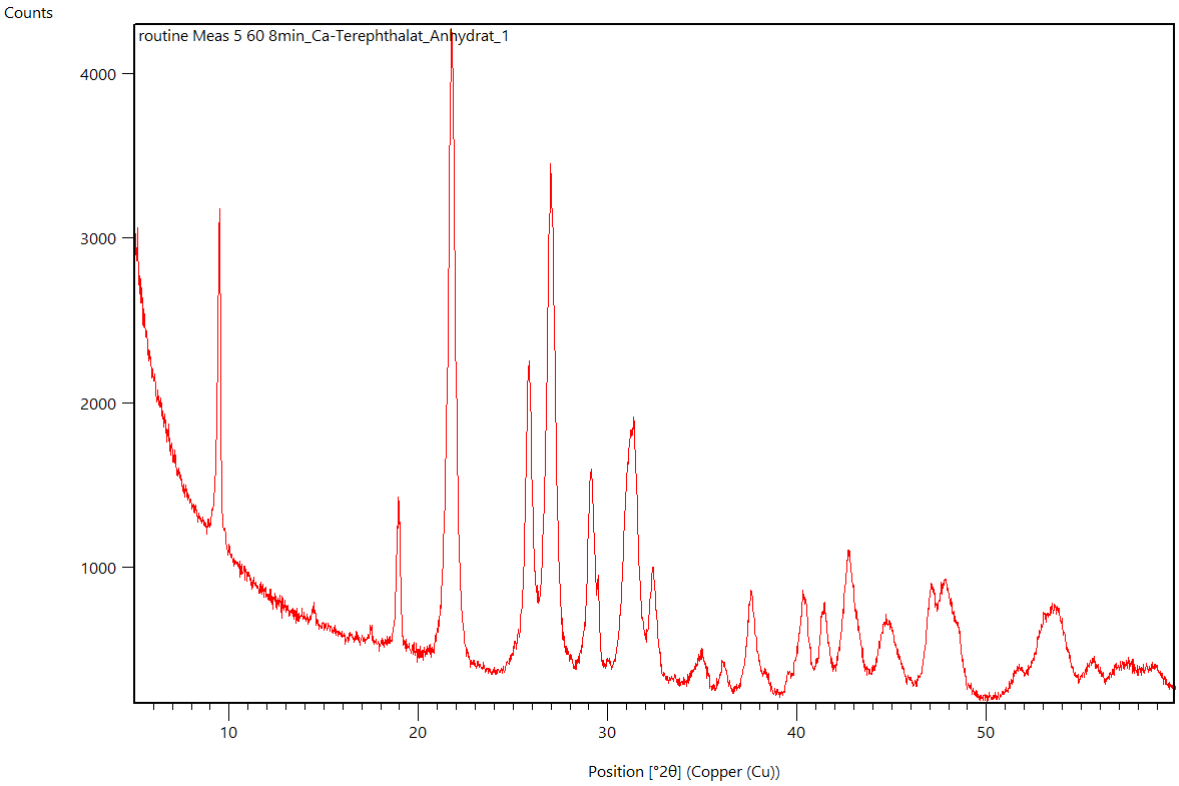

Figure 42: PXRD of Ca-terephthalate anhydrate

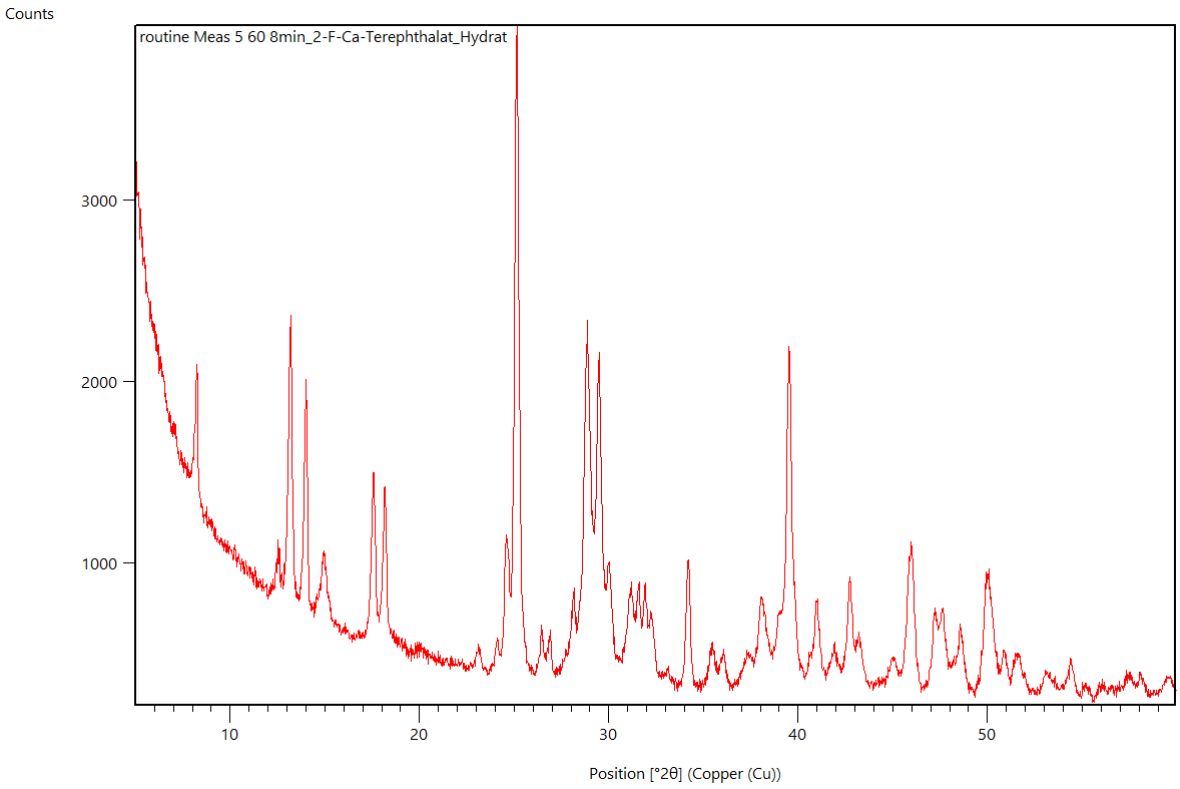

Figure 43: PXRD of 2-fluoro Ca-terephthalate trihydrate

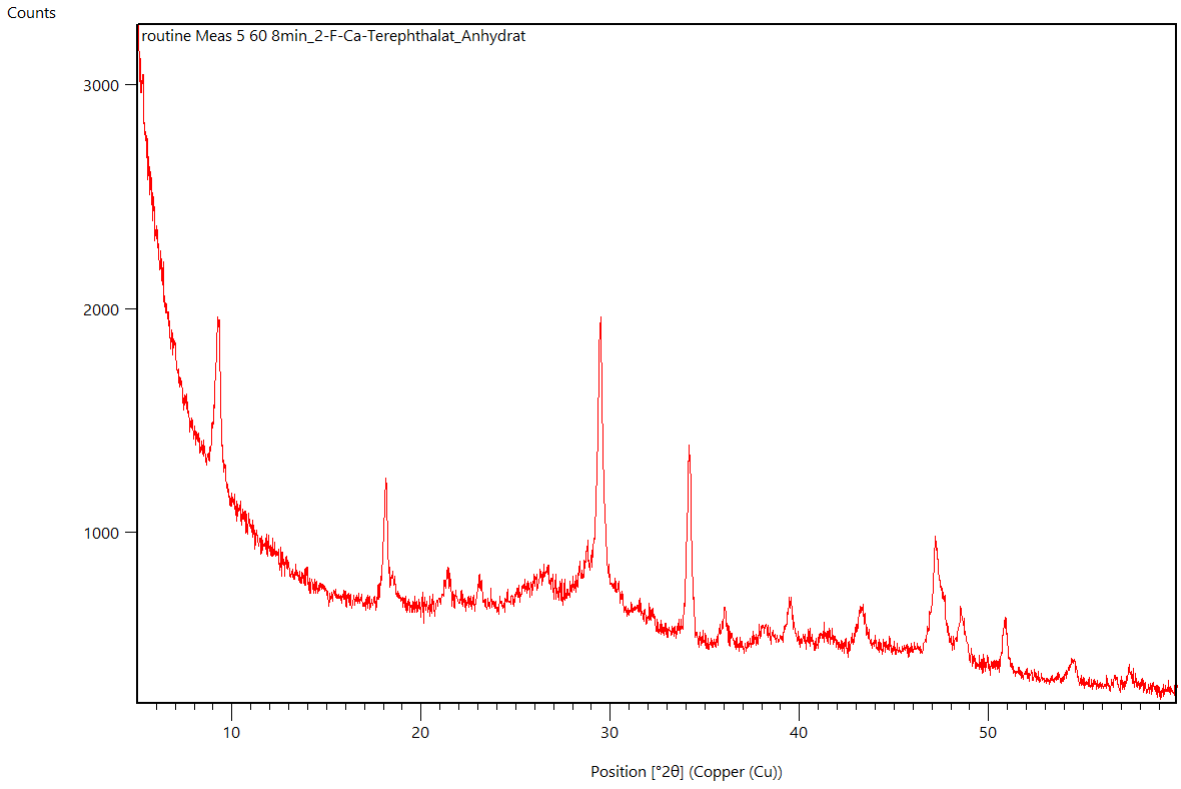

Figure 44: PXRD of 2-fluoro Ca-terephthalate anhydrate

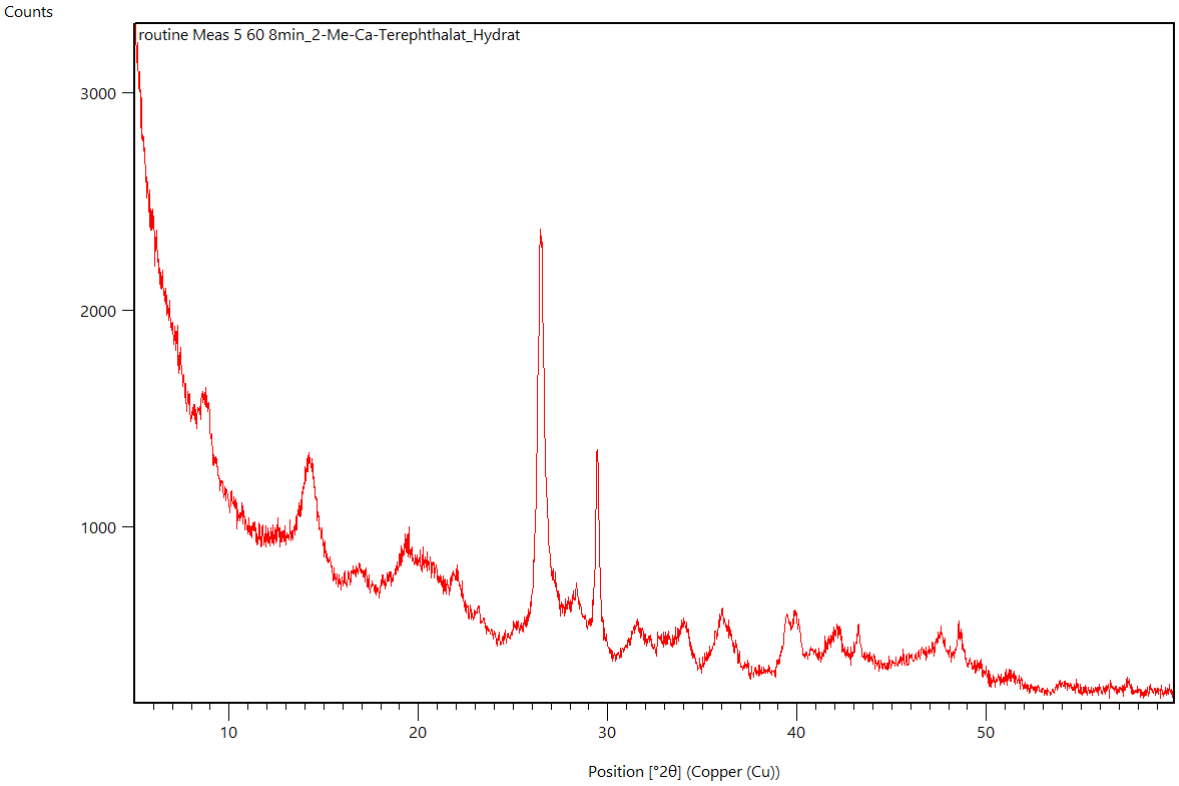

Figure 45: PXRD of 2-methyl Ca-terephthalate n-hydrate

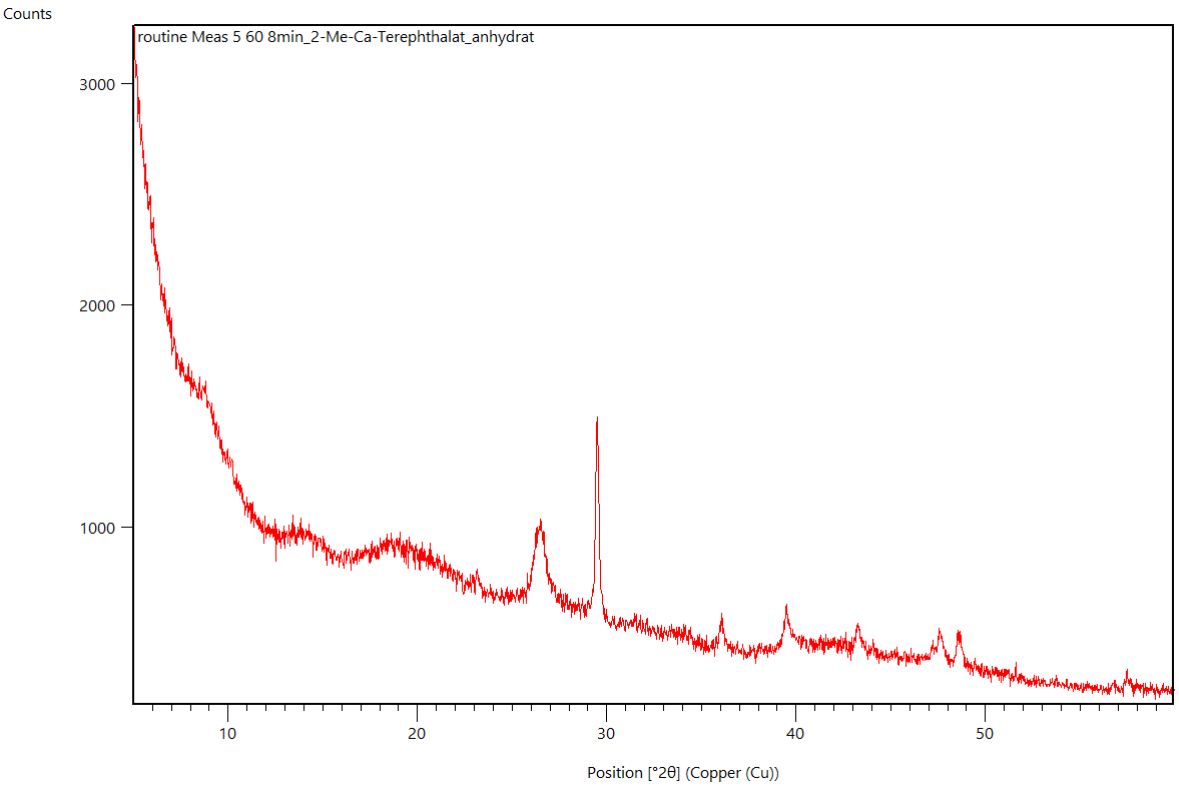

Figure 46: PXRD of 2-methyl Ca-terephthalate anhydrate

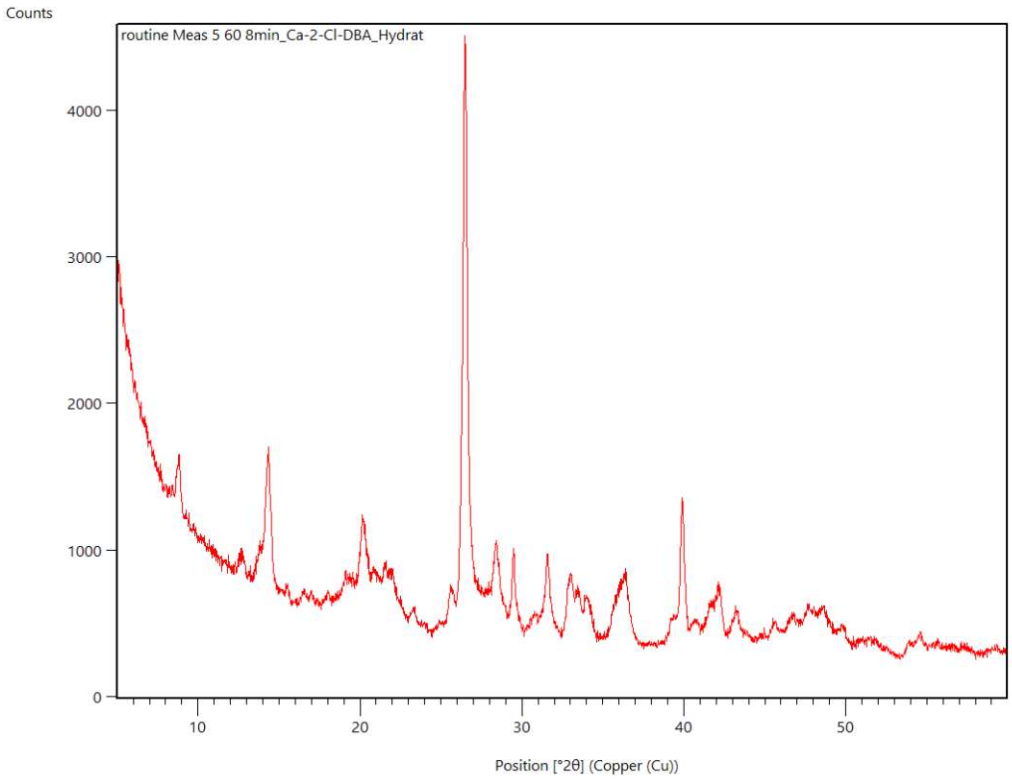

Figure 47: PXRD of 2-chloro Ca-terephthalate n-hydrate

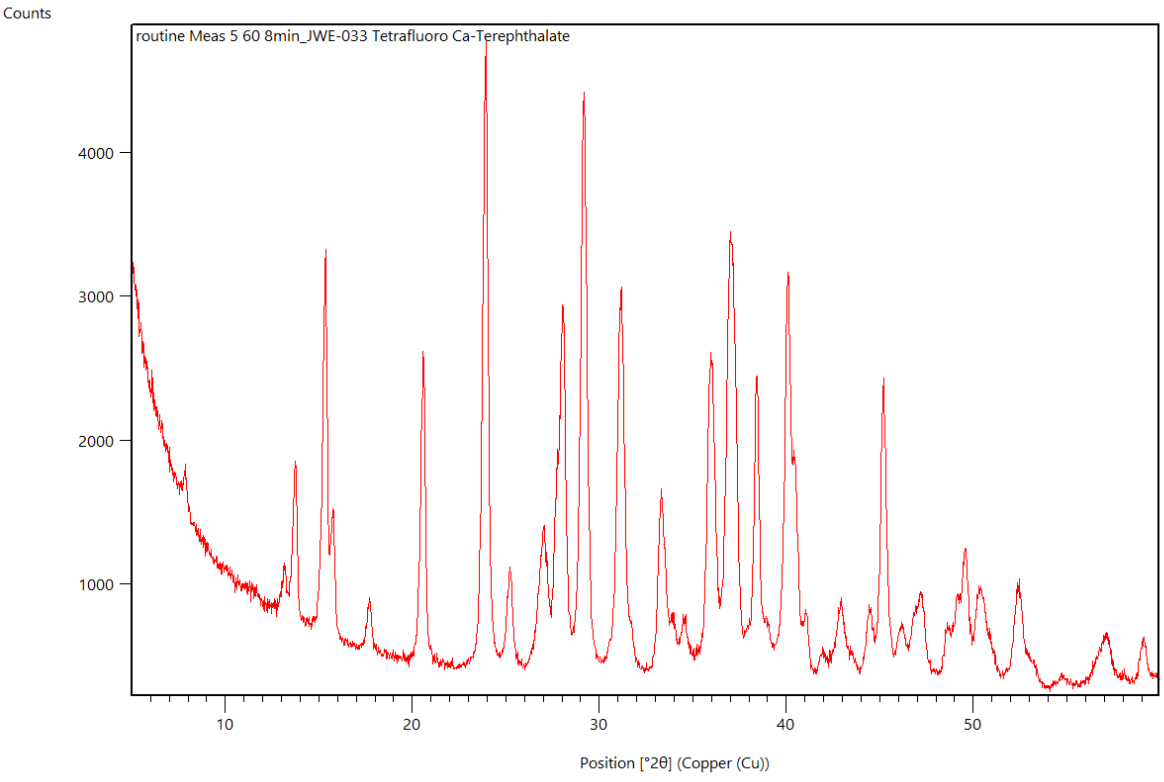

Figure 48: PXRD of tetrafluoro Ca-terephthalate tetrahydrate

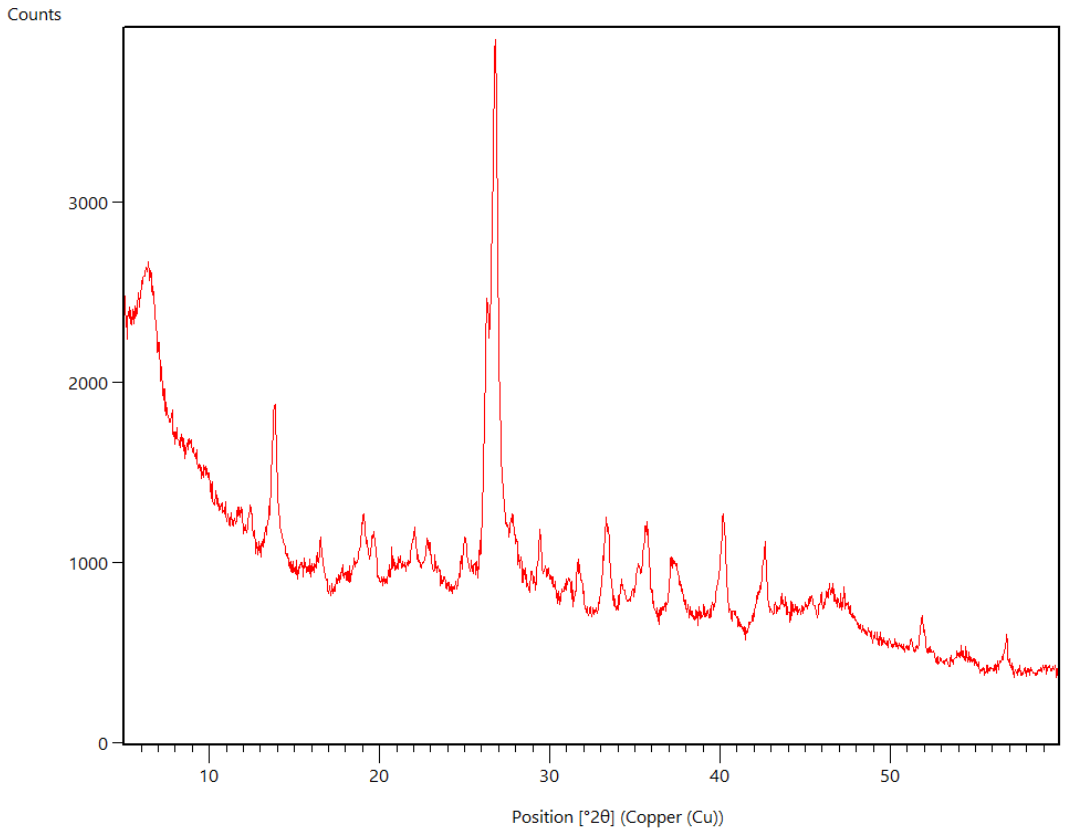

Figure 49: : PXRD of tetrafluoro Ca-terephthalate anhydrate

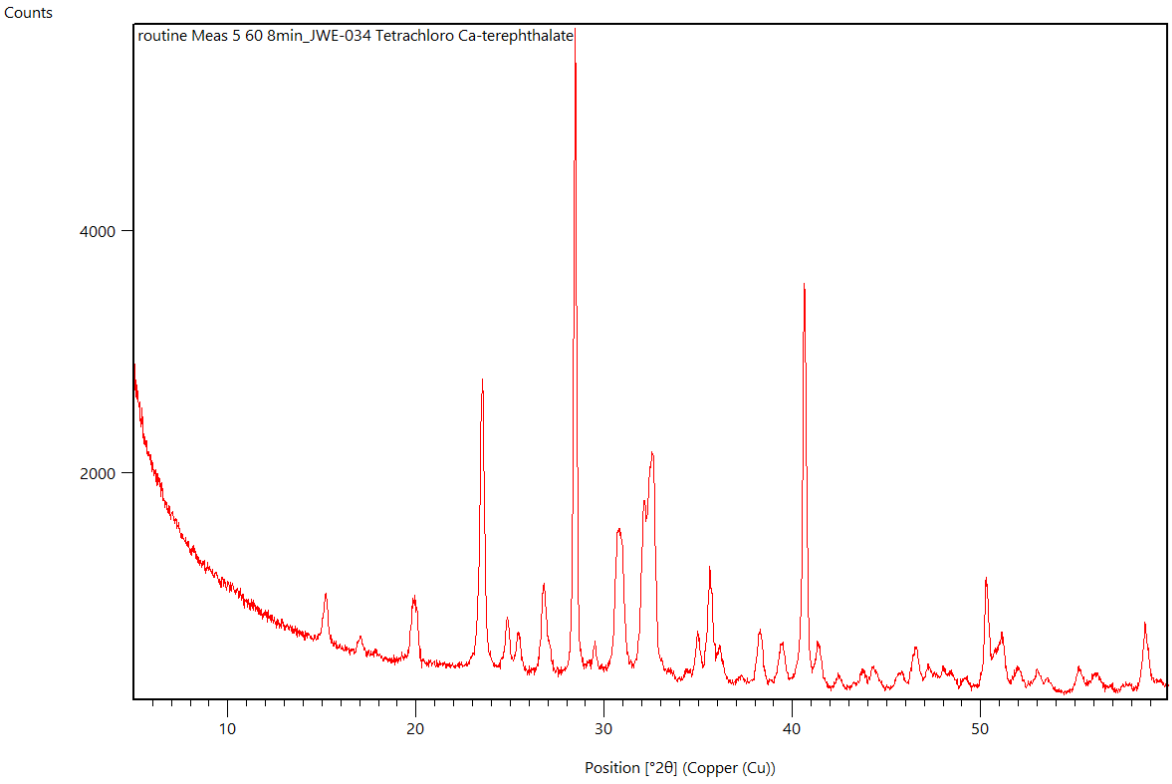

Figure 50: PXRD of tetrachloro Ca-terephthalate n-hydrate

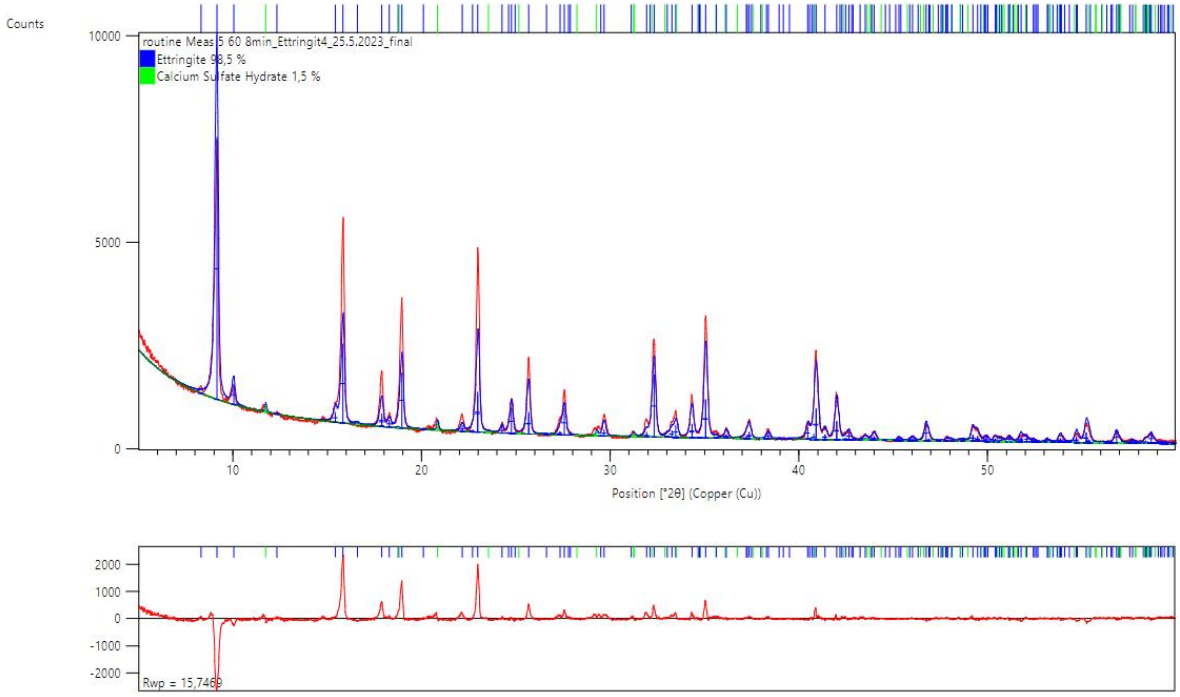

Figure 51: Rietveld refined diffractogram of ettringite

FTIR Spectra

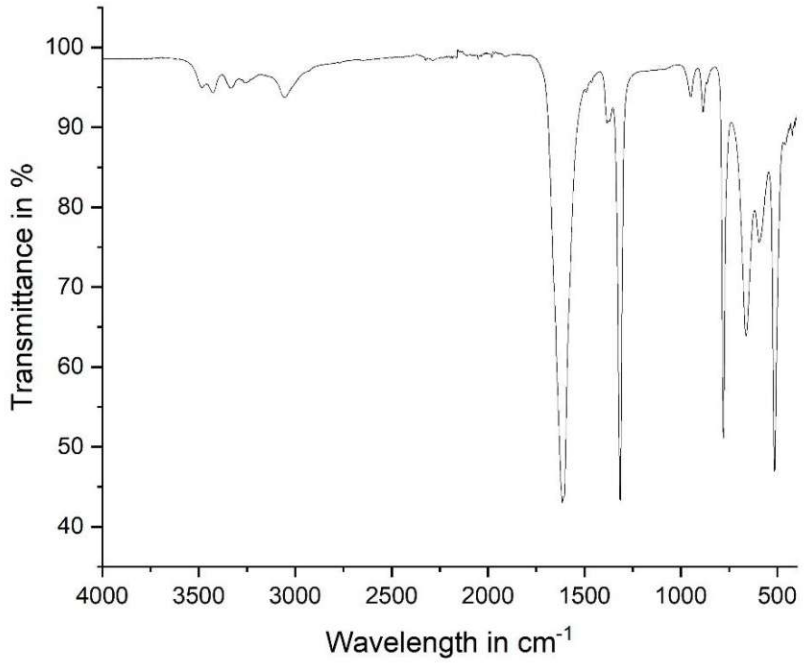

Figure 52: FTIR spectrum of Ca-oxalate monohydrate

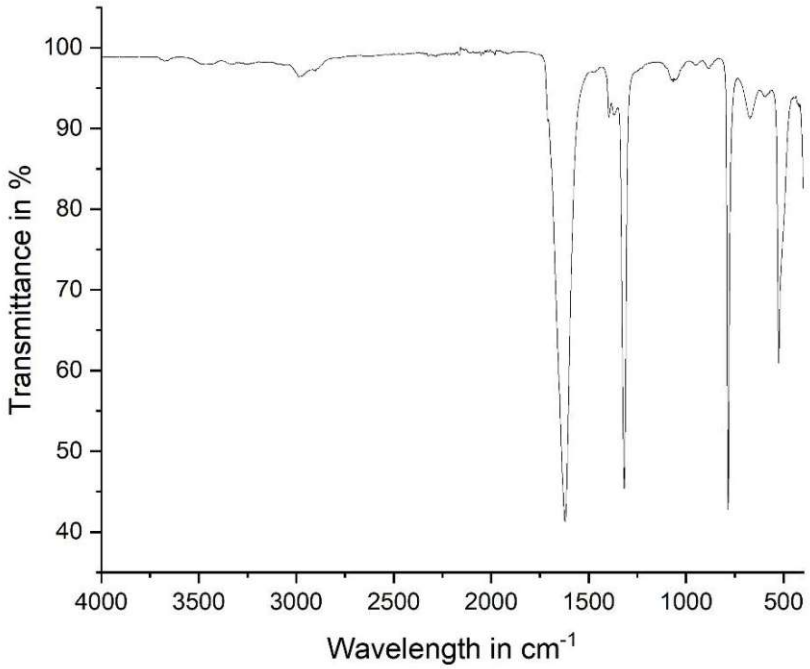

Figure 53: FTIR spectrum of Ca-oxalate monohydrate anhydrate

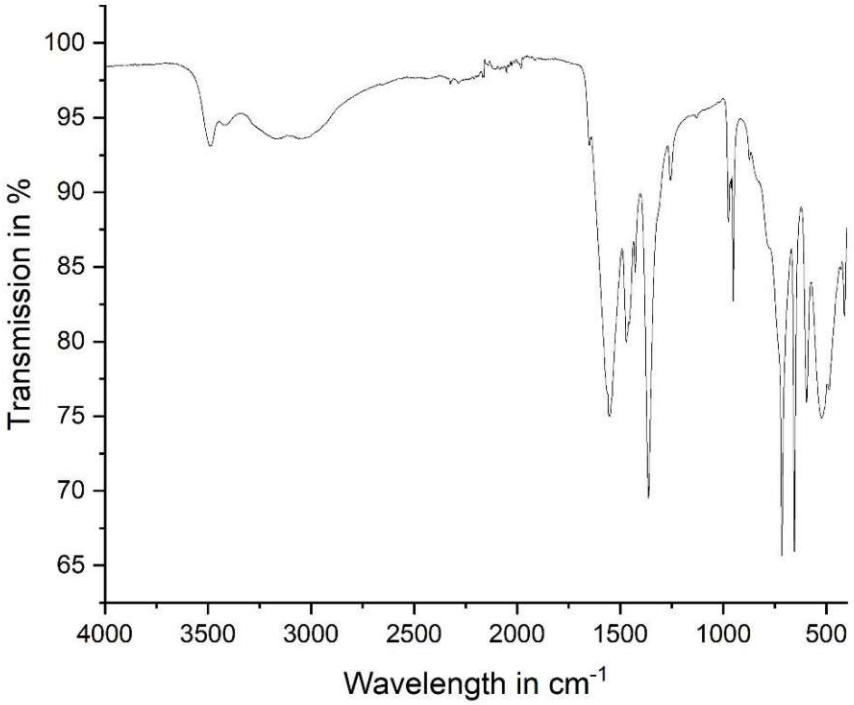

Figure 54: FTIR spectrum of Ca-malonate dihydrate

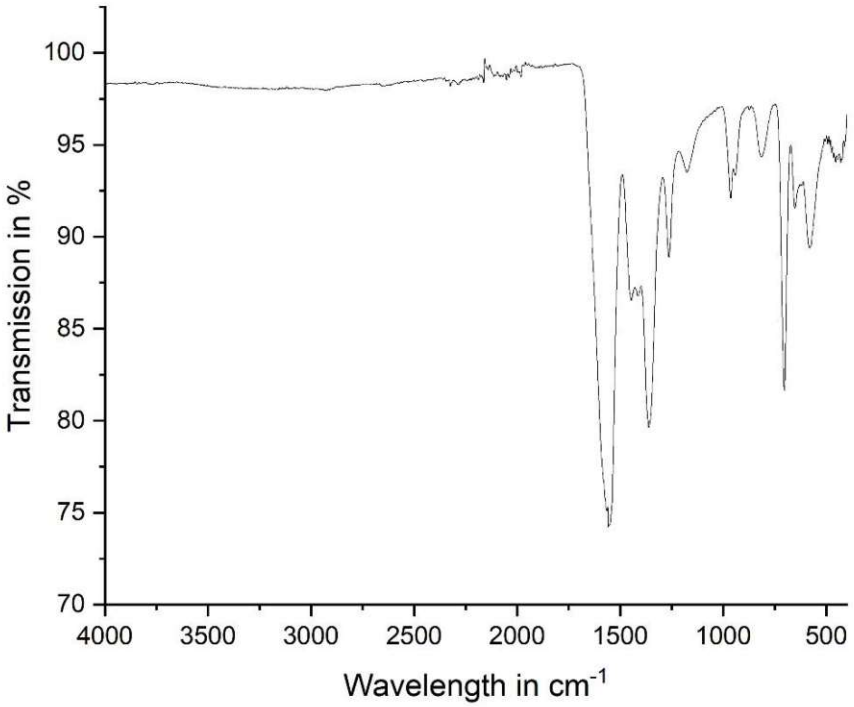

Figure 55: FTIR spectrum of Ca-malonate anhydrate

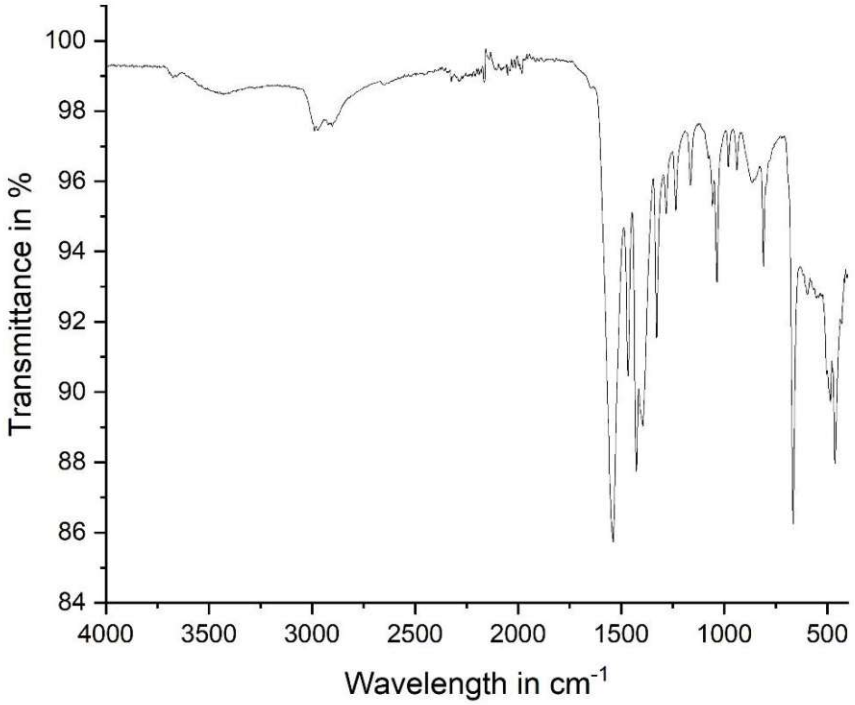

Figure 56: FTIR spectrum of Ca-succinate monohydrate

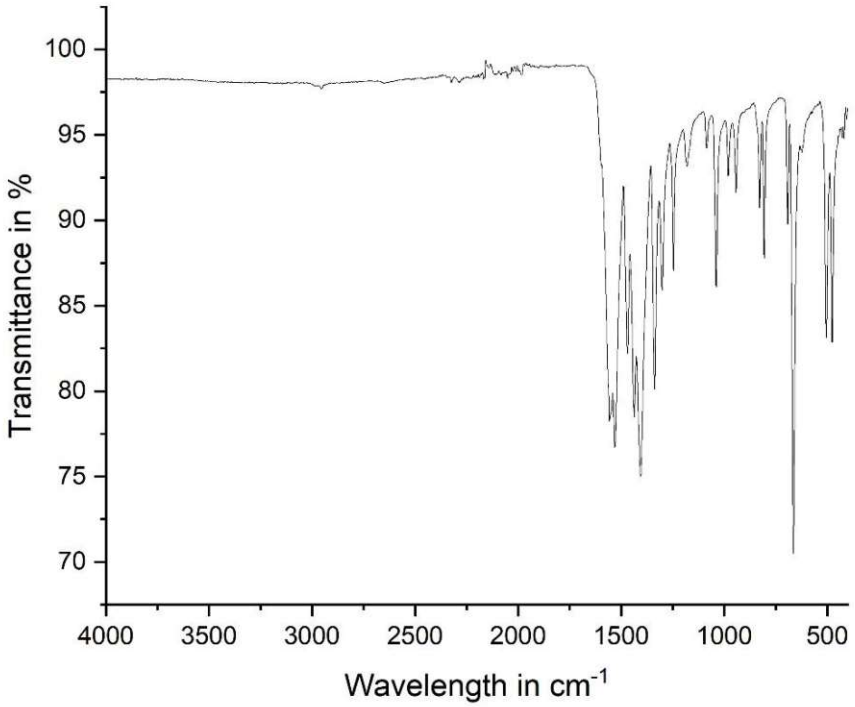

Figure 57: FTIR spectrum of Ca-succinate hydrate

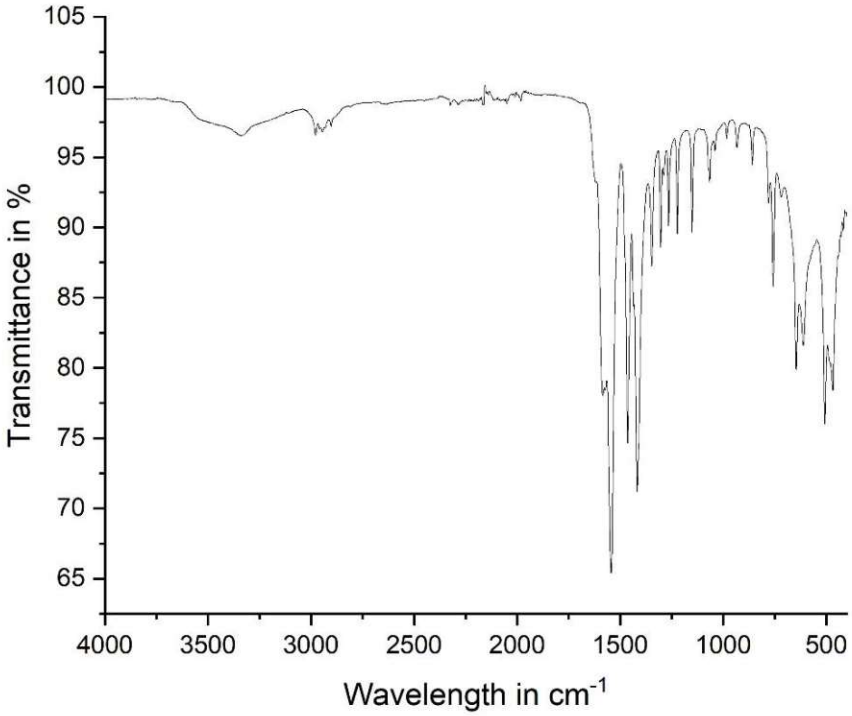

Figure 58: FTIR spectrum of Ca-glutarate monohydrate

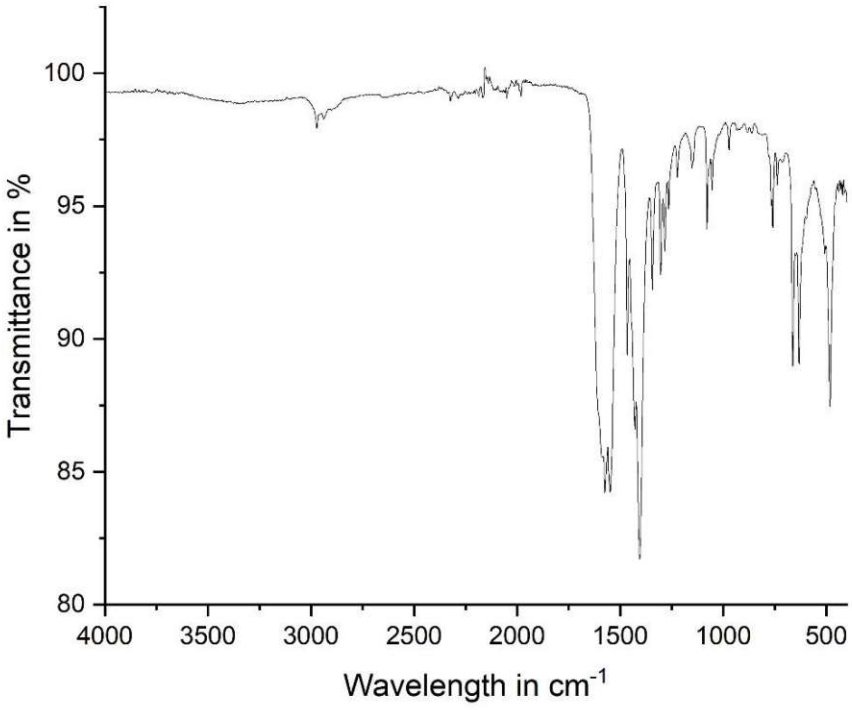

Figure 59: FTIR spectrum of Ca-glutarate anhydrate

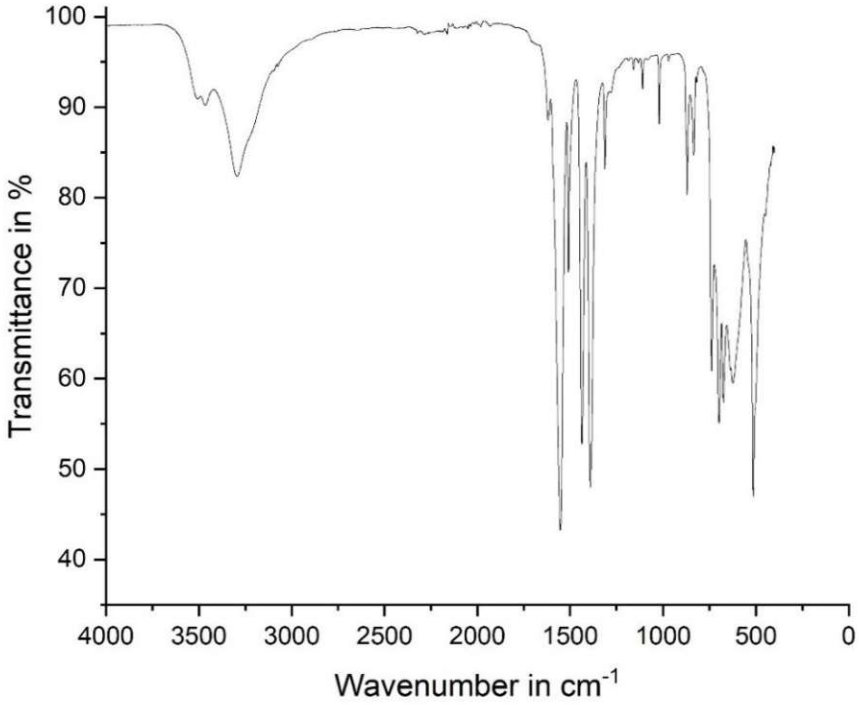

Figure 60: FTIR spectrum of Ca-terephthalate trihydrate

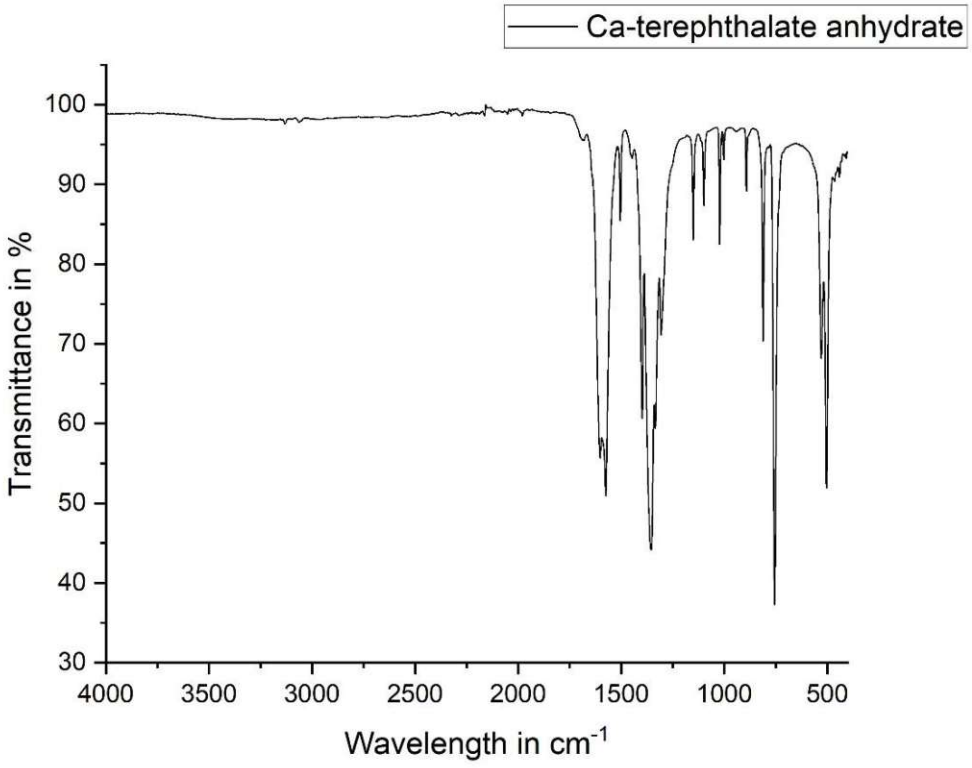

Figure 61: FTIR spectrum of Ca-terephthalate anhydrate

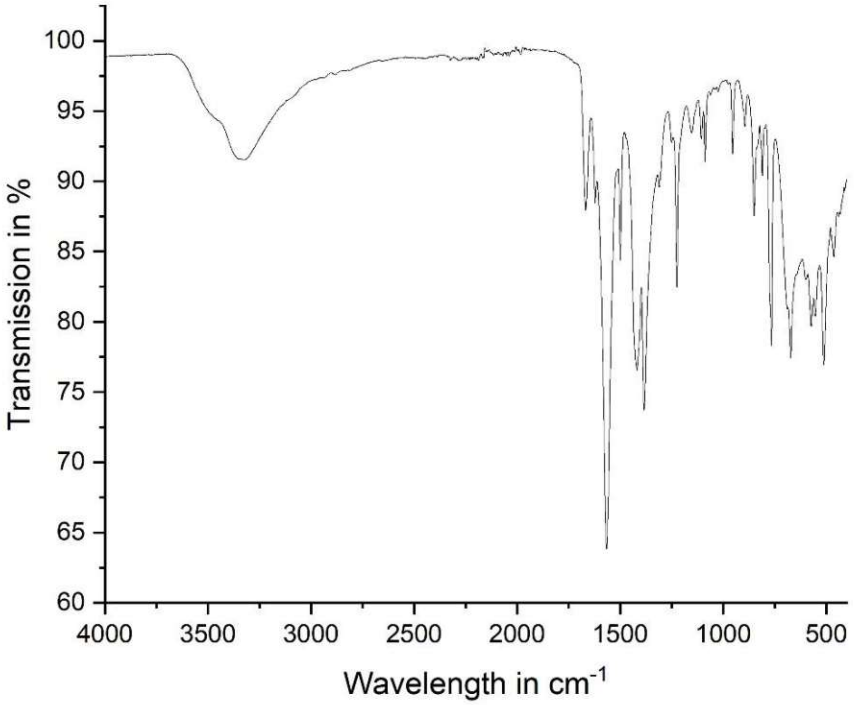

Figure 62: FTIR spectrum of 2-fluoro Ca-terephthalate trihydrate

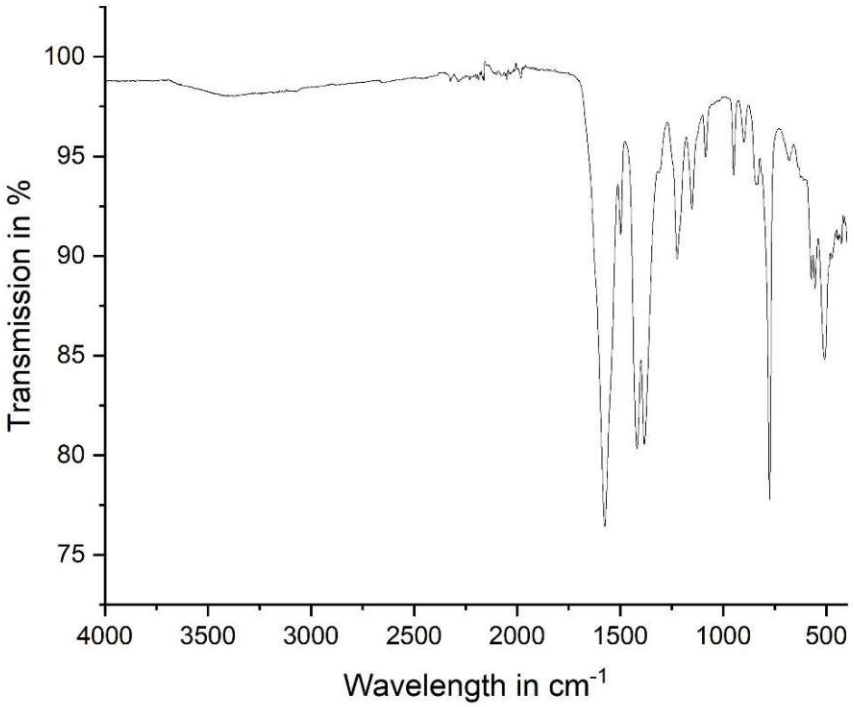

Figure 63: FTIR spectrum of 2-fluoro Ca-terephthalate anhydrate

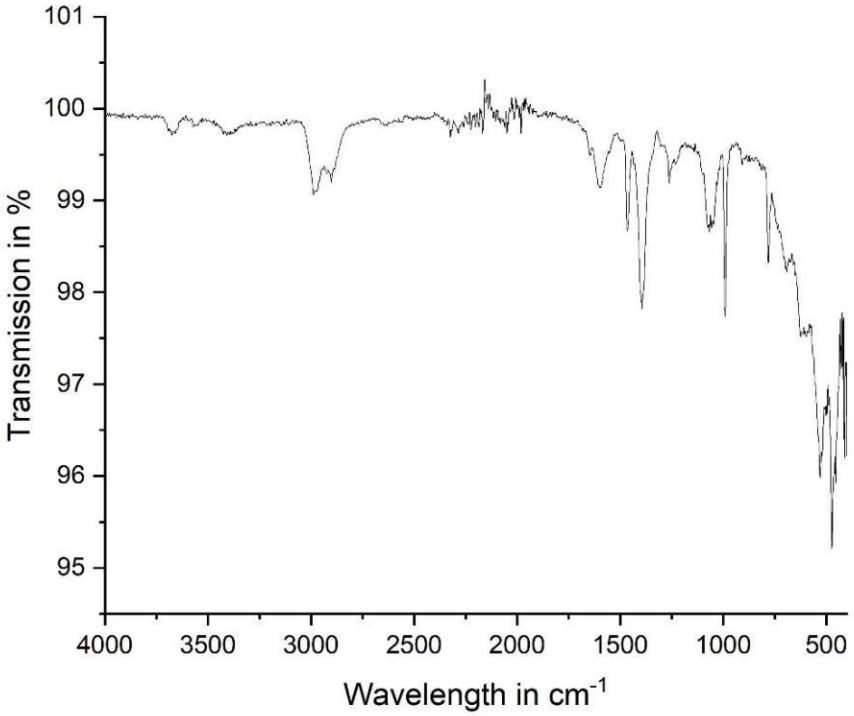

Figure 64: FTIR spectrum of tetrafluoro Ca-terephthalate tetrahydrate

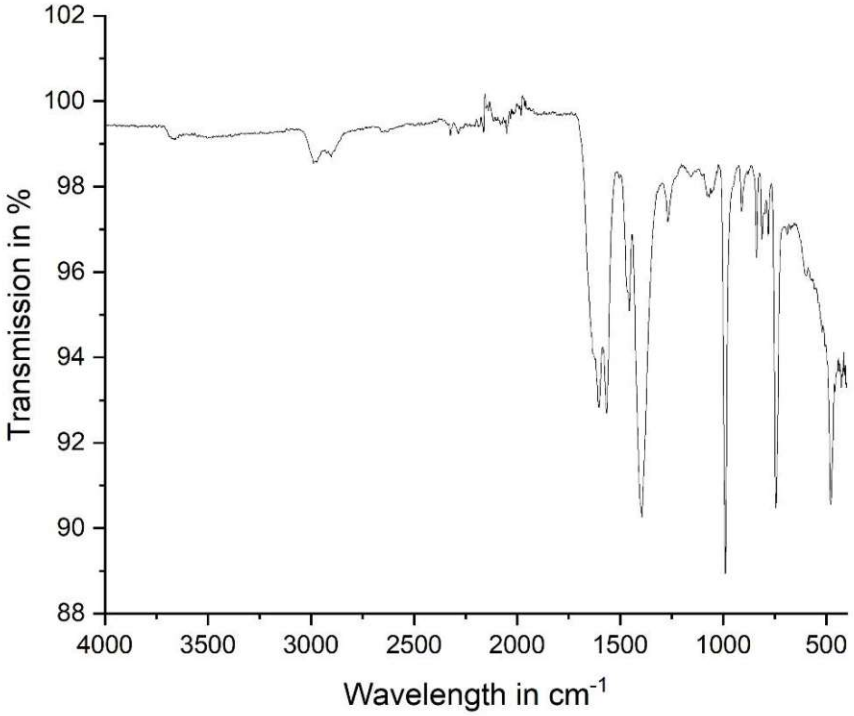

Figure 65: FTIR spectrum of tetrafluoro Ca-terephthalate anhydrate

References

1. *bp Statistical Review of World Energy 2021*. 2022. p. 60.
2. IEA, *Co-Generation and Renewables*. 2011, IEA: Paris.
3. IEA, *Heating Without Global Warming*. 2014: Paris.
4. Cot-Gores, J., A. Castell, and L.F. Cabeza, *Thermochemical energy storage and conversion: A-state-of-the-art review of the experimental research under practical conditions.* Renewable & sustainable energy reviews, 2012. **16**(ISSN: 1364-0321): p. 5224.
5. IEA, *Renewables 2019*. 2019, IEA: Paris.
6. Knoll, C., *Investigations of the reaction kinetics of thermochemical energy storage materials*. Untersuchungen der Reaktionskinetik von thermochemischen Energiespeichermaterialien. 2017, Wien. 200 Blätter, Illustrationen, Diagramme.
7. Hasnain, S.M., *Review on sustainable thermal energy storage technologies, Part I: heat storage materials and techniques.* Energy conversion and management, 1998. **39**(ISSN: 0196-8904): p. 1138.
8. Shine, K.P., et al., *Alternatives to the Global Warming Potential for Comparing Climate Impacts of Emissions of Greenhouse Gases.* Climatic Change, 2005. **68**(3): p. 281-302.
9. Wu, S., *Heat energy storage and cooling in buildings*, in *Materials for Energy Efficiency and Thermal Comfort in Buildings*, M.R. Hall, Editor. 2010, Woodhead Publishing. p. 101-126.
10. Li, G., *Sensible heat thermal storage energy and exergy performance evaluations.* Renewable and Sustainable Energy Reviews, 2016. **53**: p. 897-923.
11. Koçak, B., A.I. Fernandez, and H. Paksoy, *Review on sensible thermal energy storage for industrial solar applications and sustainability aspects.* Solar Energy, 2020. **209**: p. 135-169.
12. Engel, T. and P. Reid, *Thermodynamics, Statistical Thermodynamics & Kinetics*. 2012: Pearson.
13. Chavan, S., R. Rudrapati, and S. Manickam, *A comprehensive review on current advances of thermal energy storage and its applications.* Alexandria Engineering Journal, 2022. **61**(7): p. 5455-5463.
14. Linder, M., *Using thermochemical reactions in thermal energy storage systems*. 2015, Elsevier Ltd. p. 374.
15. Cabeza, L.F., et al., *Introduction to thermal energy storage (TES) systems*. 2015, Elsevier Ltd. p. 28.
16. Abedin, A.H., *A Critical Review of Thermochemical Energy Storage Systems.* The Open Renewable Energy Journal, 2011. **4**: p. 42-46.

17. Lager, D., *Evaluation of thermophysical properties for thermal energy storage materials - determining factors, prospects and limitations*. 2017, Wien: Wien. xii, 149, 3 Seiten, Illustrationen, Diagramme.
18. Pardo, P., et al., *A review on high temperature thermochemical heat energy storage.* Renewable and Sustainable Energy Reviews, 2014. **32**: p. 591-610.
19. N'Tsoukpoe, K.E., et al., *A review on long-term sorption solar energy storage.* Renewable and Sustainable Energy Reviews, 2009. **13**(9): p. 2385-2396.
20. Clark, R.-J., A. Mehrabadi, and M. Farid, *State of the art on salt hydrate thermochemical energy storage systems for use in building applications.* Journal of energy storage, 2020. **27**(ISSN: 2352-152X).
21. Yan, T., et al., *A review of promising candidate reactions for chemical heat storage.* Renewable and Sustainable Energy Reviews, 2015. **43**: p. 13-31.
22. Donkers, P.A.J., et al., *A review of salt hydrates for seasonal heat storage in domestic applications.* Applied energy, 2017. **199**(ISSN: 0306-2619): p. 68.
23. Hua, W., et al., *Review of salt hydrates-based thermochemical adsorption thermal storage technologies.* Journal of Energy Storage, 2022. **56**: p. 106158.
24. Yan, T. and H. Zhang, *A critical review of salt hydrates as thermochemical sorption heat storage materials: Thermophysical properties and reaction kinetics.* Solar Energy, 2022. **242**: p. 157-183.
25. Xu, J., R. Wang, and Y. Li, *A review of available technologies for seasonal thermal energy storage.* Solar energy, 2014. **103**: p. 610-638.
26. Tatsidjodoung, P., N. Le Pierrès, and L. Luo, *A review of potential materials for thermal energy storage in building applications.* Renewable and Sustainable Energy Reviews, 2013. **18**: p. 327-349.
27. van Essen, V.M., et al., *Characterization of Salt Hydrates for Compact Seasonal Thermochemical Storage*. 2009. p. 825-830.
28. Solé, A., I. Martorell, and L.F. Cabeza, *State of the art on gas–solid thermochemical energy storage systems and reactors for building applications.* Renewable and Sustainable Energy Reviews, 2015. **47**: p. 386-398.
29. Van Essen, V., et al., *Characterization of $MgSO_4$ hydrate for thermochemical seasonal heat storage.* 2009.
30. Ferchaud, C., et al. *Study of the reversible water vapour sorption process of $MgSO_4.7H_2O$ and $MgCl_2.6H_2O$ under the conditions of seasonal solar heat storage*. in *Journal of Physics: Conference Series*. 2012. IOP Publishing.
31. Whiting, G., et al., *Heats of water sorption studies on zeolite–$MgSO_4$ composites as potential thermochemical heat storage materials.* Solar Energy Materials and Solar Cells, 2013. **112**: p. 112-119.

32. Donkers, P.A.J., et al., *Water Transport in $MgSO_4 \cdot 7H_2O$ During Dehydration in View of Thermal Storage.* The Journal of Physical Chemistry C, 2015. **119**(52): p. 28711-28720.
33. Sögütoglu, L.C., et al., *In-depth investigation of thermochemical performance in a heat battery: Cyclic analysis of K_2CO_3, $MgCl_2$ and Na_2S.* Applied Energy, 2018. **215**: p. 159-173.
34. Posern, K. and C. Kaps, *Calorimetric studies of thermochemical heat storage materials based on mixtures of $MgSO_4$ and $MgCl_2$.* Thermochimica Acta, 2010. **502**(1): p. 73-76.
35. Molenda, M., et al. *Thermochemical energy storage for low temperature applications: materials and first studies in a gas-solid reactor*. in *Proceedings of 12th Int. Conference on Energy Storage (Innostock), Lleida, Spain*. 2012.
36. Donkers, P.A.J., O.C.G. Adan, and D.M.J. Smeulders, *Hydration/Dehydration Processes in Stabilized $CaCl_2$.* Poromechanics VI, 2017: p. 656-663.
37. Barsk, A., et al., *Exceptionally high energy storage density for seasonal thermochemical energy storage by encapsulation of calcium chloride into hydrophobic nanosilica capsules.* Solar Energy Materials and Solar Cells, 2023. **251**: p. 112154.
38. de Boer, R., W.G. Haije, and J.B.J. Veldhuis, *Determination of structural, thermodynamic and phase properties in the Na_2S–H_2O system for application in a chemical heat pump.* Thermochimica Acta, 2002. **395**(1): p. 3-19.
39. Sögütoglu, L.-C., et al., *Understanding the Hydration Process of Salts: The Impact of a Nucleation Barrier.* Crystal Growth & Design, 2019. **19**(4): p. 2279-2288.
40. Clark, R.-J. and M. Farid, *Hydration reaction kinetics of $SrCl_2$ and $SrCl_2$-cement composite material for thermochemical energy storage.* Solar Energy Materials and Solar Cells, 2021. **231**: p. 111311.
41. Blijlevens, M.A.R., et al., *A study of the hydration and dehydration transitions of $SrCl_2$ hydrates for use in heat storage.* Solar Energy Materials and Solar Cells, 2022. **242**: p. 111770.
42. Stengler, J., I. Bürger, and M. Linder, *Thermodynamic and kinetic investigations of the $SrBr_2$ hydration and dehydration reactions for thermochemical energy storage and heat transformation.* Applied Energy, 2020. **277**: p. 115432.
43. Ding, B., et al., *Study on long-term thermochemical thermal storage performance based on $SrBr_2$-expanded vermiculite composite materials.* Journal of Energy Storage, 2021. **42**: p. 103081.
44. N'Tsoukpoe, K.E., et al., *A systematic multi-step screening of numerous salt hydrates for low temperature thermochemical energy storage.* Applied Energy, 2014. **124**: p. 1-16.
45. Shkatulov, A., et al., *Core–Shell Encapsulation of Salt Hydrates into Mesoporous Silica Shells for Thermochemical Energy Storage.* ACS Applied Energy Materials, 2020. **3**(7): p. 6860-6869.

46. Wedler, G. and H.-J. Freund, *Lehrbuch der physikalischen Chemie*. 6., vollst. überarb. u. aktualis. Aufl. ed. 2013. 2012, Weinheim: Weinheim : Wiley-VCH. XXIX, 1141 S., Ill., graph. Darst., 24 cm.
47. Deutsch, M., et al., *Systematic search algorithm for potential thermochemical energy storage systems.* Applied energy, 2016. **183**(ISSN: 0306-2619): p. 120.
48. Knoll, C., et al., *Probing cycle stability and reversibility in thermochemical energy storage – $CaC_2O_4 \cdot H_2O$ as perfect match?* Applied Energy, 2017. **187**: p. 1-9.
49. Tomasich, J., *Conception of a new suspension reactor for calcium oxalate-based thermochemical energy storage systems*. 2020, Wien.
50. Garofalo, L., et al., *Salt Hydrates for Thermochemical Storage of Solar Energy: Modeling the Case Study of Calcium Oxalate Monohydrate Dehydration/Rehydration under Suspension Reactor Conditions.* Industrial & Engineering Chemistry Research, 2021. **60**(30): p. 11357-11372.
51. Galwey, A.K. and M. Abdel Aziz Mohamed, *Thermal decomposition of calcium malonate dihydrate.* Solid State Ionics, 1990. **42**(3): p. 135-145.
52. Brusau, E.V., et al., *A low temperature infrared study of the coordinated water in calcium malonate dihydrate.* Spectrochim Acta A Mol Biomol Spectrosc, 2002. **58**(8): p. 1769-74.
53. Binitha, M.P. and P.P. Pradyumnan, *Studies on growth, thermal and dielectric behavior of calcium succinate trihydrate single crystals.* Journal of crystal growth, 2014. **396**(ISSN: 0022-0248): p. 44.
54. D.S, C., M. C.K, and S.S. X, *Growth by free evaporation method and physico - chemical properties of calcium succinate single crystals.* Optik, 2017. **145**: p. 418-427.
55. Mazaj, M., et al., *Spectroscopic Studies of Structural Dynamics Induced by Heating and Hydration: A Case of Calcium-Terephthalate Metal–Organic Framework.* The Journal of Physical Chemistry C, 2013. **117**(15): p. 7552-7564.
56. Xiao, F., et al., *A new calcium metal organic frameworks (Ca-MOF) for sodium ion batteries.* Materials Letters, 2021. **286**: p. 129264.
57. Mazaj, M. and N. Zabukovec Logar, *Phase Formation Study of Ca-Terephthalate MOF-Type Materials.* Crystal Growth & Design, 2015. **15**(2): p. 617-624.
58. Li, Y., et al., *Scale-Up Synthesis of High Purity Calcium Terephthalate from Polyethylene Terephthalate Waste: Purification, Characterization, and Quantification.* Macromolecular Materials and Engineering, 2021. **306**(12): p. 2100591.
59. Dominici, F., et al., *Thermomechanical and morphological properties of poly(ethylene terephthalate)/anhydrous calcium terephthalate nanocomposites.* Polymers., 2020. **12**(ISSN: 2073-4360 , 2073-4360).
60. Matsuzaki, T. and Y. Iitaka, *The crystal structure of calcium terephthalate trihydrate.* Acta Crystallographica Section B, 1972. **28**(7): p. 1977-1981.

61. Scholz, G.A., Abdullah; Kemnitz, Erhard, *Mechanochemical Synthesis and Caracterization of Alkaline Earth Metal Terephtalates: $M(C_8H_4O_4)*nH_2O$.* Zeitschrift für Anorganische und Allgemeine Chemie, 2014. **640**(DOI: 10.1002/zaac.201300537): p. 317-324.
62. Yang, X., Y. Hao, and L. Cao, *Bio-Compatible Ca-BDC/Polymer Monolithic Composites Templated from Bio-Active Ca-BDC Co-Stabilized CO_2-in-Water High Internal Phase Emulsions.* Polymers, 2020. **12**(4): p. 931.
63. Groeneman, R.H. and J.L. Atwood, *Terephthlate bridged coordination polymers based upon group two metals.* Crystal engineering, 1999. **2**(ISSN: 1463-0184): p. 249.
64. Kazuo, M., *Thermal behavior of alkaline earth metal malonate hydrates and their anhydrides.* Thermochimica acta, 1996. **286**(ISSN: 0040-6031 , 1872-762X): p. 198.
65. Varughese, P., et al., *Crystallization and structural properties of calcium malonate hydrate.* Journal of Materials Science, 2004. **39**: p. 6325-6331.
66. Pruß, A. and W. Wagner, *Eine neue Fundamentalgleichung für das fluide Zustandsgebiet von Wasser für Temperaturen von der Schmelzlinie bis zu 1273 K bei Drücken bis zu 1000 MPa*. 1995: VDI-Verlag.
67. Chen, B., et al., *Physicochemical properties of ettringite/meta-ettringite for thermal energy storage: Review.* Solar Energy Materials and Solar Cells, 2019. **193**: p. 320-334.
68. Perkins, R.B. and C.D. Palmer, *Solubility of ettringite ($Ca_6[Al(OH)_6]_2(SO_4)_3 \cdot 26H_2O$) at 5–75°C.* Geochimica et Cosmochimica Acta, 1999. **63**(13): p. 1969-1980.
69. Grounds, T., H.G. Midgley, and D.V. Nowell, *The use of thermal methods to estimate the state of hydration of calciumtrisulphoaluminate hydrate $3CaO{\cdot}Al_2O_3{\cdot}3CaSO_4{\cdot}nH_2O$.* Thermochimica Acta, 1985. **85**: p. 215-218.